University of Alberta
Printing Department

THE UNIVERSITY OF ALBERTA

HYDROMETALLURGY OF A LOW-GRADE IRON-MANGANESE ORE

Thesis

Submitted to the Faculty of Graduate Studies
in Partial Fulfilment of the Requirements for
the Degree of Doctor of Philosophy

by

MAHMUD AHMAD QAZI

DEPARTMENT OF MINING AND METALLURGY

EDMONTON, ALBERTA

APRIL, 1967

UNIVERSITY OF ALBERTA

FACULTY OF GRADUATE STUDIES

We the undersigned certify that we have read the thesis entitled

HYDROMETALLURGY OF A LOW-GRADE

IRON-MANGANESE ORE

submitted by

MAHMUD AHMAD QAZI

and recommend to the Faculty of Graduate Studies for acceptance in the partial fulfilment of the requirement for the degree of Doctor of Philosophy.

ABSTRACT

A manganese-iron ore from New Brunswick, Canada, averaging 12.4% Mn and 14.2% Fe was leached and solvent extracted on a laboratory scale.

The effects of several variables: ore-to-acid and solid-to-liquid ratios, particle size, duration and temperature of leaching, were evaluated. In a typical test on a minus 65 mesh ore sample, at 60-70°C, with ore-to-acid ratio of 1:0.4 and solid-to-liquid ratio of 1:2.5, the recovery in the leach liquor in one hour was Mn 92.7%, Fe 3.2%. The concentration of Mn was further increased, and the iron content simultaneously decreased to less than 1g/litre, when the leach solution was recycled through a fresh batch of ore, in order to neutralize the free acid.

Further purification and concentration was carried out employing a solvent extraction process using kerosine solution of di (2-ethyl hexyl)-phosphoric acid (D2EHPA). A systematic study of the partition coefficient dependence on the following parameters: pH, D2EHPA concentration, concentration of Mn in aqueous phase, ratio of aqueous-to-organic phase, time of mixing and temperature, was made.

The results indicate that macro amounts of manganese can be extracted quantitatively at 25°C and at pH 4.5-5.5 according to the equation:

$$Mn^{++} + (HL)_2 = MnL_2 + 2H^+ \qquad (1)$$

The infra-red spectrum of Mn-D2EHPA indicates a shift in the P = O stretching frequency from 1227 cm^{-1} to 1192 cm^{-1}, which is attributed to the Mn-O bond formation.

Metallic manganese has been electroplated from amide baths of manganese chloride in a diaphragm cell. The metal of approximately 99% purity and the current efficiency as high as 76% have been obtained. Effects of, anode and cathode pH, concentration of salts in the electrolyte, current density etc., on the current yield have been investigated.

ACKNOWLEDGMENTS

I want here to acknowledge with thanks the facilities and the assistance provided by the Department of Mining and Metallurgy, University of Alberta, where the first part of this work was carried out.

I wish to express my sincere gratitude to Dr. Jan Leja who has been intimately and congenially associated with me during this work. His wide scientific knowledge, accurate judgement, unflagging diligence and sincerity combined with refined sense of humour made his collaboration a cheerful and valuable experience.

I owe a very special appreciation to Dr. A.G. McCalla, Dean of Graduate Studies, University of Alberta, for allowing me to complete my project under the supervision of Dr. Leja at the University of British Columbia.

Grateful acknowledgments are extended to Dr. Ian McTaggart Cowan, Dean of Graduate Studies, and the Department of Mineral Engineering, University of British Columbia, for providing research facilities, equipment, etc.

I am greatly indebted to Mrs. Elsa Guarnaschelli for typing the thesis with patience and accuracy.

Finally, my thanks are due to the External Aid Office for the award of the Colombo Plan Scholarship.

TABLE OF CONTENTS

TABLE OF CONTENTS (Continued)

TABLE OF CONTENTS (Continued)

LIST OF FIGURES

LIST OF FIGURES (Continued)

LIST OF FIGURES (Continued)

LIST OF TABLES

LIST OF TABLE (Continued)

INTRODUCTION

The continuing expansion of steel industry calls for an increased manganese production. As the rich manganese deposits are quickly being exhausted, the low grade ores will probably assume, before long, a much greater importance than heretofore.

Physical methods of beneficiating low-grade manganese ores have been studied extensively but, due to the complexity of the ore minerals and gangue present, these methods are reported to have met with very little success.

The iron-manganese ore from New Brunswick is too low in iron to be used directly as an iron ore. The first attempt[1] to exploit this deposit was made in 1848 when a blast furnace was erected in the area with a capacity of 7 tons iron per day; however, the manganese content of the ore is not high enough to be recovered by pyrometallurgical methods.

The ore is a typical example of a low-grade iron-manganese material which does not respond to the conventional physical methods of beneficiation, such as: flotation, gravity concentration etc. A small capacity experimental sink float plant was set up in 1953, near the deposit to up-grade the oxide before shipment to the blast furnace at Niagara Falls. The results indicated that a concentrate of 40% manganese grade could be obtained with an overall

manganese recovery of about 70%[1a].

During the preliminary tests in this project the sample of ore received from Woodstock, N.B., appeared to be amenable to leaching by dilute mineral acids. A detailed leaching study has been carried out using sulphuric acid. The leach liquor contained appreciable amounts of impurities that had to be removed before electrowinning metallic manganese.

Normally, the leach liquor is purified from heavy metal impurities by sulphide precipitation at an appropriate pH, while iron is removed by aeration of the liquor followed by filtration of the precipitated hydrated oxide. The sulphide treatment leaves an objectionable amount of sulphide in the liquor, necessitating its subsequent removal, while aeration and filtration of slimy precipitates involve too long and tedious procedures. These difficulties are avoided by using solvent extraction which selectively extract manganese in the organic phase leaving the impurities in the aqueous phase. Beside selectivity, simplicity, scope and speed are the additional merits of this process. The loaded solvent is stripped of its manganese content by a stoichiometric quantity of any mineral acid.

Metallic manganese can be obtained by electrolysing the aqueous solutions of manganese in the presence of a large amount of ammonium salt or from the fused manganese salts.

An attempt has been made to electroplate manga-

nese in non-aqueous media. The experimental evidence indicates that the method could be developed for useful applications, such as: electrowinning, improvement of purity and mechanical properties of the metal.

PROPERTIES AND USES OF METALLIC MANGANESE

Manganese is a very hard, grayish-white metal. In a pure state as electrolytic manganese, it scratches glass. Manganese was first isolated in 1774 by Ghan and Scheele. The physical and chemical properties of manganese are roughly the same as those of iron, the chief difference being that manganese is harder and more brittle but less refractory. It is fairly electropositive,

$$Mn = Mn^{++} + 2e^{-} \qquad E^{\circ} = 1.18V \qquad (1)$$

It occurs in four allotropic modifications: brittle or alpha (which is the common variety), beta, gamma (or ductile variety), and delta. The physical properties are given in Table I.

Manganese is readily dissolved in dilute non-oxidizing acids. It is very reactive towards oxygen and moisture, its greyish-white lustre is dulled by the formation of an oxide film in air. It is not particularly reactive towards non-metals at ordinary temperatures, but at elevated temperatures it reacts vigorously. It burns in chlorine, fluorine and nitrogen to give chloride, fluoride and nitrides, respectively. It also combines

directly with boron, carbon, silicon, and phosphorus, but not with hydrogen.

Table I

Physical Properties of Electrolytic Manganese [2]

	Alpha Manganese	Gamma Manganese
Electrical Resistivity	189.6×10^{-5} ohm cm	44.5×10^{-6} ohm cm
Hardness (Mohs' Scale)	7.1	2.3
Density	7.45 g/cm^3	7.20 g/cm^3
Magnetic Susceptibility	14×10^{-6}	8×10^{-6}
Transition temperatures (cgsm)		
Alpha-beta	723°C	
Beta-gamma	1098°C	
Gamma-delta	1135°C	
Delta-liquid	1246°C	

A. Metallurgical Uses

The primary use of manganese is in the manufacture of ordinary carbon steels and in the production of high manganese steel. In steel-making manganese acts as a deoxidizer and desulphurizer thus preventing the production of iron sulphide which causes hot embrittlement of steel and minimizing the blowhole formation in the ingot.

Manganese is added to molten steel in the form of a

ferro-manganese alloy known as spiegeleisen containing 18-22% manganese. Additions of manganese impart high tensile strength to steels, thus parts which are subjected to severe mechanical shocks, abrasions and distortion, e.g. rail crossings, automobile wheels etc. are made of high manganese steel. The so-called Hadfield steels contain 12-15% Mn and are used whenever high resistance to wear and erosion is required.

In non-ferrous metallurgy manganese is alloyed with a number of elements like copper (used for turbine propellers), manganese-bronze used for properllers. Aluminum-, magnesium-, and nickel-manganese alloys are also used, e.g. for spark plugs etc.

B. Non-metallurgical Uses

Manganese dioxide is used in electrical batteries, in glass, ceramic and enamel industry.

Manganese salts, oxides and organic compounds have application in paint and varnish industry for oil driers. Also chemicals, to be used for pigment and oxidizers for laboratory and industrial purposes.

REVIEW OF THE LITERATURE

Many extraction schemes have been developed and proposed for the recovery of manganese from ores. They may be broadly classified as pyrometallurgical and hydrometallurgical or chemical processes.

From a hydrometallurgical standpoint manganese ores may be divided into several types: (1) Ores in which manganese minerals are readily soluble in at least one solvent; (2)Ores in which manganese minerals require preliminary treatment to make it soluble; (3) Ores containing manganese in insoluble form; (4) Ores which destroy excessive amount of solvent due to soluble impurities.

To class one belong all the higher oxides of manganese, such as pyrolusite (MnO_2) psilomelane ($H_4Ba_2Mn_8O_{20}$), braunite [$3(MN,Fe)_2O_3.MnSiO_3$] and wad, as well as the manganiferous ores. These minerals are readily soluble in acids. To class two belongs rhodochrosite ($MnCO_3$), which requires calcining to expel CO_2 before the manganese is solubilized in sulphurous acid or ammonium compounds. To class three belong rhodonite ($MnSiO_3$) and the partly oxidized black silicates which are practically insoluble in the usual leaching agents. Class four is represented by ores with high lime gangue which precludes acid leaching.

In chemical processes, the active solubilizing agents are derived from chlorine, nitrogen or sulphur com-

pounds. A complete survey of the three processes has been presented in the form of a report by the author[3] (Department of Mining and Metallurgy, University of Alberta, Edmonton). The processes employing chlorine and fixed nitrogen are reviewed by Norman and Kirby[4]. Below, only a brief recapitulation of the main aspects of the three types of processes is given.

A. CHLORIDE PROCESSES

When chloride processes are applied to manganese, the latter is volatilized in the form of manganous chloride ($MnCl_2$) away from the gangue minerals. In a general classification chloride processes may be divided into leaching, and chloridization. In leaching, reagent such as aqueous hydrochloric acid is used to dissolve manganese as chloride. Most of the problems found in this technique concern the simultaneous dissolution of other constituents from the raw material, necessitating a subsequent separation of manganese.

In chloridization, on the other hand, a pyrochemical technique is employed to convert the manganese in the raw material to chloride. The manganese ore is roasted in the presence of a chloride source at temperature high enough to allow the formation of $MnCl_2$. The source may either be a gas such as hydrogen chloride (HCl), or an admixed solid such as sodium chloride (NaCl) or calcium chloride ($CaCl_2$). If the roasting temperature is low the vapor pressure of the $MnCl_2$ formed will not be high enough to cause volatilization of the chloride, in which case the $MnCl_2$ formed will remain

in the roasted material. The manganous chloride and all the other chlorides are then dissolved out with water.

The disadvantages of the chloride processes is that at higher temperature they are very corrosive. Part of the leaching agent is decomposed generating chlorine according to reaction

$$MnO_2 + 4HCl = MnCl_2 + 2H_2O + Cl_2 \qquad (2)$$

B. FIXED NITROGEN PROCESSES

Fixed-nitrogen processes for recovering manganese from its ores may employ one or more of several fixed nitrogen compounds, such as ammonia, nitric acid, or certain ammonium salts. The ore may be directly solubilized or the ore may require roasting.

The nitrogen compounds used for leaching manganese (such as nitric acid, developed by Nossen[5], and nitrogen dioxide) convert the manganese minerals [except rhodonite ($MnSiO_3$)] to soluble nitrates. The manganese nitrate can then be decomposed to an almost chemically pure manganese dioxide.

Other fixed-nitrogen processes employ ammonium sulphate [$(NH_4)_2SO_4$] and ammonia-carbon dioxide-water system that is, ammonium carbamate process. The reactions of the process may be written as:

$$NH_3 + H_2O = NH_4OH \qquad (3)$$

$$2NH_4OH + CO_2 = O{=}C\begin{matrix}ONH_4\\NH_2\end{matrix} + 2H_2O \qquad (4)$$

ammonium carbamate

$$MnO + O{=}C\begin{matrix}ONH_4\\NH_2\end{matrix} = Mn\begin{matrix}O\text{-}C\text{-}NH_2\\ \| \ O\\ONH_4\end{matrix} \qquad (5)$$

$$Mn\begin{matrix}O\text{-}C\text{-}NH_2\\ \| \ O\\ONH_4\end{matrix} + 2H_2O = Mn\begin{matrix}O\\ \diagdown\diagup\\O\end{matrix}C = O + 2NH_4OH \qquad (6)$$

manganous carbonate

Ammonium sulphate leach as in Bradley-Fitch process(6) is carried out on reduced manganese ore with a solution of 10% $(NH_4)_2SO_4$ at 90°C; the following reaction takes place:

$$MnO + (NH_4)_2SO_4 = MnSO_4 + 2NH_3 + H_2O \qquad (7)$$

Similarly, in Bruce Williams process[7], the manganese ore is roasted with ammonium salts like $(NH_4)_2SO_4$, NH_4HSO_3, NH_4Cl, etc., at 450-550°C, and the manganese oxides are converted into the corresponding salts according to the reactions:

$$3MnO_2 + 3(NH_4)_2SO_4 = 3MnSO_4 + 4NH_3 + N_2 + 6H_2O \qquad (8)$$

$$MnO_2 + NH_4HSO_3 = MnSO_4 + NH_3 + H_2O \qquad (9)$$

$$MnO + 2NH_4Cl = MnCl_2 + 2NH_3 + H_2O \quad (10)$$

C. SULPHUR PROCESSES

The sulphur processes are divided into four groups: (1) treatment with gaseous sulphur dioxide, (2) dithionate and sulphate process, (3) iron pyrite roast, and (4) sulphuric acid leaching process.

1. Sulphur Dioxide Process

The oxides of manganese may readily be converted to manganous sulphate ($MnSO_4$) by treating with gaseous sulphur dioxide or by sulphurous acid at concentrations which do not lead to iron sulphate formation. In application to carbonate ores a preliminary roasting is required.

Leaver[8] was the first to develop a commercial method of leaching manganese with SO_2 and sulphurous acid. The crushed ore was pulped with water and treated with furnace gases containing 2-6% SO_2 counter currently in a specially designed drum. The discharged pulp was filtered. The leach liquor contained about 11% $MnSO_4$ which corresponded to 65-75% of the original soluble manganese content. The filtrate was evaporated and calcined at 800-1000°C to give oxide product containing 60-64% Mn.

Blumburg and Morgan[9] used 15% SO_2 from pyrite burners at a lower temperature of 300°C. Their laboratory scale tests indicated that the leach filtrate contained less

than 0.02 g/l iron and no sulphite or dithionate.

However, it was found that at higher SO_2 concentration and higher temperatures, side reactions took place with the formation of di- and polythionates according to the reaction:

$$H_2S_2O_3 + MnO_2 = MnS_2O_6 + 2H_2O \qquad (11)$$

A recent development of the SO_2 process, which seems to have some promise has been described by Allen[10]. It differs from the early SO_2 process in two respects, viz., a high temperature autoclaving and a sintering operation. A slurry of ground manganese ore is treated with SO_2 in a packed tower. Manganese dioxide reacts to form manganese sulphate and dithionate. The reactions are represented as:

$$MnO_2 + SO_2 = MnSO_4 \qquad (12)$$

$$MnO_2 + 2SO_2 = MnS_2O_6 \qquad (13)$$

The dithionate produced is converted to sulphate by oxidation of the slurry in an autoclave. The following reaction takes place:

$$MnS_2O_6 + 1/2\ O_2 + H_2O = MnSO_4 + H_2SO_4 \qquad (14)$$

The process is recommended for ores containing 20% Mn. The recovery obtained was about 70% of the soluble manganese present in the ore.

2. Dithionate and Sulphate Processes

As an alternate to the process described above a slurry of ore in an excess of calcium dithionate is treated with smelter flue gases containing about 3% SO_2 and oxygen; the following reactions occur:

$$MnO_2 + SO_2 = Mn^{2+} + SO_4^{2-} \quad (15)$$

$$MnO_2 + 2SO_2 = Mn^{2+} + S_2O_6^{2-} \quad (16)$$

$$H_2O + SO_2 + 1/2\ O_2 = 2H^+ + SO_4^{2-} \quad (17)$$

$$H_2O + 2SO_2 + 1/2\ O_2 = 2H^+ + S_2O_6^{2-} \quad (18)$$

The sulphate formed by reactions (15) and (17) is precipitated as calcium sulphate:

$$CaS_2O_6 + SO_4^{2-} = CaSO_4 + S_2O_6^{2-} \quad (19)$$

While the manganese dithionate solution is separated by filtering the slurry. The solution is treated with slaked lime to precipitate manganese hydroxide and regenerate calcium dithionate:

$$MnS_2O_6 + Ca(OH)_2 = Mn(OH)_2 + CaS_2O_6 \quad (20)$$

Ravitz[11] pointed out that the only losses of dithionate are those due to incomplete washing of leach residue and of the precipitated hydroxide. The manganese recovery in the hydroxide is reported to be 96%. The amount of SO_2 utilized was 60-70% of that introduced, ranging from 1.5 to 2.2 lbs. per lb. of manganese extracted. The drawback of this process (as in the other sulphur processes) is the slimy form of calcium sulphate which produces scale in the evaporator.

Sulphate Process. Hoak and Coull[12] have proposed the use of waste pickle liquor from the steel industry (containing 5% free sulphuric acid and 15% ferrous sulphate), to leach manganese from low-grade ores. Experimental work on an ore containing 14.7-26.9% manganese showed that, about 98% manganese could be leached from a 60 mesh ore when treated with leach liquor for 30 minutes.

The manganese sulphate in the leach liquor was converted to chloride by treating it with calcium chloride, in order to minimize contamination of manganese with sulphur.

The separation of iron and manganese was done by selective precipitation of iron with lime, at pH below 4.2. This treatment removed about 98% of iron but 5% Mn was also lost due to coprecipitation.

The filtrate containing manganous chloride and calcium chloride was treated with lime slurry until the pH rose to 9.5. Manganese was precipitated as hydroxide.

The amount of manganese extracted was largely con-

trolled by the quantity of ferrous sulphate. The extraction reactions can be represented as:

$$MnO_2 + 2FeSO_4 + 2H_2O = MnSO_4 + Fe(OH)_3 + Fe(OH)SO_4 \quad (21)$$

followed by:

$$Fe(OH)_3 + H_2SO_4 = Fe(OH)SO_4 + 2H_2O \quad (22)$$

$$Fe(OH)SO_4 + H_2SO_4 = Fe_2(SO_4)_3 + 2H_2O \quad (23)$$

The overall leaching reaction is therefore:

$$MnO_2 + 2FeSO_4 + 2H_2SO_4 = MnSO_4 + Fe_2(SO_4)_3 + 2H_2O \quad (24)$$

Autoclaving the ore slurry improved pickle liquor leaching by increasing extraction of manganese and causing precipitation of ferric iron as alpha Fe_2O_3.

3. Sulphation Roasting with Pyrites

A method of leaching low-grade manganese ore (less than 5% Mn) utilizing pyrite as a reagent, was developed by Thomas and Whalley[13]. An aerated slurry of ore and pyrite, heated at 90°C, gave manganese extraction of about 90% in four hours; recycling the leach liquor yielded a solution practically free from iron and containing approximately 100 gram manganese sulphate per litre.

The mechanism appears to be essentially, the reduction of tetravalent manganese in pyrolusite (MnO_2) to the divalent, acid soluble, manganous form by ferrous iron. During the dissolution of manganese the iron is alternately oxidized by pyrolusite and reduced by pyrite:

$$Fe^{++} \underset{FeS_2}{\overset{MnO_2}{\rightleftharpoons}} Fe^{+++} \qquad (25)$$

In other words the ferrous ion is continuously regenerated during the leaching process.

Heating an aqueous slurry of pyrite at 110°C in an autoclave first under oxygen pressure and then in the absence of oxygen produces a concentrated acidic solution of ferrous sulphate (200 g/l). Hoak and Coull[12] found that solutions of similar composition were suitable for leaching pyrolusite ores at room temperatures.

Although the reaction of ferrous sulphate with manganese dioxide is fast, the formation of ferrous sulphate from pyrite is known to be slow:

$$FeS_2 + 3\ 1/2\ O_2 + H_2O = FeSO_4 + H_2SO_4 \qquad (26)$$

For example, only 5% of the pyrite was oxidized in 4 hours, when a slurry of minus 200 mesh pyrite in dilute sulphuric acid of pH 1.0 at 90°C was oxygenated. The ferrous sulphate formed may be oxidized by oxygen according to the reaction:

$$2FeSO_4 + H_2SO_4 + 1/2\ O_2 = Fe_2(SO_4)_3 + H_2O \qquad (27)$$

The removal of ferrous ion by this reaction might be expected to interfere with the leaching pyrolusite by reaction (25).

4. Sulphuric Acid Leaching Process

Schrier and Hoffman[14] suggested a method of treatment for low-grade manganese ores to produce high grade manganese dioxide. The gound ore and oil was mixed in a roaster feeder, and reduced in the kiln at 750°C for 20-40 minutes. The roasted oxide was leached with a solution containing 75 g/l H_2SO_4, at 60°C for 2 hours. About 76% manganese was extracted in the leach liquor.

Engel and Heinen[15] studied the action of sulphuric acid in the presence of organic reducing agents in the solution like sawdust, lignin, sugar, oils and coal.

Sulphation reduction of manganese oxides is based on the exothermic reaction:

$$2MnO_2 + 2H_2SO_4 + C = 2MnSO_4 + 2H_2O + CO_2 \qquad (28)$$

The manganese sulphate produced is extracted by leaching with cold water.

The principal advantages of this process are that the ore does not have to be roasted before leaching and the process can be applied to small scale manganese mining operations.

The extraction figures and the corresponding sulphuric acid consumptions compare favourably with results obtained in the laboratory from sulphuric acid leaches of calcine produced from reduction roasts of the ores.

D. PURIFICATION OF LEACH SOLUTION

It appears that one of the most important factors in producing manganese by electrolysis is the level of impurities in the electrolyte. Manganese has quite a high oxidation potential (1.18V). Since the only metals less noble than manganese are aluminum, the alkali and the alkaline earth metals, all other metals are deleterious to the deposition of manganese. The range of the tolerance of various elements evaluated by Jacobs[16] is listed in the table (II). The data were obtained on the basis that the decrease in current efficiency was about 2% in two hours with standard electrolyte.

Table II

Effect of Impurities in Cell Solution

Impurities	Max. Allowable Conctn. mg/litre
Co	5
Ni	5
Cu	10-15
As	6-9
As (V)	24

Table II (Cont'd)

Fe (II)	30
Pb	No effect up to the limit of solubility
Sb	5
Zn	10

The chief impurity in the leach liquor is iron. The most common method of its removal is by aeration.

Inspection of the Eh-pH diagrams for Fe-H_2O and Mn-H_2O systems (in Fig. 1 and 2) leads to the conclusion that iron can be selectively precipitated from solution containing iron and manganese at a pH range of 6-8 on aeration. The Eh-pH diagrams are particularly useful to predict the conditions of potential and pH under which a given solid/liquid system is in an equilibrium. For a metal M, considering a general reaction with water:

$$xM + aH_2O = yN + bH^+ \tag{29}$$

in which M is the acidic form and N is the alkaline form of the metal; the condition of equilibrium is given by

$$K = \frac{(N)^y}{(M)^x} (H^+)^b \tag{30}$$

assuming x = y, and taking logarithm

$$\log K = \log \frac{(N)}{(M)} - b\,pH \tag{31}$$

This equation indicates that the ratio of pH concentration of the alkaline form to the concentration of acidic form increases linearly with pH.

In the case of an electrochemical reaction of the form:

$$xM + aH_2O + ne^- = yN + bH^+ \tag{32}$$

the condition of electrochemical equilibrium will be given by

$$E_o = E_o^o - \frac{RT}{nF} .b.pH + \frac{RT}{nF} \log \frac{(M)}{(N)} \tag{33}$$

considering x = y as before.

It will be noted that the activity of the oxidized form is in the numerator of the term $\log \frac{M}{N}$: the equilibrium potential E_o, therefore, increases when the amount of the oxidized form increases.

Considering the electrode potential and pH as independent variables and the logarithmic function of the concentrations of the substances M and N as a parameter, the potential -pH diagram can be drawn for a particular system.

Figures 1 and 2 are the Eh-pH diagrams for Fe-H_2O[17] and Mn-H_2O systems[18] respectively. The lines (a) and (b)

express respectively the reduction equilibrium of water according to the reaction

$$H_2 = 2H^+ + 2e^- \qquad \text{(line a)} \tag{34}$$

with $E_{oa} = 0.000 - o,0591\ pH$ (volts)

and its oxidation equilibrium according to the reaction

$$2H_2O = O_2 + 4H^+ + 4e^- \quad \text{(line b)} \tag{35}$$

with $E_{ob} = 1.228 - 0.0591\ pH$ (volt)

at a hydrogen or oxygen pressure of one atmosphere.

The lines express the equilibrium condition under which the species represented by a chemical reaction are stable. For example, assuming that the reaction taking place on the precipitation of iron from the leach liquor by aeration be

$$Fe^{++} + 3H_2O = Fe(OH)_3 + 3H^+ \tag{36}$$

The solubility of iron and its hydroxide is represented by line 28 on Figure (1). The iron is precipitated from the solution by raising the pH and/or blowing air, whereupon the very sparingly soluble ferric hydroxide is precipitated and

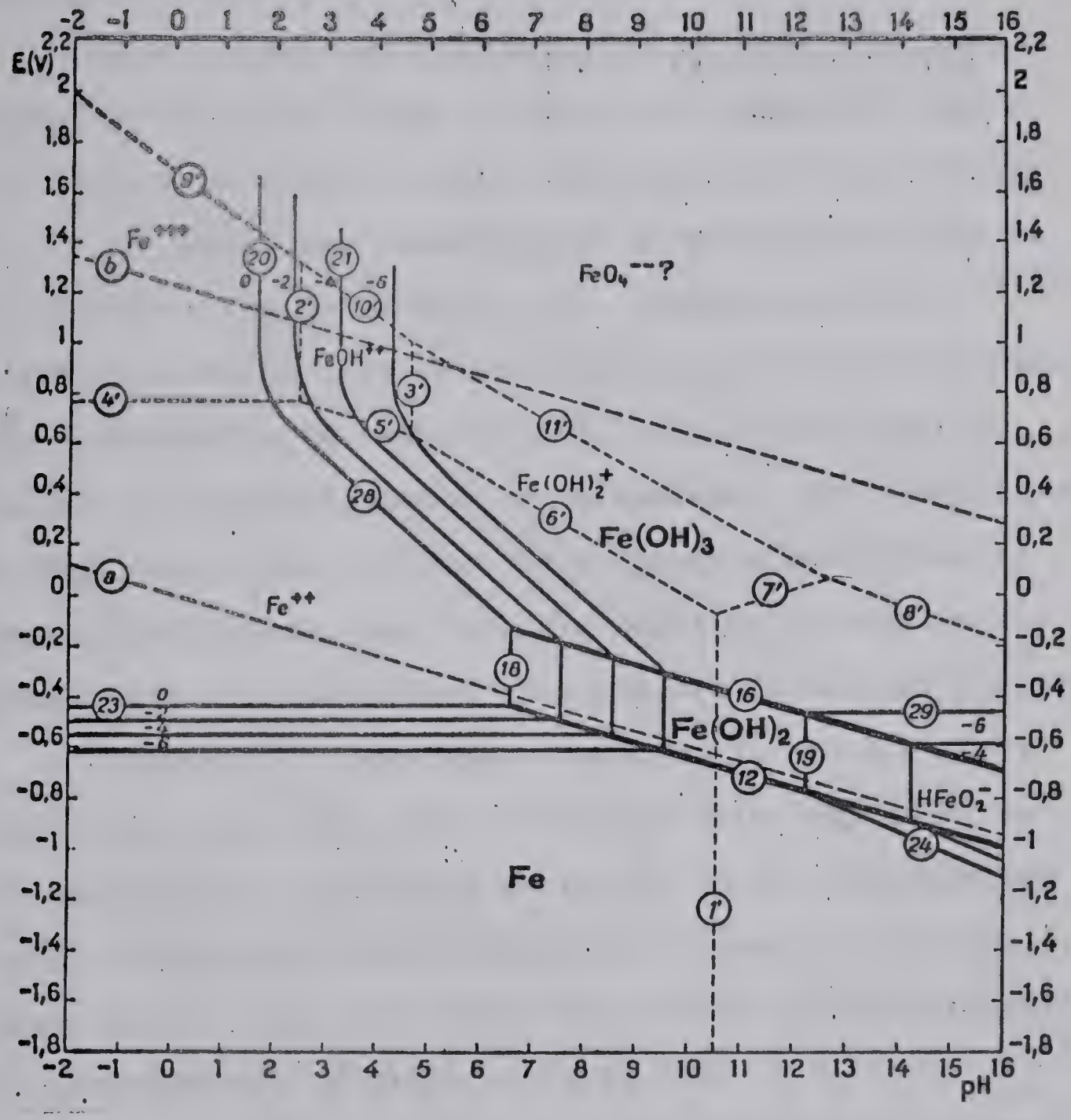

Fig. 1. Potential-pH equilibrium diagram for the system iron-water, at 25°C [considering as solid substances only Fe, $Fe(OH)_2$ and $Fe(OH)_3$]. From M. Pourbais Atlas of Electrochemical Equilibrium Aqueous Solutions (1966) p. 313

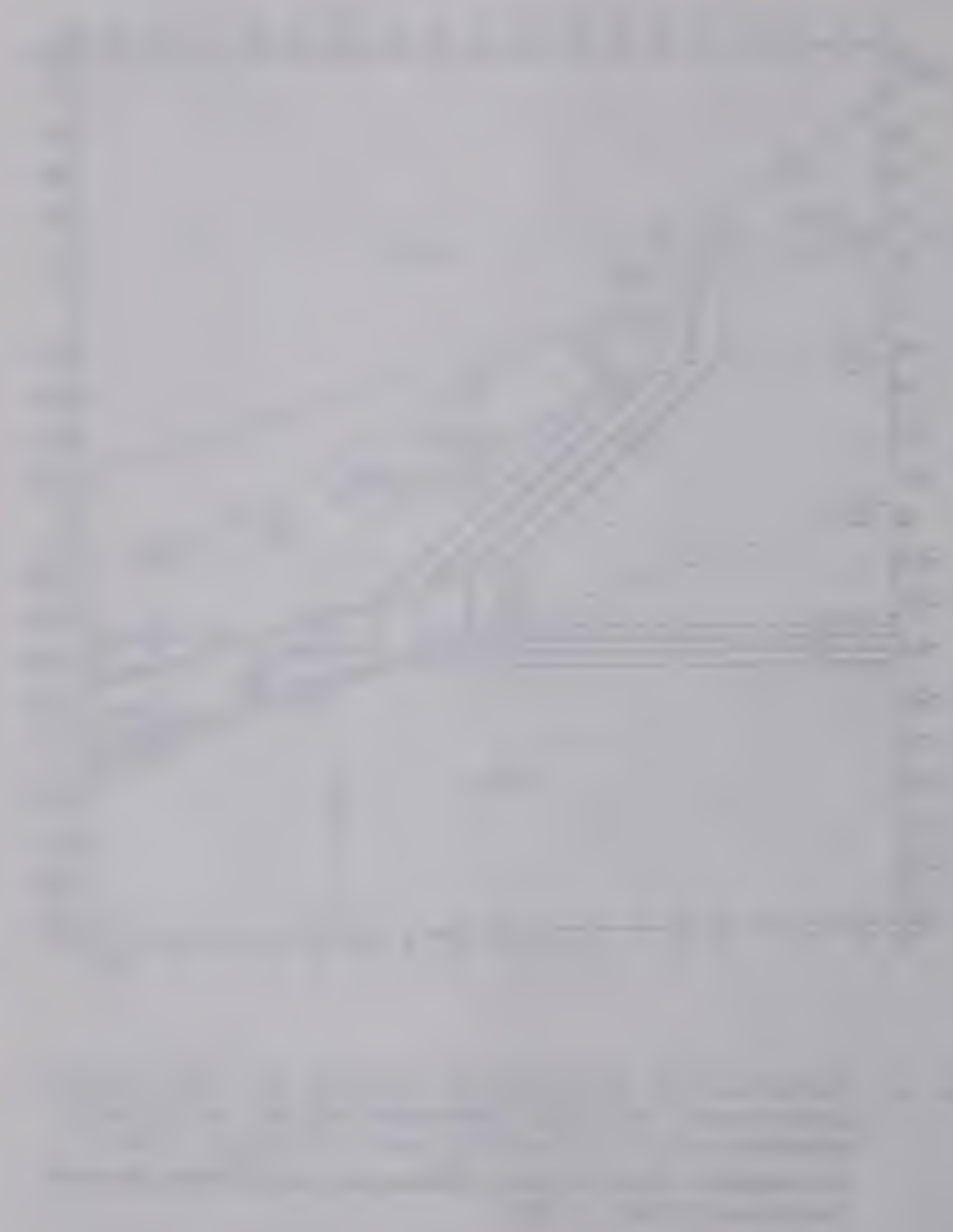

can be removed by filtration. As can be seen in Figure (1) both the rise of pH, and the presence of oxygen effect oxidation and to raise the redox potential, contribute to the precipitation of $Fe(OH)_3$.

Considering the unit activity of both iron and manganese in solution it can be noted from Figures 1 and 2, that a rise of pH above 6 causes the precipitation of manganese. It is therefore, advantageous to precipitate iron at lower pH and in the presence of air. Levan and others[19,20] successfully removed iron on aeration at a pH of 5.5 maintaining the temperature between 60-65°C. The use of lower pH restricted the coprecipitation of manganese. The leach liquor freed from iron still contains objectionable quantities of copper, nickel, cobalt and zinc, in addition to calcium and magnesium sulphates dissolved from the ore in sulphur processes.

Ambrose[21] developed a process in which copper, nickel, cobalt and zinc were removed as sulphide, using ammonium sulphide and activated charcoal. Manganese sulphide at first precipitates in the nearly pure state, but after standing for an hour, the nickel and cobalt sulphides precipitate provided the solution is at pH 7.0.

Jacobs[22] used hydrogen sulphide instead of ammonium sulphide. The amount of H_2S required was found to be 0.1 to 0.15 g/l. The amount of Mn lost in this process was only 0.5 gram per litre. After filtration the solution was treated with $FeSO_4$ and oxidized to precipitate iron as oxide.

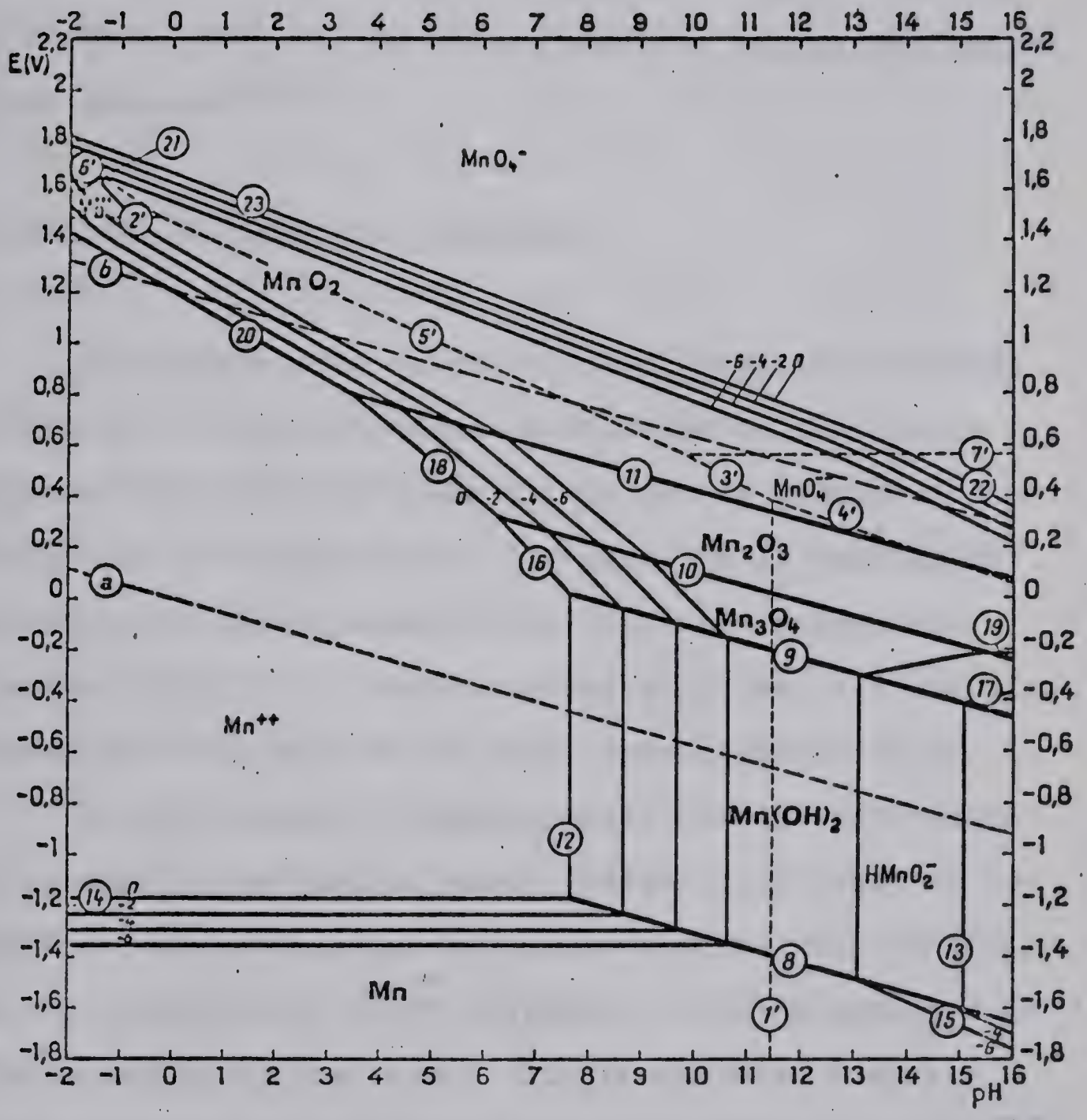

Fig. 2. Potential-pH equilibrium diagram for the system manganese-water, at 25°C [considering β-MnO_2 (pyrolusite).] From M. Pourbais, Atlas of Electrochemical Equilibria in Aqueous Solutions (1966) p. 290.

Magnesium in some of the ores is dissolved in the leaching process. Magnesium sulphate does not have an adverse effect on the electrolysis, if the temperature is not allowed to rise above 15°C. Above this temperature Mg precipitates in the electrolytic cell as triple salts of magnesium, manganese, and ammonia.[22a]

E. PRODUCTION OF METALLIC MANGANESE

Considering the potential-pH diagram representing the conditions of thermodynamic equilibrium of the system manganese-water at 25°C (Figure 2), it can be predicted that electrowinning of manganese will be possible in neutral or acidic solutions whose potential is below the potentials shown by the line (14). For one molar solution, for example, this potential will have to be below approximately -1.2V.

As the region of thermodynamic stability of manganese lies well below that of water (whose lower limit is represented by the dotted line (a)), the electrolysis of manganese in the presence of water therefore, will be accompanied with the evolution of hydrogen. Due to the base reducing property of manganese the deposited metal tends to react with aqueous electrolyte with the evolution of hydrogen. In practice, this reaction is slow[23] probably on account of the large hydrogen overpotential of the metal. The affinity to evolve hydrogen is measured by the difference between the

potentials of the cathode and the potential relating to line (a) in Figure (2). The affinity and, consequently, the rate of hydrogen evolution will be larger the smaller is the pH of the solution, all other conditions remaining constant. The current efficiency will therefore, be improved with the increase in the cathodic pH. However, this pH cannot exceed a certain limit beyond which the manganese may get precipitated as $Mn(OH)_2$. The best conditions of yield and metal purity (free from oxide) will be obtained at cathodic pH slightly below that for manganese hydroxide formation, i.e. for 1.0 M solution of manganese the predicted pH is 7.4. This value is in agreement with the results of Jacobs et al[24], who obtained a current efficiency of 65% and 62.7% for solutions of pH 7.2 containing approximately 14 and 32.37 g Mn/l.

It has been observed that as the electrolysis proceeds the cathodic pH decreases, probably due to the diffusion of acid from the anolyte compartment. Thus it is necessary to buffer the electrolyte using ammonium salts.

The only process in operation for an electrolytic production of manganese is that developed by U.S. Bureau of Mines and Electro Manganese Corporation, Knoxville, Tennessee. It has been described in a number of publications, issued by the Bureau.

The study of the literature on electrowinning manganese reveal that the essential constituents of the electro-

lyte are as follows:

1. Reasonable concentration of manganese in the catholyte (optimum concentration being approximately 12 g/l)
2. Substantial amount of ammonium salts to keep the solution properly buffered (about 100-140 g/l ammonium sulphate)
3. A sulphur compound capable of being reduced at the cathode (0.05 - 0.1 g/l SO_2 has been found to be adequate).

The electrolysis of manganese is carried out in a compartment cell. The first cell used by Bureau of Mines was developed by Jacobs and Yarroll[25] and was a compartment cell in which the cathodes were freely suspended in the catholyte compartments while each of the anodes was surrounded by a canvas diaphragm.

Several types of lead anodes alloyed with tin, cobalt, silver, antimony, arsenic etc. were suggested. The essential features of a successful anode is the formation of a porous, adherent and self-limiting coating, i.e. a coating that remains porous and adherent until a thickness capable of reducing further manganese dioxide formation is reached.

A variety of materials have been tried for cathode. Stainless steel cathodes have proved by far the most satisfactory. The other cathode materials worth mentioning are Cr, Ni and Mo alloyed with iron. Carosella[26] used Haste-

alloy cathods.

The process currently in operation at Knoxville is based upon more than a dozen United States and foreign patents. The data on the production of electrolytic manganese are given in Table III.

Table III

Data on Production of Electrolytic Mn by Electro Manganese Corporation

Anolyte	
Mn g/l as $MnSO_4$	10-18
H_2SO_4 g/l	25-35
$(NH_4)_2SO_4$ g/l	120-140
pH	1-1.4
Catholyte feed:	
Mn g/l as $MnSO_4$	25-35
$(NH_4)_2SO_4$ g/l	125-135
pH	7.2-7.6
Anodes comp.	Lead loose with Sn, Sb and Co.
Cathode comp.	Stainless steel 18% Cr, 12% Ni, 25% Mo
Temp. °C	35-40
Cathode C.D.amp/sq.ft.	40
Diaphragm	woven textile
Cell voltage	5
Current efficiency	65-70
Purity of Mn%	99.97

THERMODYNAMIC CONSIDERATIONS

All spontaneous processes are accompanied by a decrease in the free energy of the system; at equilibrium the free energy must therefore be a minimum. It follows, also, that a reaction cannot proceed spontaneously if the accompanying free energy change is positive. However, a negative value of free energy change does not necessarily mean that a reaction will proceed at a measurable rate under a given set of conditions, but indicates only that the reaction is thermodynamically possible. Whether or not the reaction will proceed to equilibrium at an appreciable rate depends on the kinetics of the reaction.

Considering a reaction between a pure solid metal M and gaseous oxygen to form the pure solid oxide MO:

$$2M_{(s)} + O_{2(g)} \rightleftharpoons 2MO_{(s)} \tag{38}$$

the change in the Gibbs free energy, for the reaction (ΔG) at constant temperature and pressure, is given by:

$$(\Delta G) = 2\Delta G_{MO} - 2\Delta G_{M} - \Delta G_{O_2} \tag{39}$$

For the reaction where all the components are in their standard states the free energy change is given by:

$$(\Delta G^\circ) = 2\Delta G^\circ_{MO} - 2\Delta G^\circ_{M} - \Delta G^\circ_{O_2} \tag{39a}$$

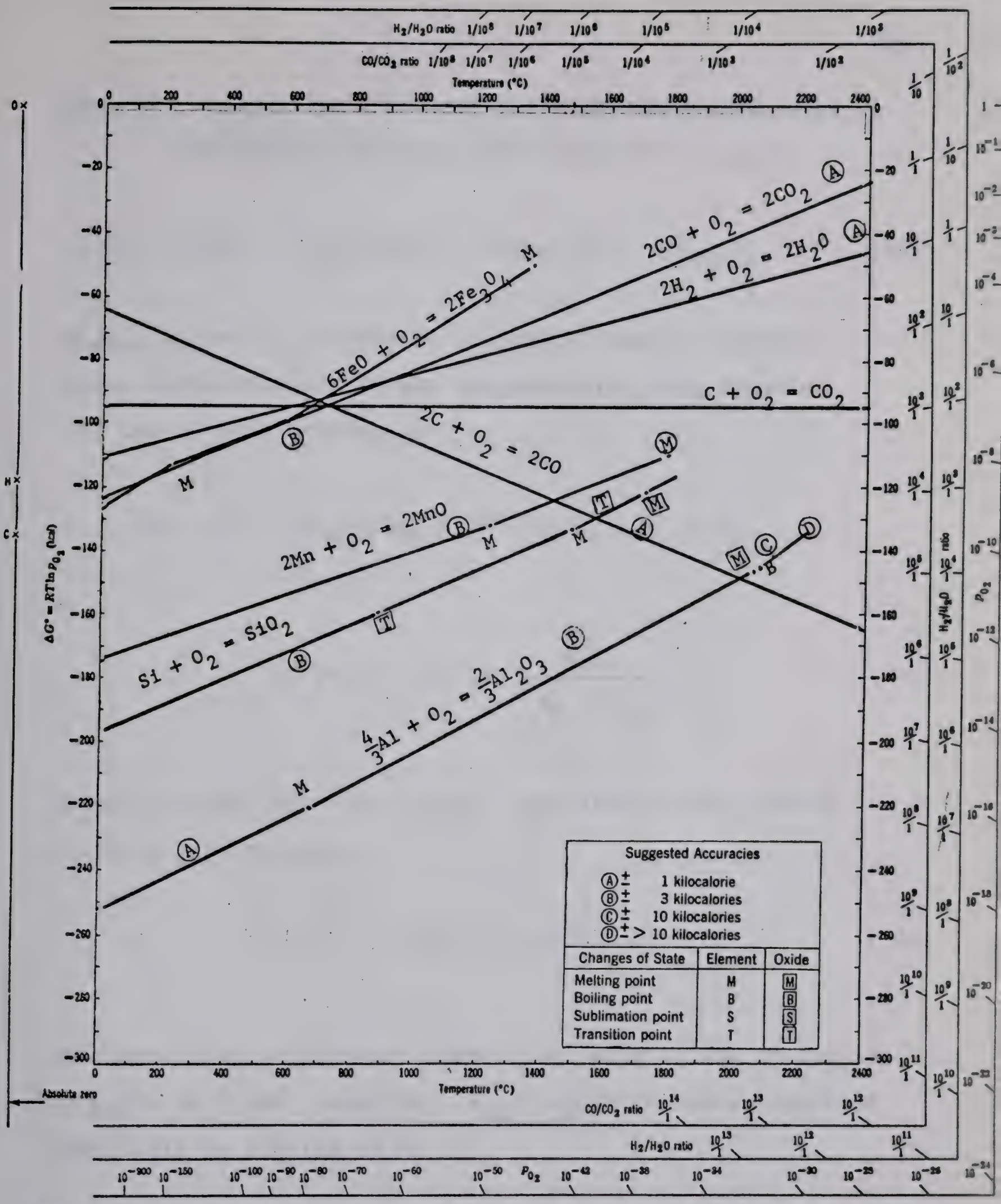

Fig. 3 Standard free energy of formation of oxides as a function of temperature. From F. D. Richardson and J. H. E. Jeffes, *J. Iron Steel Inst.*, 160, 261 (1948). Modified by L. S. Darken and R. W. Gurry, *Physical Chemistry of Metals*, McGraw-Hill, New York, 1953.

where the superscript (°) denotes the standard free energy.

Subtracting equation (39a) from (39), we get:

$$(\Delta G) - (\Delta G^\circ) = 2\Delta(G_{MO} - G^\circ_{MO}) - 2\Delta(G_M - G^\circ_M) - \Delta(G_{O_2} - G^\circ_{O_2}) \qquad (40)$$

If a_{MO}, a_M and a_{O_2} represent the activities of the metal oxide, pure metal and oxygen respectively, then equation (40) can also be written as:

$$\Delta G - \Delta G^\circ = 2RT \ln a_{MO} - 2RT \ln a_M - RT \ln a_{O_2}$$

or

$$\Delta G = \Delta G^\circ + RT \ln \left[\frac{a^2_{MO}}{a^2_M \cdot a_{O_2}}\right] . \qquad (40a)$$

At equilibrium $(\Delta G) = 0$. Hence, the standard free energy charge of the reaction

$$(\Delta G^\circ) = -RT \ln \left[\frac{a^2_{MO}}{a^2_M \cdot a_{O_2}}\right] \qquad (40b)$$

For substances at standard state, i.e. pure solids or liquids, or gases at 1 atm. pressure, $a_{MO} = a_M = 1$. Hence, equation (40b) will be simplified to

$$\Delta G^\circ_2 - RT \ln 1/a_{O_2} = RT \ln a_{O_2} = RT \ln p_{O_2} \qquad (40c)$$

line for the formation of an oxide (in the diagram), the greater the stability of oxide. Hence a pure element is able to reduce the oxide of any other element whose ΔG° curve lies higher on the diagram. For example, Si and Al curves lie below that of Mn-MnO reaction, so MnO will be reduced to metal by Al and Si, where as carbon reacts with MnO to form metal and carbon monoxide only at temperatures well above the melting point of manganese.

The hydrogen reduction equilibria of the manganese oxides, however, would involve the following steps:

$$2MnO_2(c) + H_2(g) = Mn_2O_3(c) + H_2O(g) \quad (42)$$

$$3Mn_2O_3(c) + H_2(g) = 2Mn_3O_4(c) + H_2O(g) \quad (43)$$

$$Mn_3O_4(c) + H_2(g) = 3MnO(c) + H_2O(g) \quad (44)$$

and $$MnO(c) + H_2(g) = Mn(c) + H_2O(g) \quad (45)$$

The free energies of formation for the reactions (42) to (45) are given in table IV[29].

Table IV

Free Energy of Formation ΔG°(k.cal/mole) for the Reactions 42 to 45

	Free Energy ΔG° at		
Reaction	298.15°K	800°K	1000°K
42	-41.85	-48.55	-50.90
43	-36.90	-39.35	-39.85
44	- 8.95	-19.10	-22.80
45	+32.1	+29.45	+28.60

The reduction of manganese oxides with carbon involves the following equilibria:

$$2MnO_2(c) + C\ (graphite) = Mn_2O_3(c) + CO(g) \quad (46)$$

$$4MnO_2(c) + C\ (graphite) = 2Mn_2O_3 + CO_2(g) \quad (47)$$

$$3Mn_2O_3(c) + C\ (graphite) = 2Mn_3O_4(c) + CO(g) \quad (48)$$

and $$6Mn_2O_3(c) + C\ (graphite) = 4Mn_3O_4(c) + CO_2(g) \quad (49)$$

$$Mn_3O_4(c) + C\ (graphite) = 3MnO(c) + CO(g) \quad (50)$$

and $$2Mn_3O_4(c) + C\ (graphite) = 6MnO(c) + CO_2(g) \quad (51)$$

$$MnO(c) + C\ (graphite) = Mn(c) + CO(g) \quad (52)$$

$$2MnO(c) + C\ (graphite) = 2Mn(c) + CO_2(g) \quad (53)$$

The thermodynamic data for the carbon reduction equilibria are given in Table V.

Table V.

Free Energies of Formation $\Delta G°$ (in °K.cal/mole) for the Reactions 46 to 53

	Free Energy $\Delta G°$ at		
Reaction	298.15°K	800°K	1000°K
46	-20.0	-43.55	-52.8
47	-68.7	-94.25	-104.3
48	-15.05	-34.4	-41.75
49	-58.75	-75.95	-82.2
50	+12.85	-14.1	-24.65
51	-2.90	-35.4	-48.0
52	+53.9	+34.4	+26.7
53	-79.2	-61.65	+54.7

The equilibrium reactions for the reduction of manganese oxides by carbon monoxide are:

$$2MnO_2(c) + CO(g) = Mn_2O_3(c) + CO_2(g) \quad (54)$$

$$3Mn_2O_3(c) + CO(g) = 2Mn_3O_4(c) + CO_2(g) \quad (55)$$

$$Mn_3O_4(c) + CO(g) = 3MnO(c) + CO_2(g) \quad (56)$$

$$MnO(c) + CO(g) = Mn(c) + CO_2(g) \quad (57)$$

The thermodynamic data for the free energy of formation, for the reactions at different temperatures are given in the Table VI.

Table VI

Free Energy of the Reactions (54) to (57)
G° (in K.cal/mole)

	Free Energy G° at		
Reaction	298.15°K	800°K	1000°K
54	-48.65	-50.70	-51.50
55	-43.70	-41.55	-40.45
56	-15.75	-21.30	-23.35
57	+25.30	+27.25	+28.00

Thermodynamic considerations indicate that the direct reduction of manganese oxides to the metallic manganese is not feasible with hydrogen, carbon monoxide and carbon at ordinary conditions, temperature above 1430°C as can be seen from the free energy diagram (Figure 3). It is therefore essential to investigate an alternate process capable of reducing Mn(II) to Mn according to equation 1.

EXPERIMENTAL

A. Description of Ore

In order to understand the leaching characteristics and to design a chemical process suitable for the ore it is essential to study the origin and mineralogy of the ore deposit.

The iron-manganese ore deposit at Woodstock, New Brunswick, was discovered in 1836 by Dr. C.T. Jackson. To date six ore bodies have been outlined in the area, estimated to contain approximately 194,000,000 tons of ore averaging 9% manganese[1]. The ore is of two types: oxide and carbonate, occurring roughly in three groups. Group 1 includes grey-green slates and sandstone. The rocks of group 2 are grey and red slates and those of group 3 are contorted calcarious slates.

The iron and manganese minerals have been deposited within five distinct conformable units namely: silicified slates, manganiferous hematite, red to purplish ferruginous slates, green chlorite slates, and brown cherty slates. Of the five units, the silicified slates and manganiferous hematite contain the bulk of iron and manganese. An idealized section would show the following sequence: dark-grey slates (foot wall), chlorite slates, silicified slates, and grey calcarious banded slates (hanging wall). The brown

cherty slates may occur anywhere within the sequence but generally occur with the silicified slates.

The red ferruginous slates thus far have been found to be present with either manganiferous hematite or silicified slates or with both.

The manganiferous hematite, the highest grade unit is dark-red to black, finely banded rock with, occasionally, alternating red and black or dark-red laminae. It has a blocky fracture and is frequently replaced with quartz. The unit is also cut by narrow quartz stringers and by veinlets of pink granular rhodochrosite and quartz which occasionally carry minute specks of chalcopyrite, galena, and sphalerite. Pyrite is a more prominent sulphide and is found particularly near the base of the unit.

The manganese minerals in the manganiferous hematite are too finely divided to be identified. The manganiferous hematite has a specific gravity of 3.8 and contains up to 45 per cent combined metal with iron and manganese in the ratio of 5 to 4, although occasionally this ratio may be reversed. It occurs both in the form of definite beds in widths up to 100 feet and as narrow lenses (up to 5 feet in depth) in the red ferruginous slates.

Table VII gives maximum, minimum and estimated average, iron and manganese contents in each of the five units as determined from the drill core analyses.

Table VII

Analysis of the Ore from Each of the Five Zones

Unit	Iron %			Manganese %		
	Min	Max	Est.Av.	Min	Max	Est.Av.
Manganiferous hem.	11	30	22	12	25	14-16
Silicified slates	10	25	16	9	20	12-14
Red Ferrug. slates	5	9	6	1	6	2-3
Green slates	3	11	7	2	7	4
Brown cherty slates	2	12	8	2	9	6

The six known deposits are: Plymouth, North Hartford, South Hartford, Moody Hill, Iron Ore Hill, Sharpe Farm.

The complexity of the ore can be visualized from the photomicrographs in Figures 4 and 5. The ore is moderately coarse grained showing white magnetite, grey quartz, dark grey calcity or chlorite, black manganiferous hematite and black crystalline pyrolusite. Petrographic analysis shows that rhodochrosite and pyrolusite crystals are randomly present. The gangue minerals detected are chlorite, calcite, dolomite, feldspar, fine crystalline pyrite, and quartz. The quartz is present as stringers cutting the veinlets of rhodochrosite and banded manganiferous hematite.

X-ray diffraction indicated that the main manganese mineral is braunite [$3(Mn,Fe)_2O_3.MnSiO_3$].[1] The chemical analy-

(4) Rhodochrosite and pyrolusite in chloritic and carbonacious gangue x 600

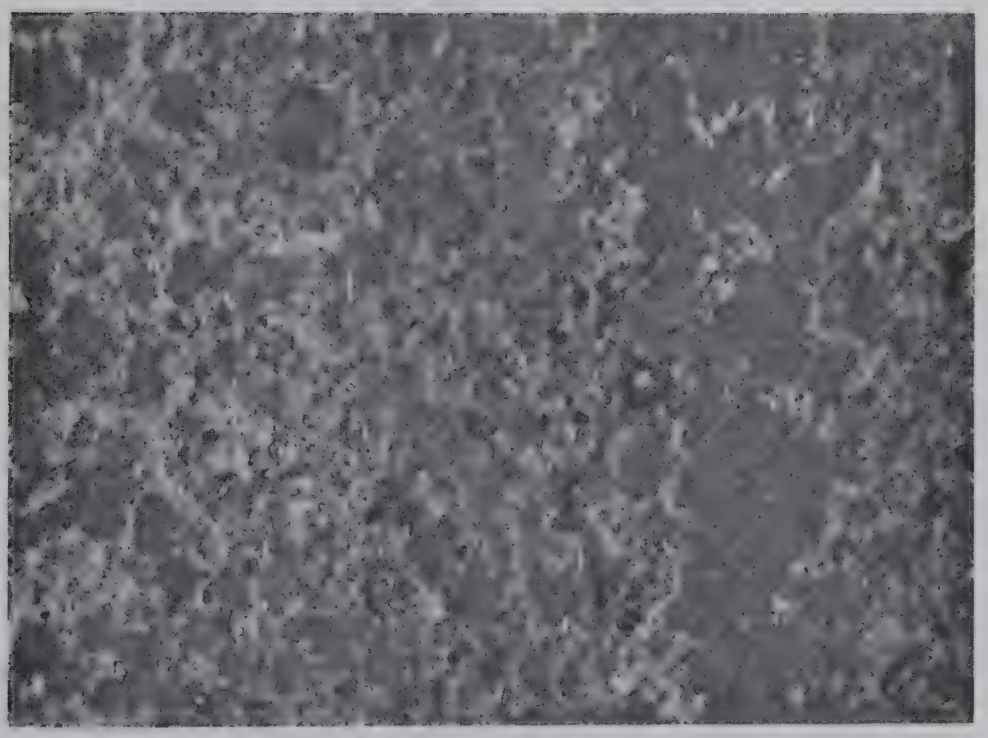

(5) Manganiferous hematite with pyrolusite crystals and quartz lenses x 600

sis of the ore sample received for the investigation is given in table VIII.

The ore sample contained 2-3 per cent pyrolusite, estimated by decomposing the ore with concentrated hydrochloric acid and determining the amount of chlorine evolved.

Table VIII

Analysis of Ore

Mn	12.4	Percent
Fe	14.2	"
SiO_2	32.25	"
Al_2O_3	9.28	"
CaO	3.12	"
MgO	10.65	"
TiO_2	0.18	"
Na_2O	1.00	"
K_2O	1.37	"
P_2O_5	1.24	"
S	0.10	"
Loss on ignition	11.7	"
CO_2	5.7	"

B. Reagents

Sulphuric acid. 95-98 per cent analytical reagent grade from Fisher Scientific Company.

Di(2-ethylhexyl)-phosphoric acid. The (D2EHPA) used in the

investigation was supplied by the Virginia-Carolina Chemical Company, Virginia, U.S.A. The reagent was purified from the monoalkyl derivatives by scrubbing with 5% sodium carbonate. The organic phase was separated from the aqueous phase and neutralized with sulphuric acid. The purity of the product was determined by potentiometric titration and was found to be 99.4%.

Table IX

Physical Properties of Purified D2EHPA

Experimental equivalent weight	319.8
Density 23°C (g/ml)	0.968
Viscosity (centipoises)	4.14
Refractive Index 22°C	1.4459

The molecular weight of D2EHPA in benzene was determined by the cryoscopic method. The following results were obtained

Molar depression of temperature with 0.18 M solution of D2EHPA in benzene,	T = 0.468°C
Cryoscopic constant of benzene	K = 4.9
Molecular weight of D2EHPA determined	= 628
Theoretical dimeric M.W	= 645

Dissociation Constant

The determination of the dissociation constant was carried out by polarmetric titration of the saturated solution of D2EHPA in conductivity water. The pK value was calculated from the pH of half-neutralization by the formula due to Dyrssen[27]:

$$pK = pH + \log[HL] - \log[L^-]$$

$$pK = 2.8 \pm 0.1$$

Formamide, kerosene, and ammonium chloride were analytical reagent grade as received from Fischer Scientific company.

Hydrochloric acid. 36-38% HCl, analytical reagent grade as received from Fischer Scientific Company.

C. Leaching Procedure

Pulverized ore samples 20 gram each of the sizes ranging between -20 to -200 mesh were leached with dilute sulphuric acid in a round bottom flask fitted with a reflux condenser. The leaching tests are carried out at temperatures ranging between 25 and 98°C for a time of 10 to 120 minutes. The pulp is vacuum filtered and washed with water. The leach liquor was analysed for Mn and Fe by an x-ray fluorescence scintillation counter or colorimetrically by Perkin Elmer

spectrophotometer Model 450. Free acid content was determined by potentiometric titration with 0.1 NaOH.

pH was controlled by a Beckman Zeromatic pH meter. The conductivity of solutions was measured using Radiometer conductivity meter type CD M2.

D. Solvent Extraction

The distribution ratio (D) was determined by equilibrating 25-50 ml of organic phase (solution of D2EHPA in kerosene) with solution of manganese leach liquor in a separatory funnel, maintaining a constant temperature in a thermostat, adjusting pH with NaOH. The equilibrated phases were analysed for Mn by measuring counts per second with Norelco x-ray fluorescence counter. The distribution is defined as

$$D = \frac{\text{counts per second per ml of organic phase}}{\text{count per second per ml of aqueous phase}} \qquad (37)$$

Viscosity measurements were made by Ostwald viscometers.

E. Equipment for Electrolysis

The apparatus for the electrodeposition of manganese is illustrated in Figure (26). The direct current is supplied by a Sorensen Model 560 BB, with an output of 0-500 volts and the current can be varied from 10 to 300 m. amps. The electrolysis is done in an H-type cell with a fritted-

glass diaphragm.

The anode was a spectrograde graphite rod while the cathode was a 18% Cr, 8% Ni stainless steel. The amount of current passed was determined using a copper coulometer in series with the cell. The applied voltage was controlled manually.

Infrared spectra of the samples were obtained using Perkin-Elmer spectrophotometer Model 521. The samples for the infrared study were prepared as liquid film of the pure compound or diluted with nujol mull; KBr pellets were made for the solid compounds.

RESULTS AND DISCUSSION

A. Leaching

1. Effect of Particle Size. This series of experiments was designed to determine the optimum particle size of the ore, so as to avoid overgrinding and at the same time to obtain maximum leaching efficiency. The size fractions from -20 to -200 mesh were subjected to the lixiviation with sulphuric acid. The acid/ore and solid/liquid ratios in all the tests were arbitrarily fixed at 1:2. The leaching was carried out with constant stirring for a period of 1 hour at 97± 2°C. The results of the tests are summarized in Table X.

The variations of the manganese and iron dissolution with the particle size are graphed in Figure 6. It is seen that the amounts of manganese and iron in solution increase as the particle size decreases, reaching their respective maxima of approximately 92% Mn and approximately 6% Fe extraction at particle size around 65 mesh. It was noted that at particle size smaller than 48-mesh separation of solids by filtration became more difficult. The optimum particle size appears therefore to be approximately 65 mesh.

The acid consumption also increases with the decreasing particle size. The amount of free H_2SO_4 in the leach liquor is quite high, and it is essential to neutralize it before subjecting the solution to further processing. The

Table X

Effect of Particle Size

H_2SO_4 = 250 g/l

Solid:Liquid = 1:2

Temp = 92-95°

Time = 1 hr

	Leach Liq. Analysis g/l			% Extn.		Acid used %	
Mesh	Mn	Fe	free acid	Mn	Fe		Remarks
-20 + 30	42.4	2.74	79.40	68.4	3.85	68.3	
-30 + 48	48.3	3.12	75.58	77.9	4.40	69.6	
-48 + 65	54.3	3.41	72.86	87.5	4.80	71.0	
-65 + 80	55.4	3.84	70.00	91.3	5.40	72.0	
80 +100	56.6	4.30	67.75	93.2	6.05	72.9	Pulp became
-100+150	58.5	4.34	66.28	94.4	6.10	73.5	slimy and
-150+200	59.0	4.36	65.60	95.2	6.15	73.9	difficult to
-200	59.3	4.36	65.35	95.6	6.15	74.0	filter

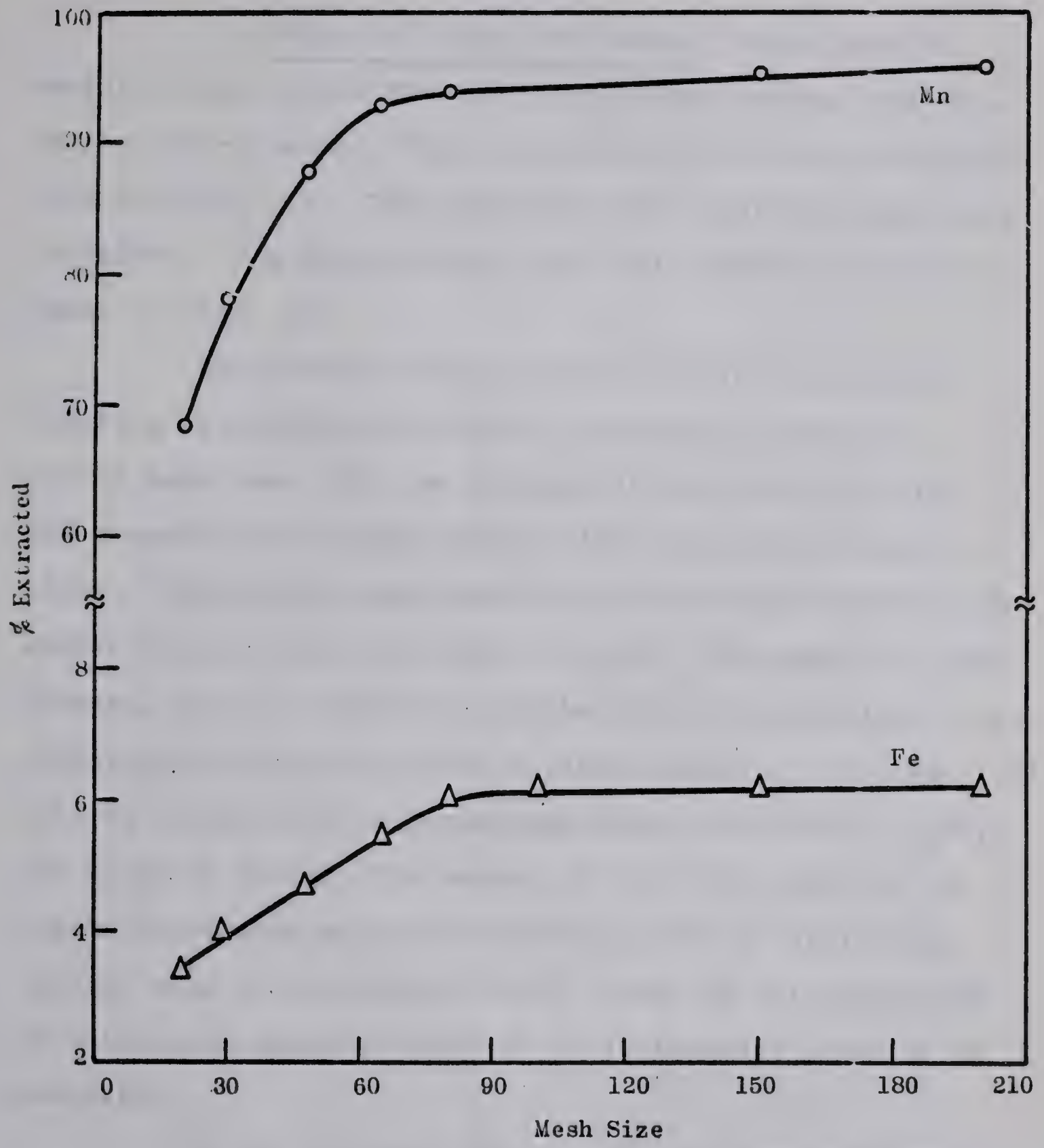

Fig. 6 Effect of particle size on the extraction of manganese and iron.

next problem therefore, is to ascertain the amount of sulphuric acid required to leach the ore sample.

2. Effect of H_2SO_4/Ore Ratio. Based upon the particle size established in the previous series, the size chosen was -65 mesh. The initial acid/ore ratio was varied from 0.2:1 to 1:1. The remaining test conditions were held as before. The data obtained from this series of tests are shown in Table XI.

The effect of the acid concentration on the extraction of manganese and iron is plotted in Figure 7. It can be seen that with the increase in the acid/ore ratio the dissolution of manganese at first increases rather rapidly. It reaches a maximum representing approximately 94% extraction at H_2SO_4/ore ratio of 0.6:1. The amount of iron, however, goes on increasing in the H_2SO_4 concentration range studied. For example, at an acid/ore ratio of 1:1 about 7.5% iron is leached out in comparison with 4.5% iron for H_2SO_4/ore ratio of 0.4:1. The amount of free H_2SO_4 left in the leach liquor also goes on increasing with the increasing initial acid concentration ratio. From the data tabulated in Table X an acid/ore ratio of 0.2:1 to 0.4:1 seems to be adequate.

It was observed that beyond the above mentioned concentration range the leaching pulp becomes slimy and difficult to filter.

TABLE XI

Effect of acid concentration.

Ore = 20 g

Solid to Liquid = 1:2

Temperature = 90-94°

Time = 1 hr

ACID TO ORE RATIO	H_2SO_4 g/1	LEACH LIQUOR ANAL. g/1			%EXTRACTION		% H_2SO_4 USED	REMARKS
		Mn	Fe	H_2SO_4	Mn	Fe		
0.2:1	100	42.6	2.74	7.5	68.7	3.85	92.5	
0.4:1	200	55.4	3.41	32.0	89.3	4.80	84.0	
0.5:1	250	58.8	3.69	76.8	94.8	5.20	69.2	
0.6:1	300	59.7	4.29	125.0	96.2	6.04	55.0	
0.8:1	400	60.1	4.86	227.2	97.0	6.85	43.2	
1:1	500	60.5	5.54	32].6	97.6	7.80	35.7	

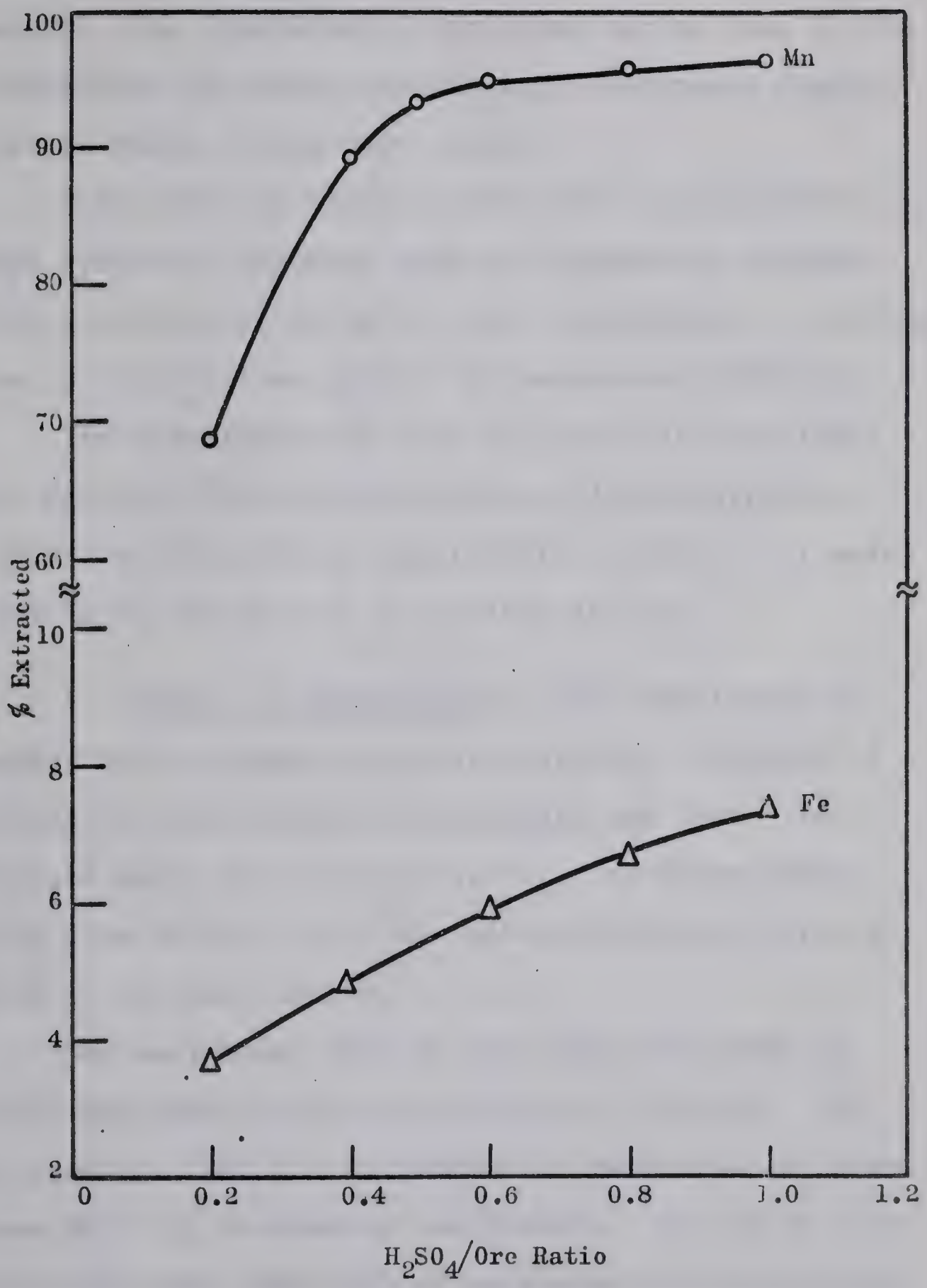

Fig. 7 Effect of acid/ore ratio on the extraction of manganese and iron..

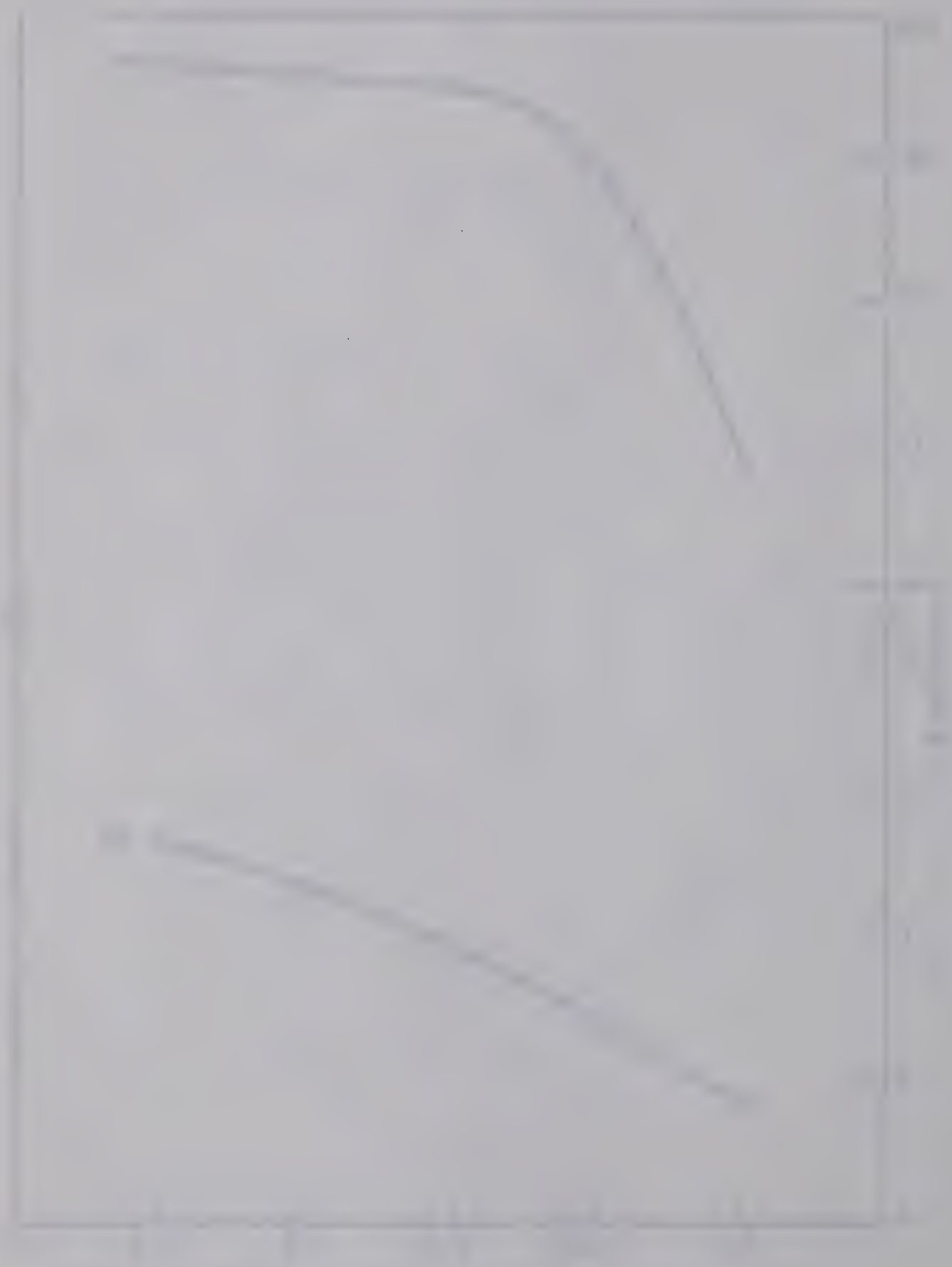

3. Effect of Liquid/Solid Ratio (Dilution). In this series the H_2SO_4 to ore ratio was chosen as 0.4:1 on the basis of the results obtained in the previous set of experiments. The liquid/solid ratio was varied from 1:1 to 4:1, maintaining the other experimental conditions almost identical to those in the last tests.

Table XII and Figure 8 show that the extraction of manganese gradually improves with the increasing dilution until the liquid/solid ratio of 2.5:1 is obtained. A further increase in the dilution lowers the manganese extraction.

The dissolution of iron on the other hand shows a steady decline with the decreasing acid concentration. About 9% Fe is extracted at liquid/solid ratio of 1:1 which decreases to as low as 1.4% at a ratio of 4:1.

4. Effect of Temperature. The experiments in this series were designed to investigate the influence of temperature on the leaching of manganese and iron. The liquid/solid ratio was fixed at 2.5:1. The temperature range was from 30-97°C while the other conditions were as specified in the last series.

The analytical data of the tests are given in Table XIII and graphically illustrated in Figure 9. The results indicate that the extraction of manganese and iron increases with the increasing temperature. It can be seen from the curve that about 92% of manganese is extracted at about 60°C. A further rise in temperature does not seem

TABLE XII

Effect of Liquid to Solid Ratio

Ore = 20 g

H_2SO_4 = 8 g

Size = -65+100 mesh

Temp. = 92±2 °C

Time = 1 hr

SOL. LIQ. RATIO W/V	H_2SO_4 g/l	LEACH LIQUOR ANAL. g/l			% EXTRACTION		% H_2SO_4 USED	REMARKS
		Mn	Fe	H_2SO_4	Mn	Fe		
1:1	400	98.7	9.70	39.5	79.6	6.8	90.0	
1:15	270	69.7	4.91	27.9	84.2	5.2	89.5	
1:2	200	55.8	3.08	20.2	90.0	4.5	89.9	
1:2.5	160	45.9	2.39	21.0	92.4	4.2	86.9	
1:3	133	37.7	1.84	12.3	91.3	3.9	90.8	
1:3.5	114	31.6	1.38	10.5	87.5	3.4	91.2	
1:4	100	25.2	1.05	15.7	81.4	2.9	84.3	

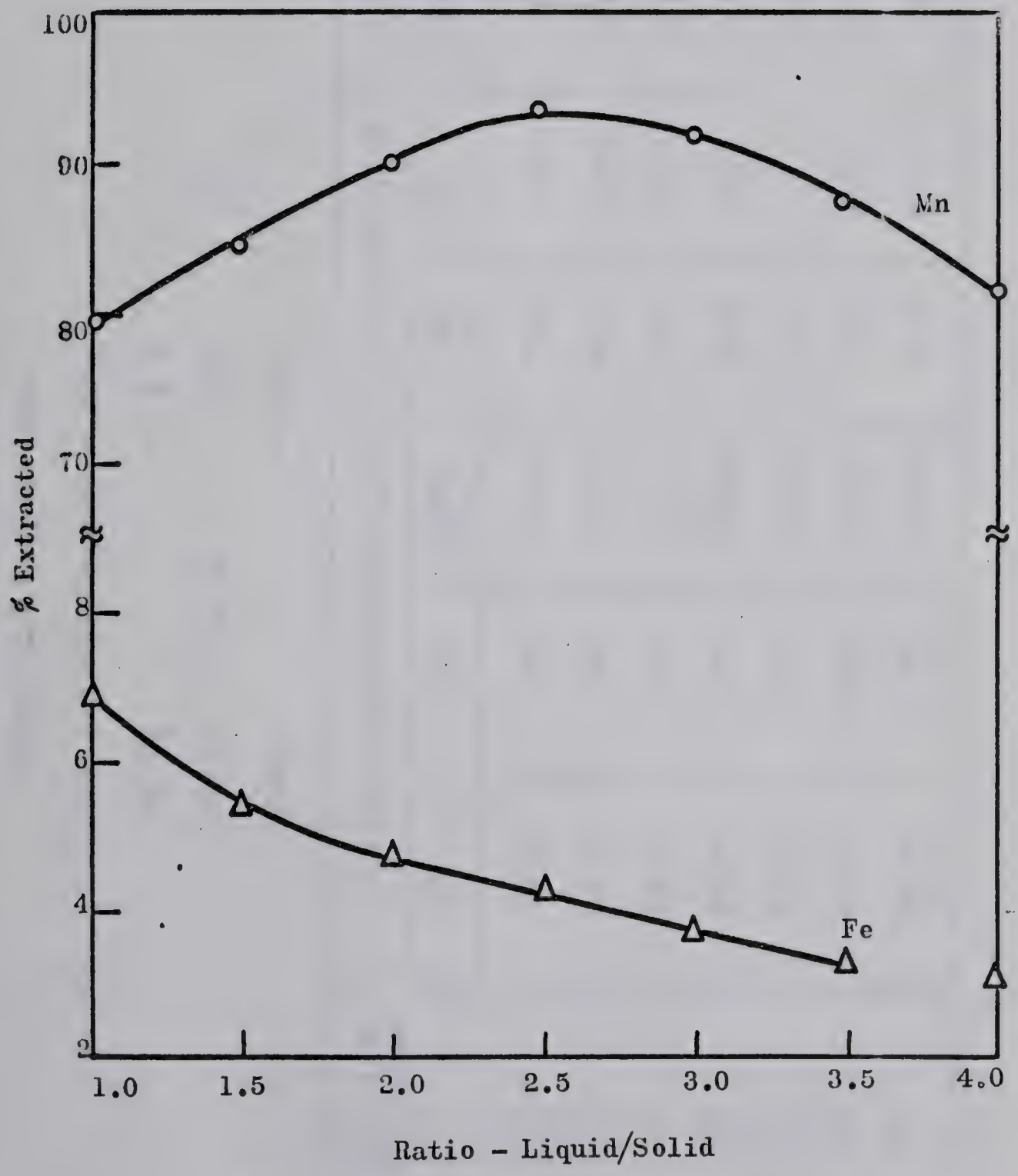

Fig. 8 Effect of liquid/solid ratio on the extraction of manganese and iron.

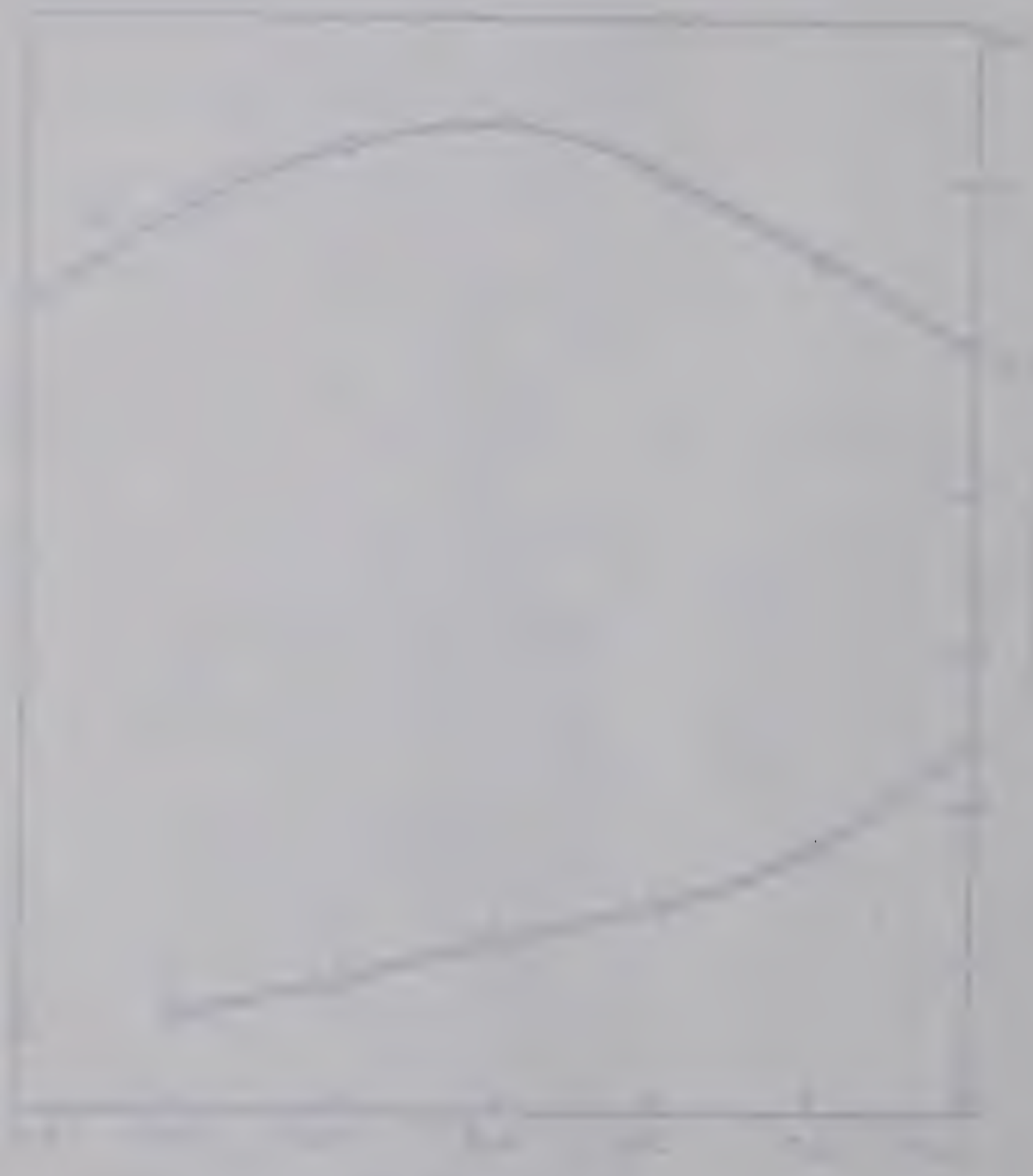

TABLE XIII

Effect of temperature.

Ore (-65+100 mesh) = 20 g

H_2SO_4 = 8 g

Solid : Liquid = 1.25

Time = 1 hr

EXTRACTION TEMPERATURE °C	LEACH LIQUOR ANAL. g/l			% EXTRACTION		% H_2SO_4 USED	REMARKS
	Mn	Fe	H_2SO_4	Mn	Fe		
25	36.2	1.65	26.00	72.5	2.90	83.9	
35	41.5	1.67	25.00	83.0	2.95	84.2	
56	44.7	1.70	23.75	89.5	3.00	85.2	
65	45.9	1.82	22.06	91.8	3.20	86.2	
71	46.0	1.87	21.18	92.0	3.30	86.8	
85	46.5	2.30	20.30	93.0	4.05	87.3	
96	46.8	2.44	18.95	93.6	4.30	88.2	

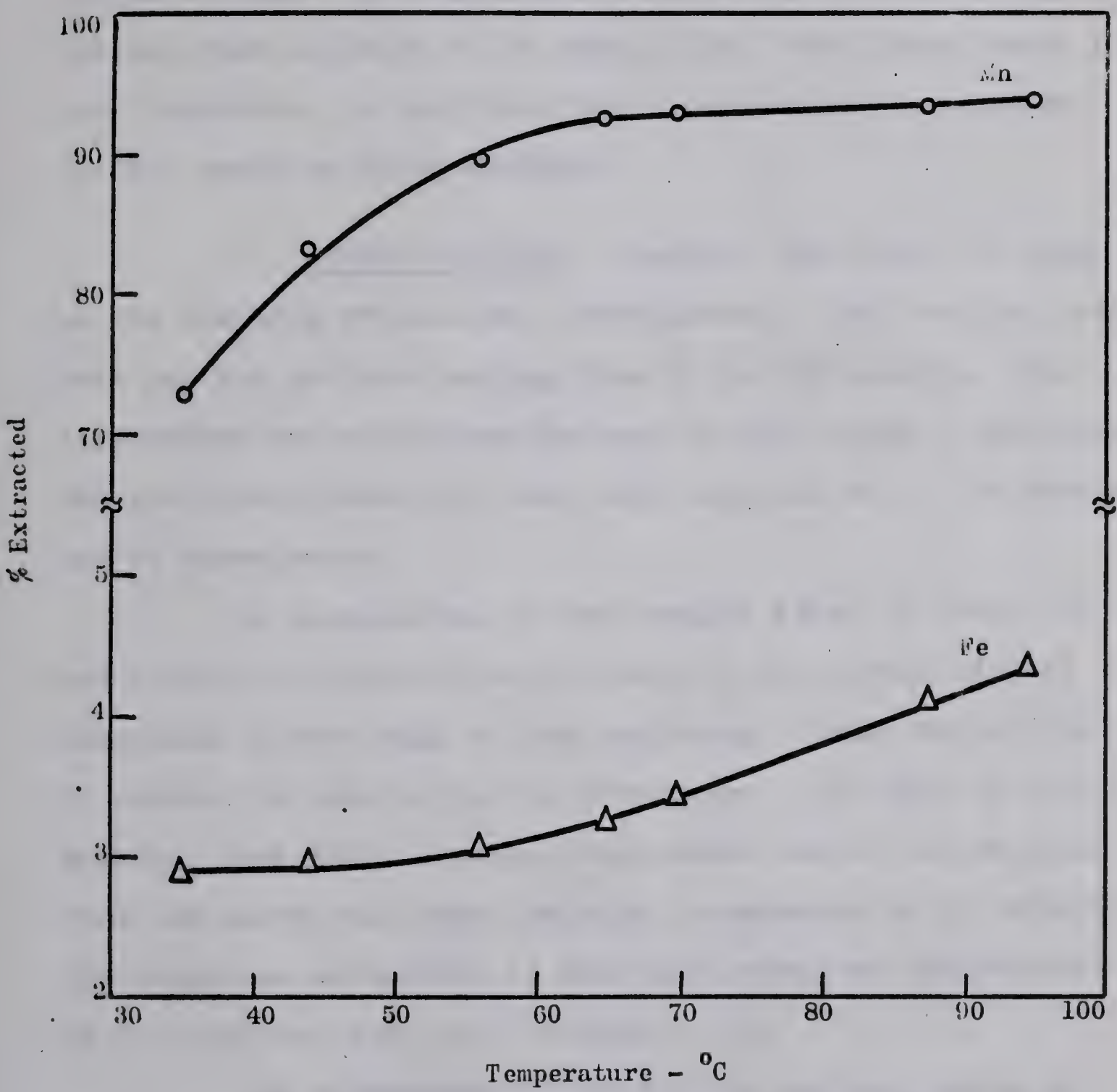

Fig. 9 Effect of temperature on the extraction of manganese and iron.

to have much beneficial effect.

The dissolution of iron on the other hand increases only slightly up to 60°C, when it is about 3% in the leach liquor. Further rise in temperature accelerates the dissolution of iron. Consequently, at 90°C the amount of iron in the solution is found to be about 4.5%. From these tests it can, therefore, be concluded that leaching process between 60-70°C would be quite adequate.

5. Effect of Time. Finally, the effect of time on the leaching process was investigated. The leaching tests were run for periods ranging from 10 to 120 minutes. The temperature was maintained between 60-65°C using a thermostat, and the other conditions were kept constant as in the previous set of experiments.

An examination of the results given in Table XIV and Figure 10 reveals that the rate of the dissolution of manganese is very high at the beginning. About 89% of the Mn content is leached out in 30 minutes. The rate of dissolution thereafter, becomes much lower and it can be seen from the curve that when leaching is extended to 120 minutes the manganese extraction is 94% which means an improvement of only 5% over that of a 30 minute run.

The extraction of iron on the contrary shows an unusual behaviour; at the beginning its amount in the leach liquor increases with time, reaches a maximum and then, it gradually decreases as the leaching process continues.

TABLE XIV

Effect of time.

Ore 20 g

H_2SO_4 8 g

Solid:Liquid 1:2.5

Temperature 93±2 °C

TIME IN MINUTES	LEACH LIQUOR ANAL. g/l			% EXTRACTION		% H_2SO_4 USED	REMARKS
	Mn	Fe	H_2SO_4	Mn	Fe		
10	30.4	2.86	35.9	60.9	5.05	77.6	
20	36.2	3.02	27.3	72.4	5.35	82.9	
30	44.4	2.97	23.8	88.7	5.25	85.2	
40	45.3	2.66	23.9	90.5	4.70	85.0	
60	46.4	1.81	21.0	92.6	3.20	86.9	
90	46.5	1.67	20.2	93.0	2.95	87.5	
120	46.8	1.59	19.6	93.5	2.82	87.7	

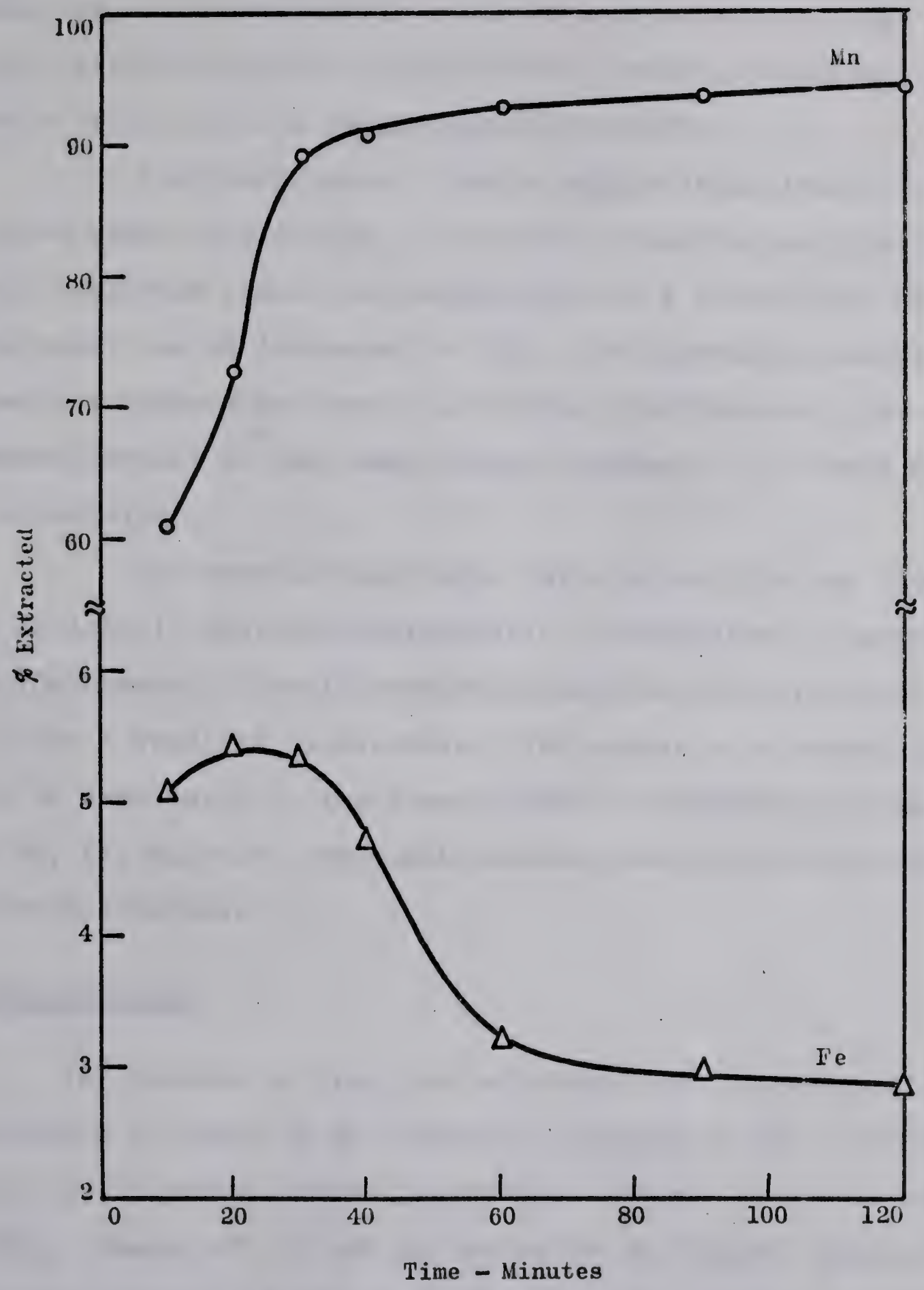

Fig. 10 Effect of time on the extraction of manganese and iron.

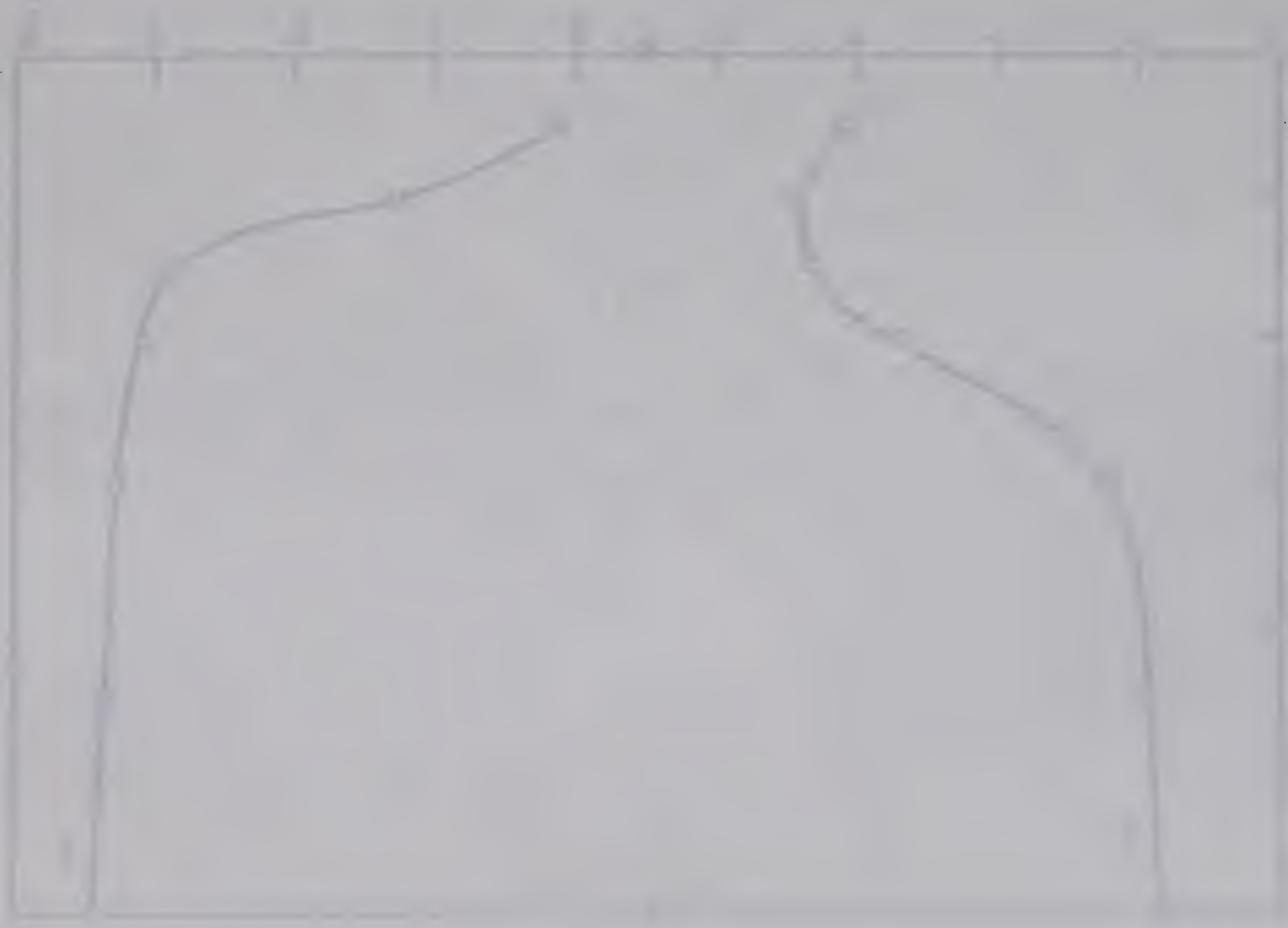

To summarize, about 92% of the manganese content and about 3.5% of the iron content are leached out when -65 mesh ore is lixiviated for about 40 minutes with dilute H_2SO_4 (at an acid/ore ratio of 0.4:1), with a liquid/solid ratio of 2.5:1, at a temperature of 60-65°C.

The final liquor after a single stage leach contained about 25 g/l H_2SO_4. In order to neutralize this free acid the leach liquor was contacted with a fresh batch of ore until the pH increased to 3.5. This operation reduced the iron content to about 1 g/l while simultaneously the manganese content of the leach liquor increased to as much as 1 mole/litre.

The experimental molar ratio of acid/Mn was found to be 1:1.51, whereas theoretically, the divalent manganese in the braunite should require an acid/Mn molar ratio of 1:1 for a complete dissolution. The excess acid consumption may be attributed to the dissolution of carbonates and oxides of Fe, Ca, Mg which eventually become precipitated and removed on filtration.

Side Reactions

The amounts of iron leached along with manganese are excessive and have to be removed or reduced to the ferrous-iron (Fe^{++}) before solvent extraction process can be undertaken, (since Fe^{++} is not extracted by the dialkyl phosphate). However, an examination of Figure 10 reveals that the amount

of Fe decreases over prolonged leaching periods. The explanation of this phenomenon is that the free acid is neutralized on prolonged contact with the ore, and this causes pH to rise to 3.5 in the final leach liquor; ferric hydroxide is thus precipitated and is subsequently removed by filtration. Oxidation of ferrous to ferric ion may be accomplished by oxygen diffusing from the atmosphere or by MnO_2 contained in the ore (in the amounts of up to 2.5%); the precipitation of Fe^{++} may take place according to the following reactions:

$$2Fe^{++} + 2H_2SO_4 + MnO_2 = 2Fe^{+++} + MnSO_4 + 2H_2O \qquad (58)$$

$$2Fe^{+++} + H_2O + 3/2\ O_2 = 2FeO.(OH) \qquad (59)$$

$$FeO.(OH) + H_2SO_4 = Fe(OH)SO_4 + H_2O \qquad (60)$$

After removal of precipitated iron the leach liquor contains varying amounts of other impurities. Analysis of a typical leach liquor is given in Table XV.

Table XV

Analysis of Leach Liquor

	g/l
Mn	45.3
Fe	3.8
Al_2O_3	0.38
CaO	0.04
MgO	0.18
P_2O_5	0.21
SiO_2	7.4

Mn was selectively extracted by solvent extraction with di-2 ethylhexyl phosphoric acid D2EHPA in kerosene.

B. Solvent Extraction

1. Chemistry of Extraction. Kimura[30] and Peppard[31] have indicated qualitatively that manganese can be extracted from HCl solutions into alkyl phosphates even when present in trace amounts. Since they dealt with trace concentrations rather than macro-quantities, the direct evaluation of the solvent extraction potentiality for a large scale process has not been worked out. According to Brown[32], dialkyl phosphoric acids are very weak extractants for Al, Ca, Mg, Zn, Cr(III), Fe(II), Mn(II), Cu, Ni, Tl and other

tetravalent metals. The present work contradicts this generalization of Brown and shows that manganese can be quantitatively and selectively extracted by di-(2-ethyl hexyl)-phosphoric acid (D2EHPA) at a pH range of 5-6.

The extraction of a cation M of charge x by di-(2-ethyl hexyl) -phosphoric acid denoted as HL has been described to take place according to the following mechanism:

$$M^{+x}_{(a)} + xHL_{(o)} = MLx_{(o)} + xH^{+}_{(a)} \qquad (61)$$

provided the aqueous cationic concentration is low (subscripts (a) and (o) denote aqueous and oil phases, respectively). Since the acid is found to dimeric in many organic solvents[33,34] (dimerization constant Kd in benzene = 2.9±0.14, in CCl_4 = 1.98±0.11)[35], the extraction reaction could be written as:

$$M^{x}_{(a)} + \frac{x}{2}(HL)_{2(o)} = ML_{x(o)} + xH^{+}_{(a)} \qquad (62)$$

Applying the law of mass action to the reaction (49)

$$K_e = [(ML)_x]\ [H^+]^x\ [HL]^{-x}\ [M^x]^{-1} \qquad (63)$$

Considering the above as general extraction reaction, we may write for manganese, omitting for simplicity the subscripts and valencies:

$$Mn + (HL)_2 = MnL_2 + 2H \tag{64}$$

and $$K_e = [MnL_2]\ [H]^2\ [Mn]^{-1}\ \ [(HL)_2]^{-1} \tag{65}$$

The extraction process is characterized by a distribution coefficient D, i.e.,

$$D = \frac{C^o_{Mn}}{C_{Mn}} \tag{66}$$

Where C^o_{Mn} and C_{Mn} are the quantities of manganese in organic and aqueous phases, respectively. Assuming that the phases are completely immiscible and the organic phase contains only $[MnL_2]_o$ as shown in equation (65), then the distribution ratio will be given by

$$D = [MnL_2]_o\ [Mn^{++}]^{-1}_{(a)} \tag{67}$$

From equation (65) and (67)

$$K_e = D\ [H]^2\ [(HL_2)]^{2/2} \tag{68}$$

or $$D = K_e\ \frac{[HL]^2}{[H]^2} \tag{69}$$

taking logarithm

$$\log D = 2[-\log[H] + \log(HL)] \tag{70}$$

or $$\log D = 2(pH + \log [HI]) \quad (71)$$

A plot of log D as a function of pH + log[HL] should give a straight line with a slope 2. This slope indicates the number of ligand molecules attached to the extracted cation. If the cation concentration in the aqueous phase is very small compared to the ligand, the change in the hydrogen ion concentration in aqueous phase could be neglected, consequently, the equation (69) simplifies to:

$$D = K_e[(HL)_2]^{2/2} = K_e[HL]^2 \quad (72)$$

Thus for low cation concentrations a plot of log D vs log [HL] should give a straight line with a slope 2.

2. Effect of pH on the Distribution Ratio. Equal volumes of 0.5 M D2EHPA were equilibrated with 0.20 M $MnSO_4$ solution at different pH (1.8-6) at 25±1°C. Figure 11 represents the extraction isotherm as a linear function of pH up to pH 4.95; above this pH the isotherm departs from linearity. At pH 5 a distribution ratio of 3.98×10^2 is obtained. This complete extraction around pH 5 coincides with the pH range in which manganese hydroxide is precipitated; therefore, the suggested mechanism is represented as follows:

$$Mn^{++} + 2\bar{O}H = Mn(OH)_2 \quad (73)$$

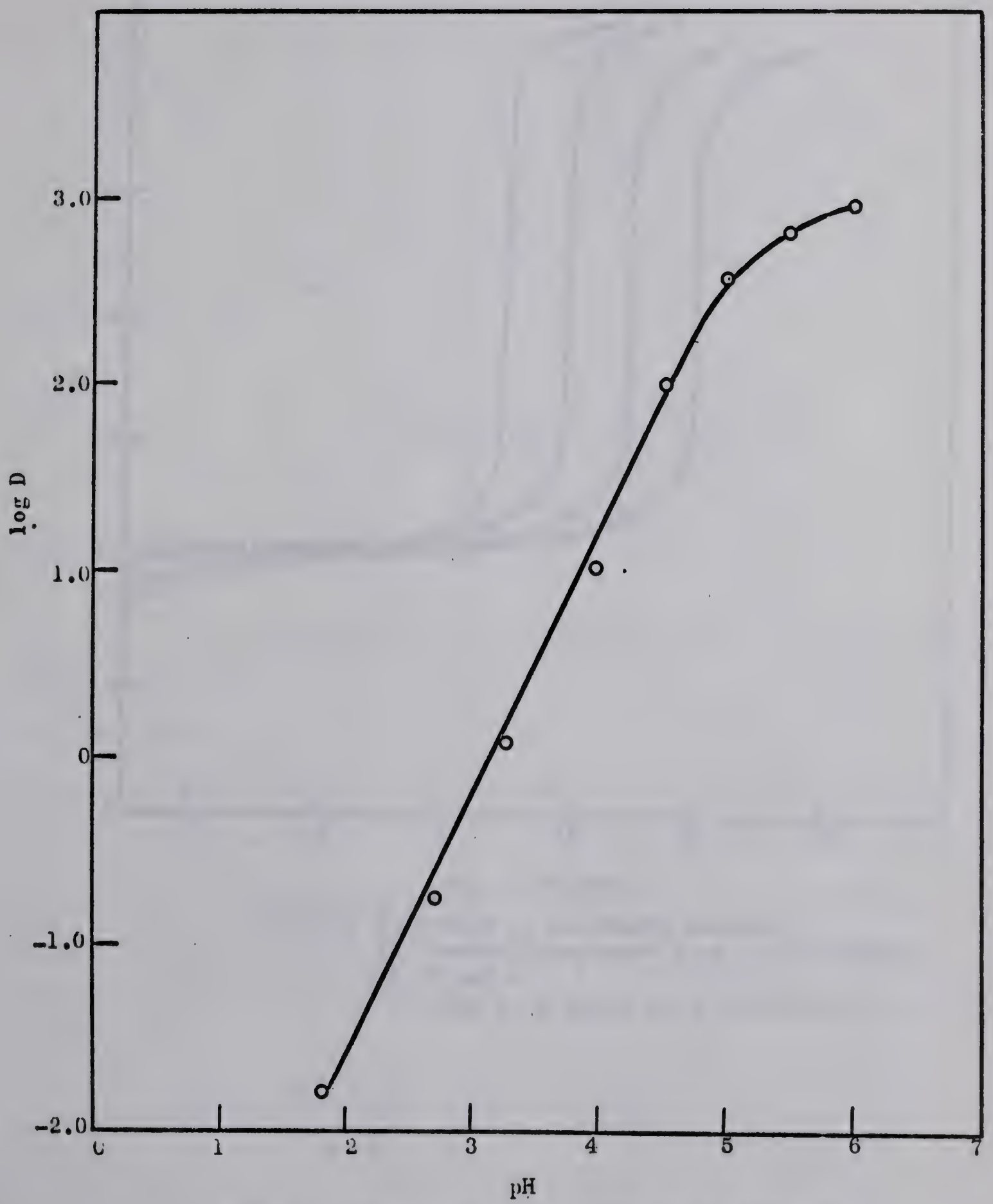

Fig. 11 Distribution coefficient as a function of pH.

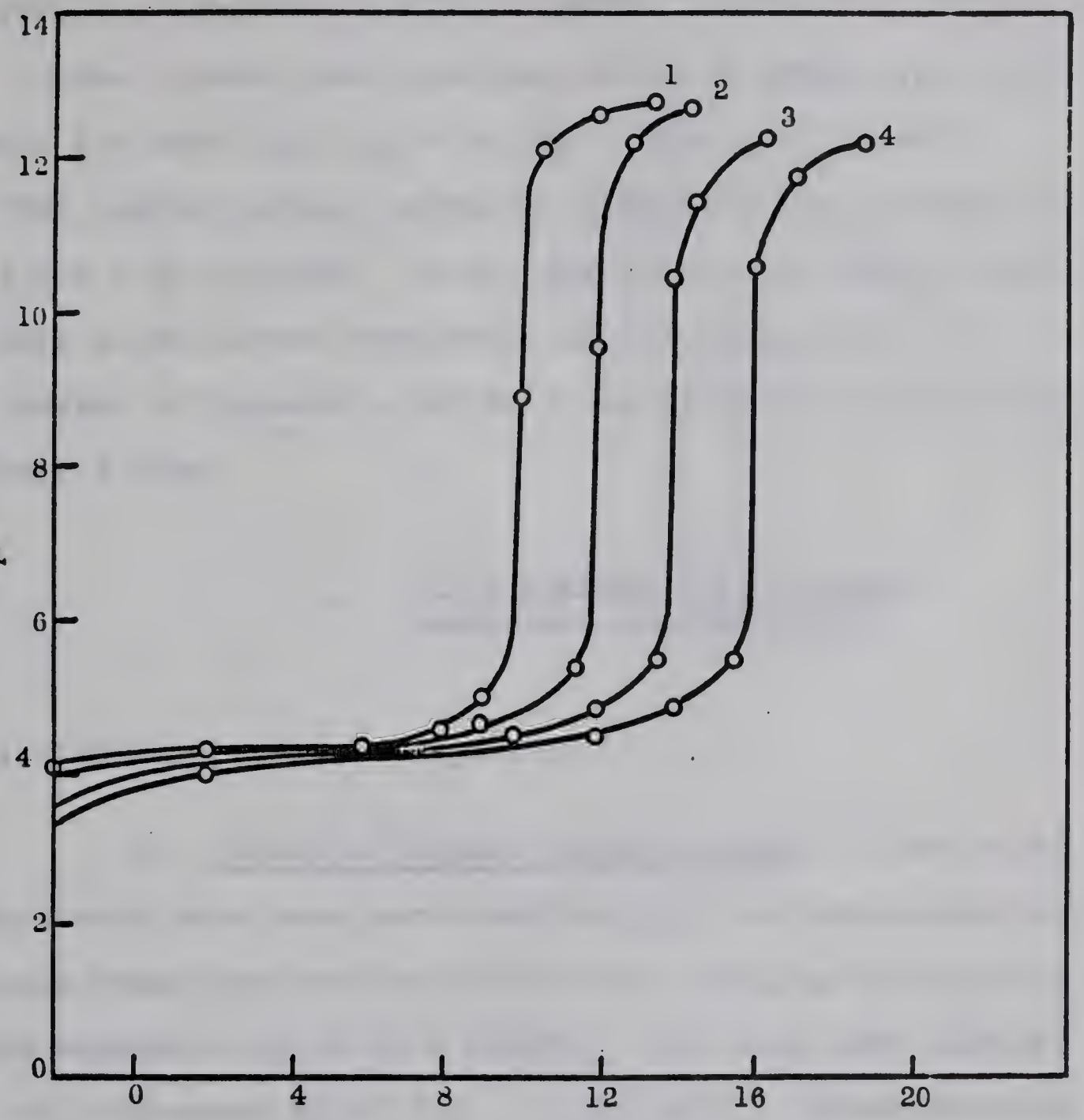

Fig. 12 Formation of Mn-D2EHPA complex
1. Neutralization of 10 ml. 0.1M D2EHPA
2, 3 and 4 " " " " "
plus 1, 2 and 3 ml of 0.1M $MnCl_2$.

$$Mn(OH)_2 + (HL)_2 = MnL_2 + 2H_2O \qquad (74)$$

Figure 12 shows a series of curves depicting the progressive formation of [Mn - D2EHPA] complex at different pH. Curve 1 shows the titration of 0.1 M D2EHPA (in C_6H_6) with 0.1 N NaOH (in C_6H_6 + CH_3OH). Curves 2, 3, and 4 are the neutralization curves of D2EHPA in the presence of 1, 2 and 3 ml 0.1M Mn. In all the curves the [MnL_2] complex appears to be formed completely in the range of pH 5 to 6. The number of ligands L per Mn^{++} ion is found to be approximately 2 from

$$n = \frac{\text{Total ligand - free ligand}}{\text{manganese concentration}} \qquad (75)$$

evaluated for curves in Figure 12.

3. Effect of Ligand Concentration. A series of experiments have been performed keeping the composition of aqueous phase constant at 0.1M Mn and changing the organic phase between 0.025-0.25 M D2EHPA; the tests were carried out at a constant pH of 5.4. A plot of C^o_{Mn} (concentration of Mn in organic phase) against concentration of D2EHPA on a log-log scale, Figure 13a gives a straight line up to 0.2 M D2EHPA resulting in complete extraction of the manganese into the organic phase.

Figure 14 shows a plot of [pH + log C_{D2EHPA}] vs

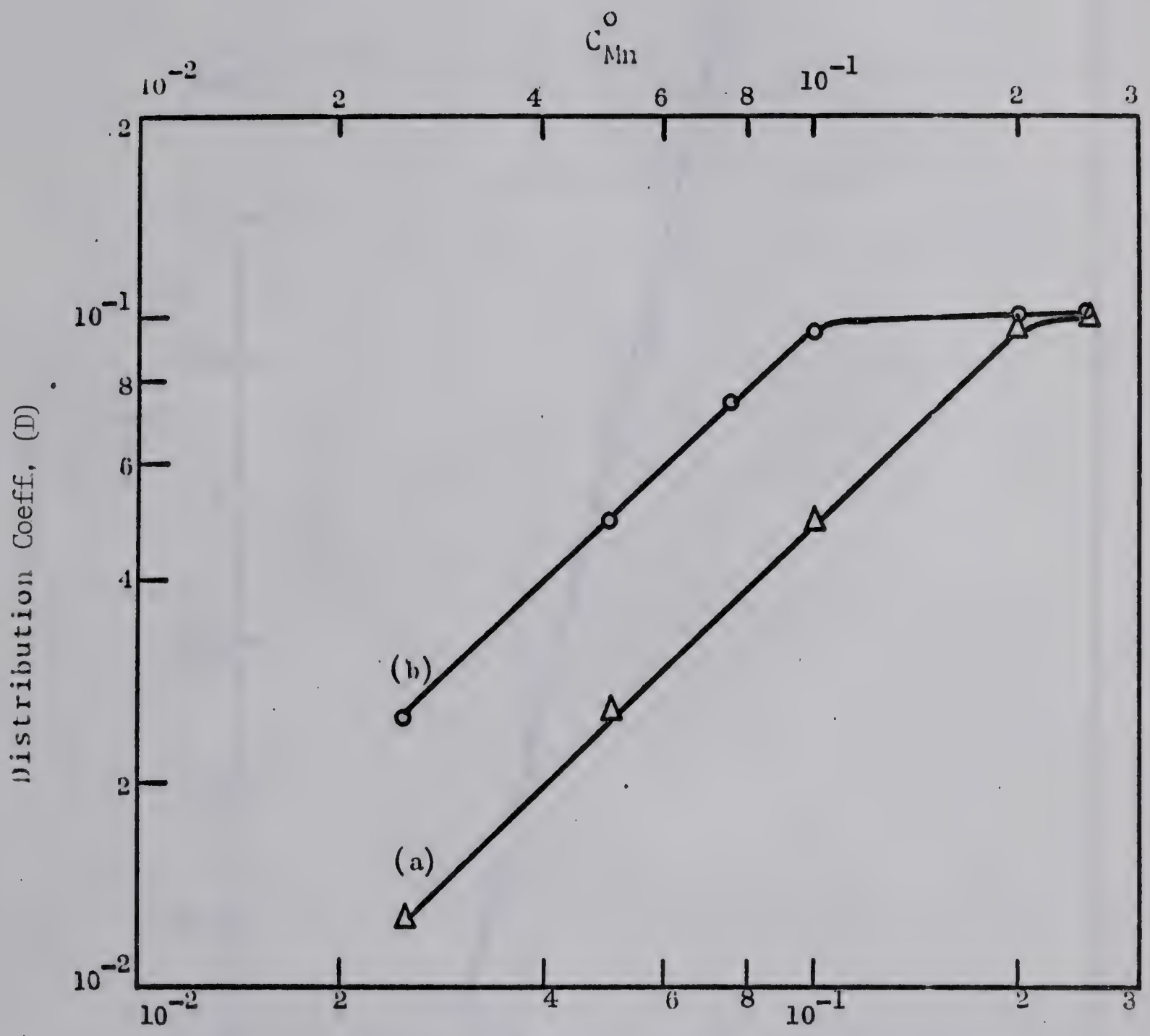

Fig. 13 (a) Solvent extraction of Mn at constant Mn^{++} concentration of 0.1M

(b) Solvent extraction of Mn at constant ligand concentration of 0.2M.

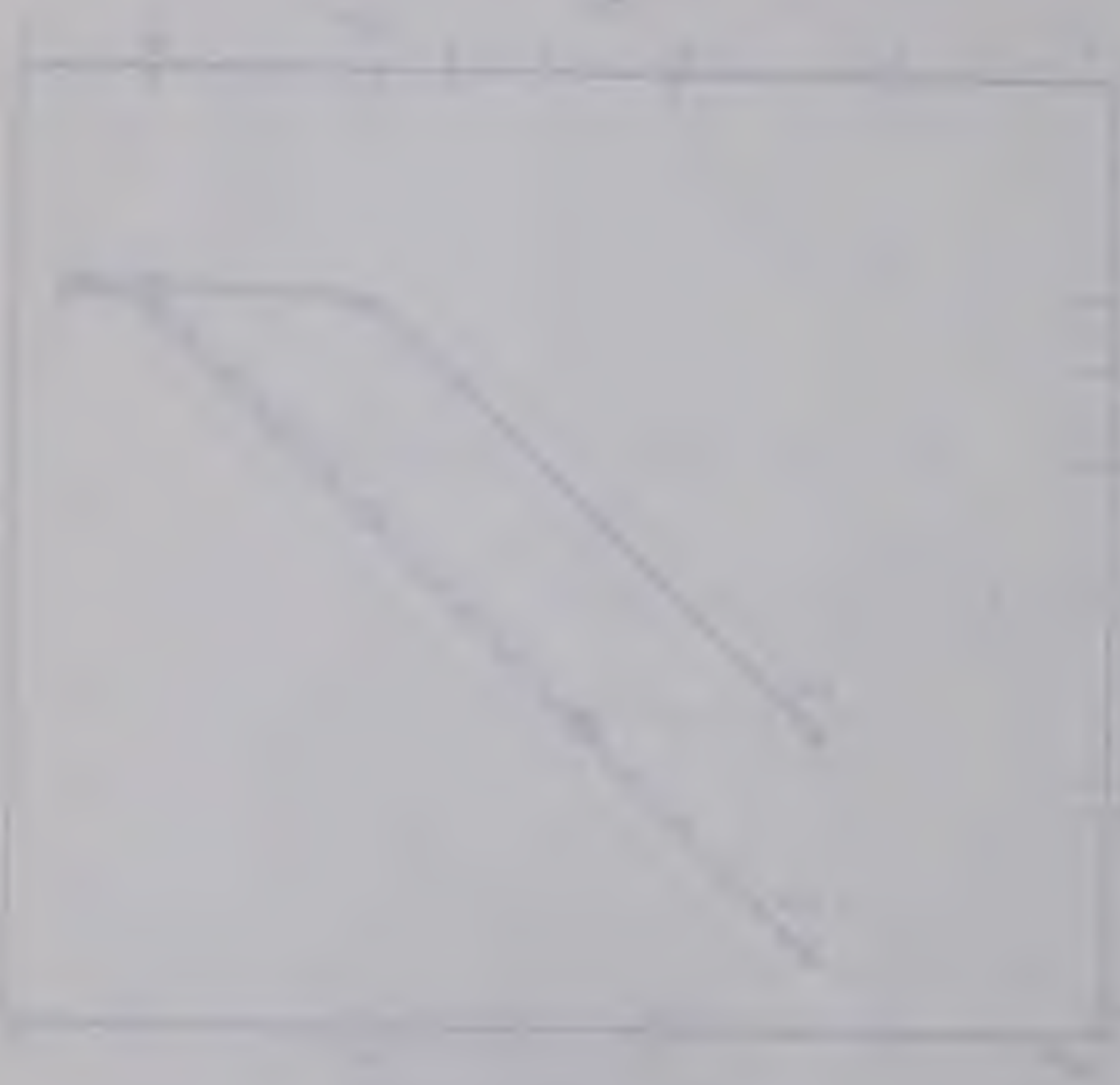

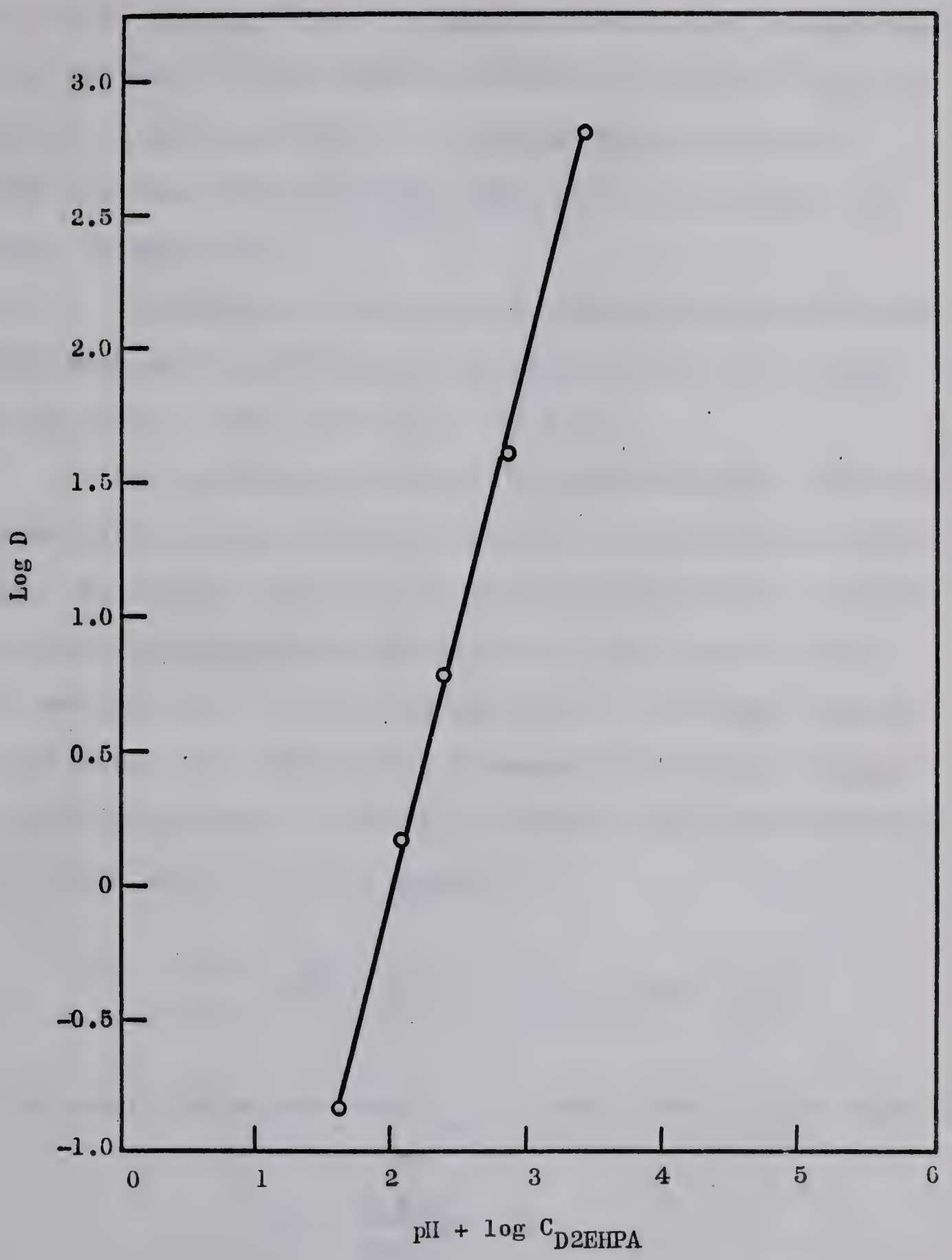

Fig.14 Dependence of distribution coefficient on pH at constant D2EHPA concentration.

log D, equation 71, for 0.25 M D2EHPA contacted with 0.025 M $MnSO_4$ at different pH values. The slope of the line is equal to 2, showing that 2 ligands are attached to each manganese cation. A confirmation of this ligand/Mn ratio was obtained in another test in which the concentration of D2EHPA was held constant while that of aqueous phase was changed (Figure 13b).

The chemical analysis of the saturated undiluted D2EHPA with extracted $MnSO_4$ is given in Table XVI. It can be seen the molar ratio of Mn to P is 1 to 2.

At a lower concentration of solvent the number of ligands attached to the metal ion can be predicted by the slope, the change in pH or the saturation method, but above a certain ion-to-ligand concentration ratio none of the above methods can be reliably employed. At higher ligand concentration the association between cation M and ligand L may occur (according to several authors) with the formation of an "acid salt" of the ligand:

$$M^{n+} + n(HL)_2 = M(L)_n \cdot nHL + nH^+ \qquad (76)$$

and the equilibrium constant K_e is then given by the equation:

$$K_e = \frac{D \cdot [H]^n}{[HL]^n} \qquad (77)$$

On taking logarithm and rearranging, the following is obtained

$$\text{Log } D = \log K_e + n \log[HL] - n \log[H] \tag{78}$$

At fixed ligand concentration one obtains on partially differentiating equation (78) with respect to log [H]

$$\frac{\delta(\log D)}{\delta(\log[H])} = -n \tag{79}$$

that is when the ligand concentration is fixed the plot of experimental value of log[D] versus log[H] should give a slope of -n.

Similarly, at fixed hydrogen ion concentration the plot of the logarithm variation of distribution when plotted against the equilibrium ligand concentration should give a straight line with slope 'n', i.e.

$$\frac{\delta(\log D)}{\delta(\log[(Hx)_2])} = n \tag{80}$$

According to Healy and Kennedy[36] when the amount of ligand in the organic phase is insufficient to give an "acid salt", the mechanism of extraction is as follows:

$$M^{n+} + (n/2 + 1)(HL)_2 = M(L)_n \cdot 2HL + nH^+ \tag{81}$$

that is, only two undissociated ligand molecules are giving molecular association with the cation-ligand complex.

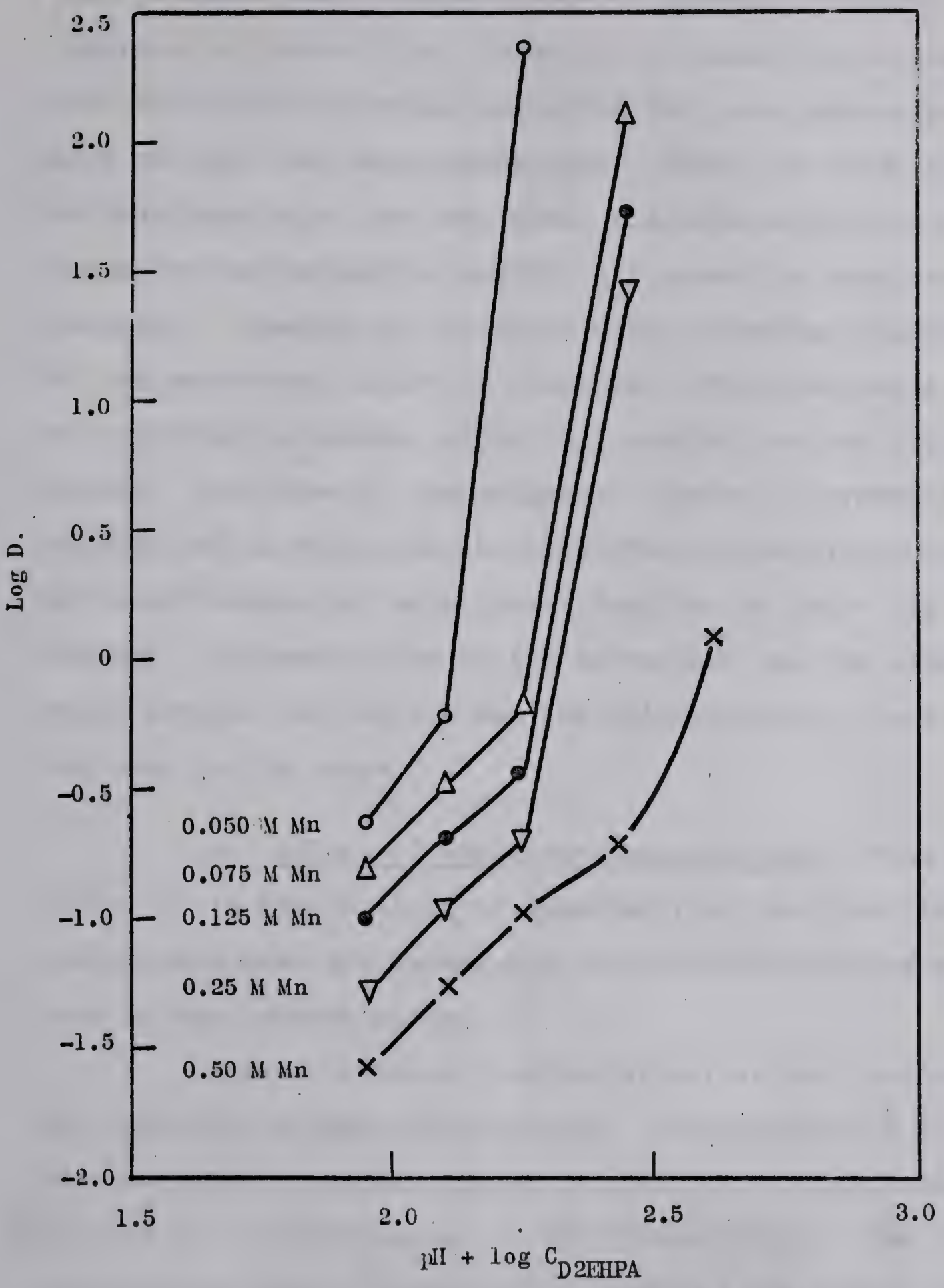

Fig. 1 5 Extraction of Mn at 0.05 - 0.5M D2EHPA concentration and constant pH 5.4

Figure 15 shows a family of curves where the pH is kept constant while concentration of D2EHPA is changed. The departure of curves from linearity is indicative of the fact that the extraction model suggested for lower concentrations does not hold for macro-quantities. Since the activities of various quantities are not known, the behavior of the complex formation and extraction coefficient cannot be predicted accurately. Lowering of the slope with increasing concentration of the extractant cannot be connected with a decreased number of solvating molecules, since this contradicts the law of mass action. Furthermore, the manganese complex is probably polymerized and in this case the logarithm of the distribution coefficient should not be a linear function of [pH + log C D2EHPA]. Polymerization of the extractant and the association between the solvate and the diluent have to lead to a decrease in the slope.

4. Effect of Manganese Concentration. From the curve 'b' in Figure 13 it is observed that the distribution coefficient does not depend upon the concentration of manganese in the aqueous phase.

Figure 16 shows a series of extraction isotherms for different D2EHPA concentration. The quantity of Mn extracted into the organic phase is plotted as a function of initial Mn^{++} concentration in the aqueous phase. The linear portions of these curves indicate complete extraction of Mn into the organic phase. At the sharp bend in the curves

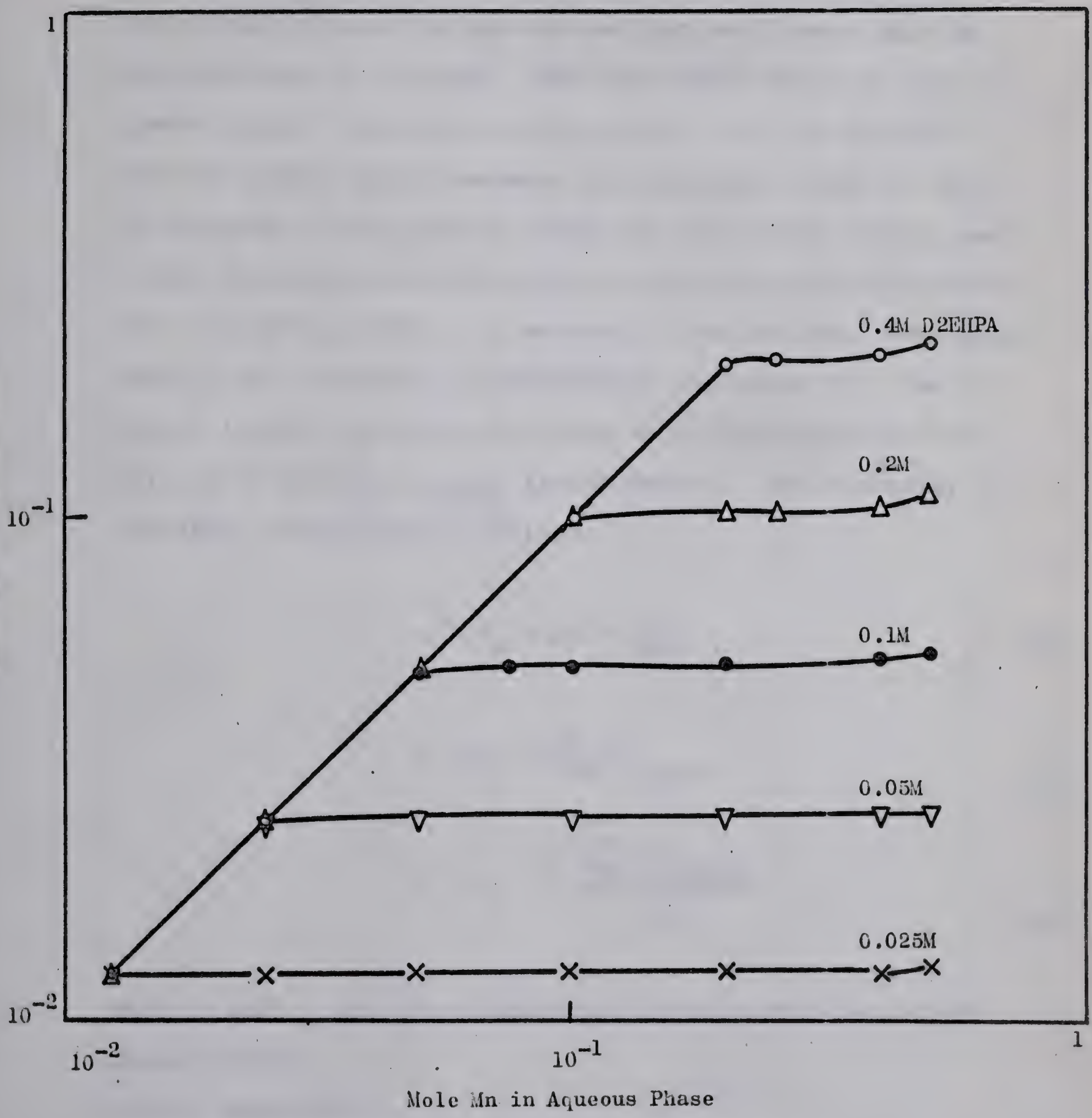

Fig. 16 Effect of the concentration of Mn on its extraction into the organic phase.

the condition of maximum extraction is obtained at a C^{o}_{Mn}/C D2EHPA ratio of 0.5. For higher manganese concentration in the aqueous phase no further extraction into the organic phase takes place, the curves are flat until very high Mn concentration is reached; then the curves begin to have an upward trend. The molar ratio exceeds 0.5, (up to 0.62) and the organic phase becomes very viscous. Since no $SO_4^{"}$ is detected in the organic phase the additional loading may be due to the active bond formation between alkyl phosphate (-P = O and Mn O(OH), i.e. molecular association. The sharp rise in the viscosity is represented in Figure 17. The increase in the viscosity was found to be dependent on pH as well as on the C^{o}_{Mn}/C_{D2EHPA} stoichiometry. The viscosity is therefore correlated as follows:

$$\eta - \eta_s \propto pH \propto \frac{1}{[H]^+} \tag{82}$$

$$\eta - \eta_s \propto C^{o}_{Mn}/C_{D2EHPA} \tag{83}$$

$$\eta - \eta_s = k \frac{C^{o}_{Mn}/C_{D2EHPA}}{[H^+]} \tag{84}$$

where η and η_s are the viscosities of Mn-D2EHPA and D2EHPA respectively.

Taking logarithm:

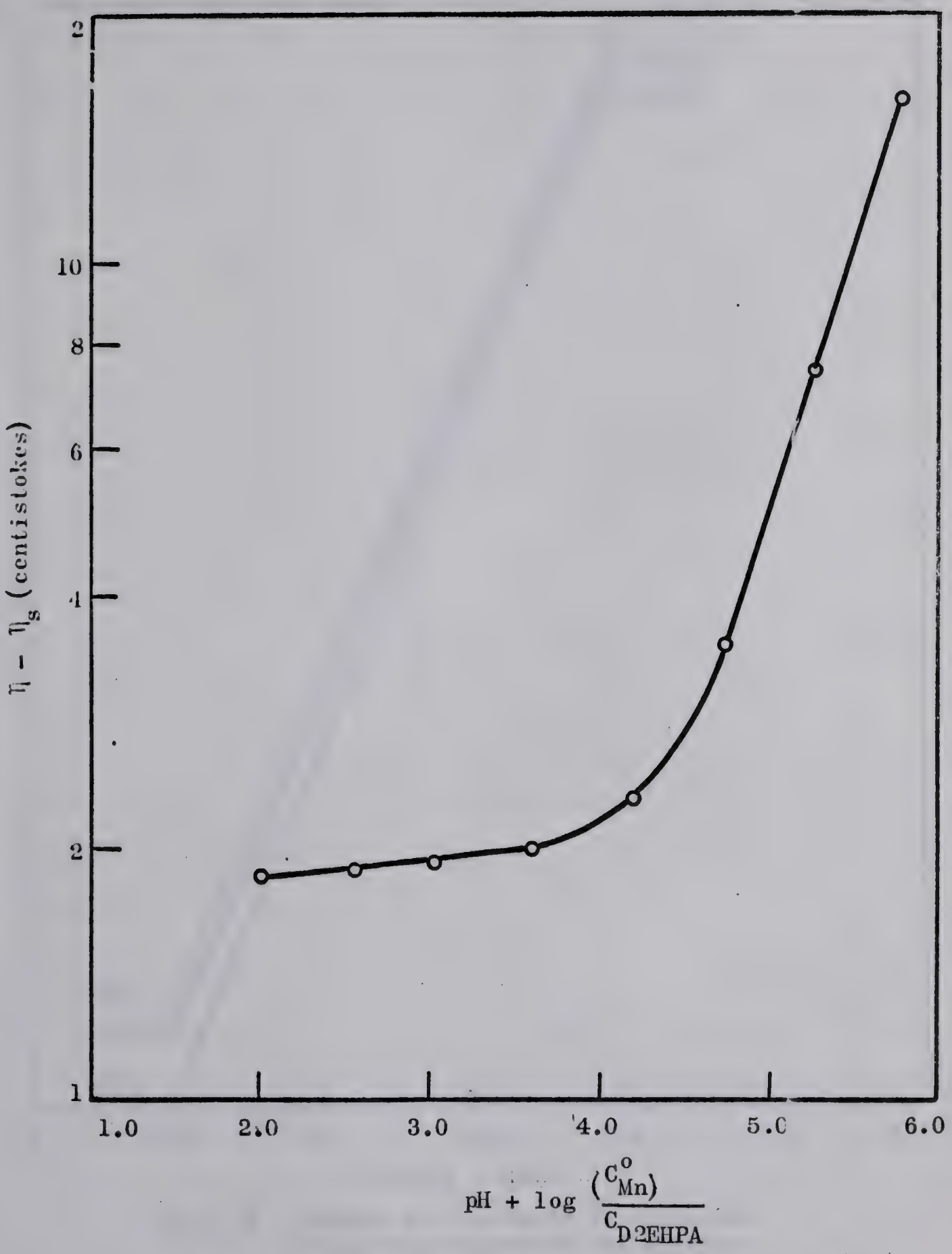

Fig. 17 Changes in viscosity with pH at 50°C, for 0.5M D2EHPA and 0.3M $MnSO_4$ in the equilibrating phases.

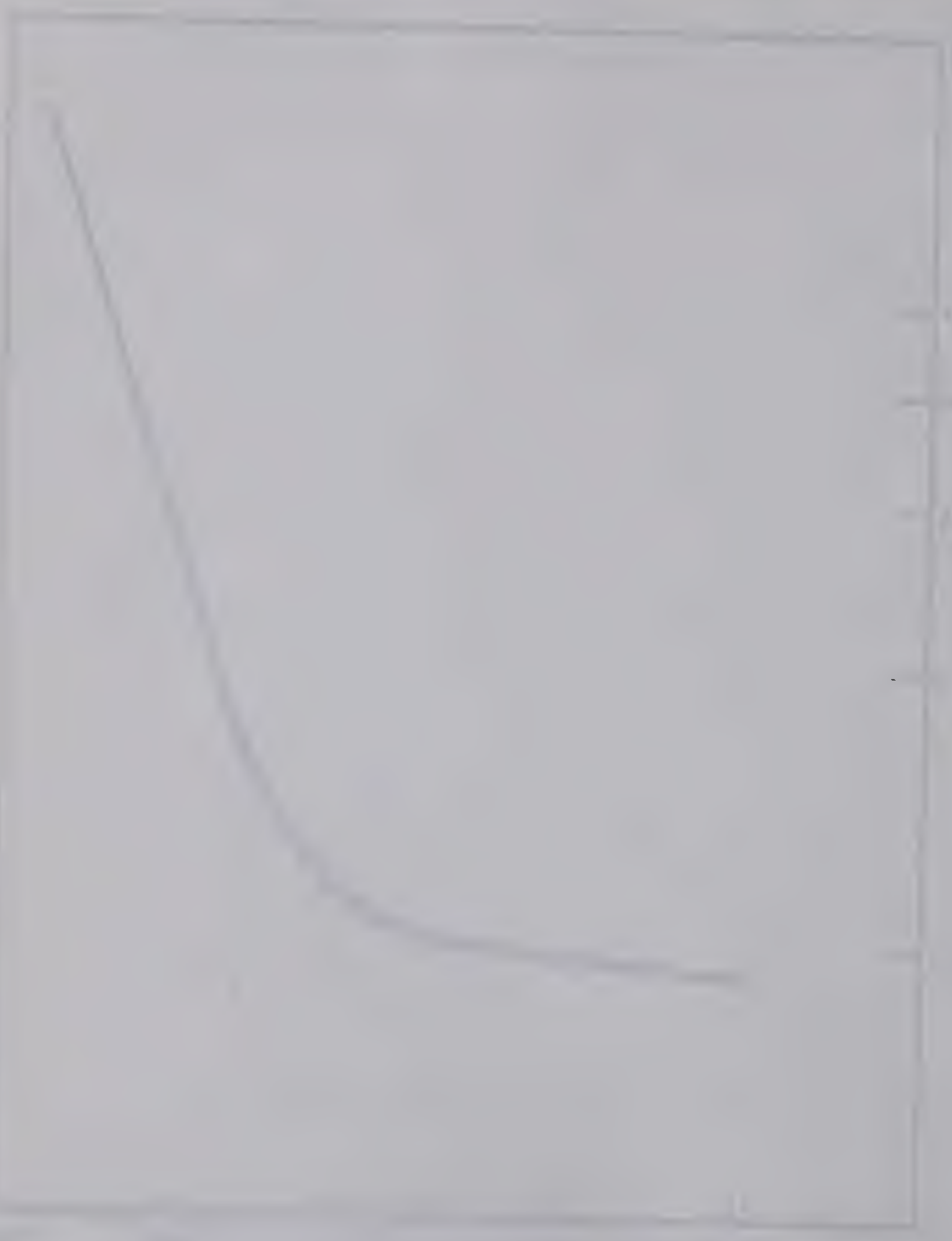

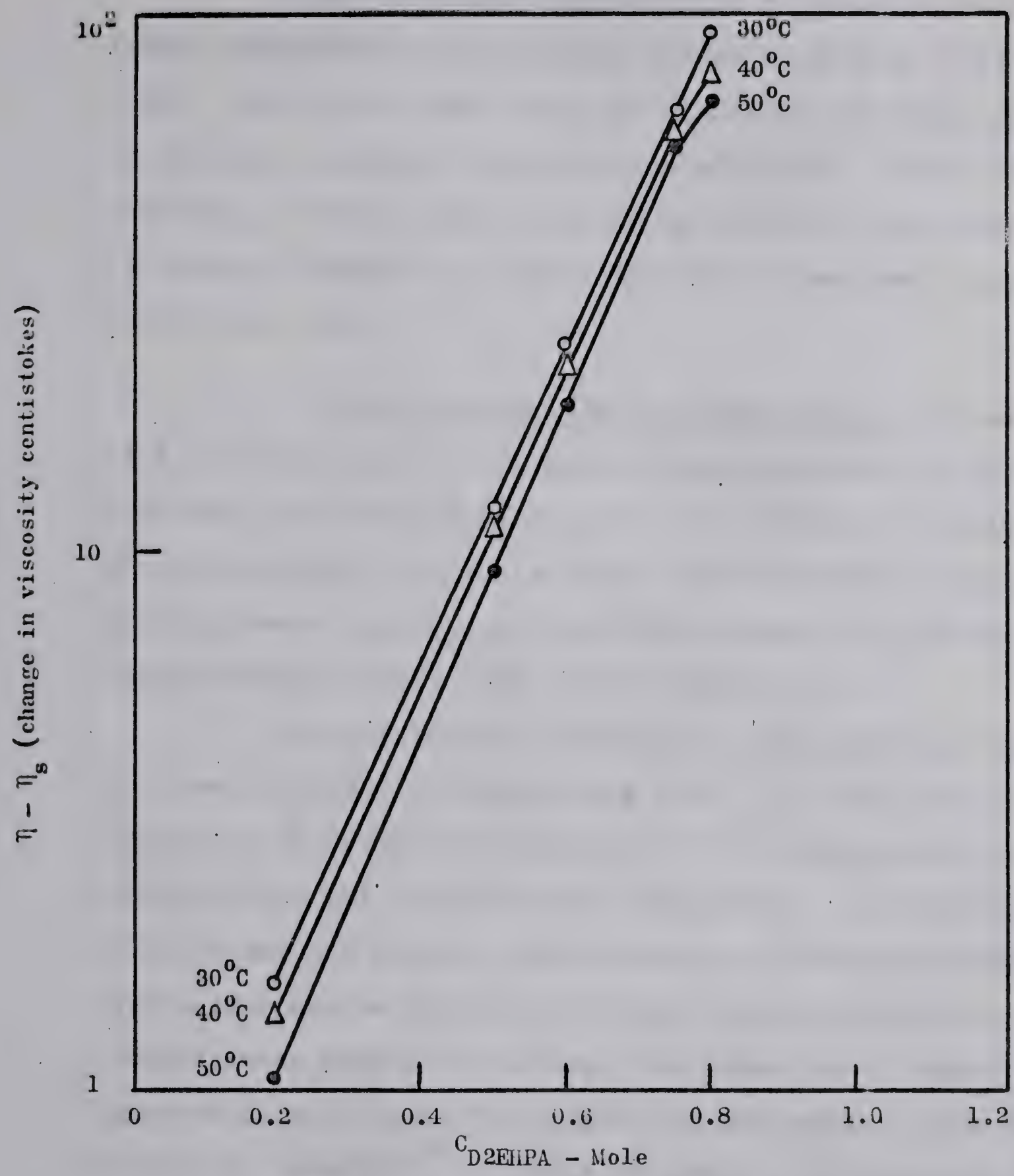

Fig. 18 Changes in viscosity at different ligand concentration but constant C^o_{Mn}/C_{D2EHPA} mole ratio of 0.48

$$\text{Log}(\eta - \eta_s) = \text{pH} + \log C^{o}_{Mn}/C_{D2EHPA} \qquad (85)$$

Figure 18 shows the variation of viscosity at different temperatures of saturated D2EHPA (0.1, 0.5, 0.75 and 0.8M). The figure shows that the viscosity increases sharply with the increased concentration of D2EHPA. It was not possible to measure the viscosity of 1M D2EHPA with the set of Ostwald viscometers, since the solution was too viscous to fill the tube.

5. Effect of Aqueous to Organic Ratio. Aliquots of 0.05, 0.1, 0.25 and 0.5 molar D2EHPA solutions in kerosine were equilibrated at 25 $\pm$ 1°C with different volumes of aqueous $MnSO_4$ solution so that the mole ratio of the contacting phases C_{Mn}/C_{D2EHPA} remained constant at 0.48 and aqueous/organic phase ratio varied from 0.4 to 3.

The distribution ratio in all the curves in Figure 19 shows in general, a decreasing trend. At very low concentration of cation the solubility of the complex in the aqueous phase was assumed to be negligible. In extraction of macro-amounts however, the decrease in the distribution coefficient may be due to an increase in the solubility of the manganese complex resulting from formation of hydrophilic aggregates, micelles. The complex in the aqueous phase may further be hydrated[37]. Since the degree of hydration is generally higher in aqueous phase than in organic the hydrated complex species may go on increasing with the increase of

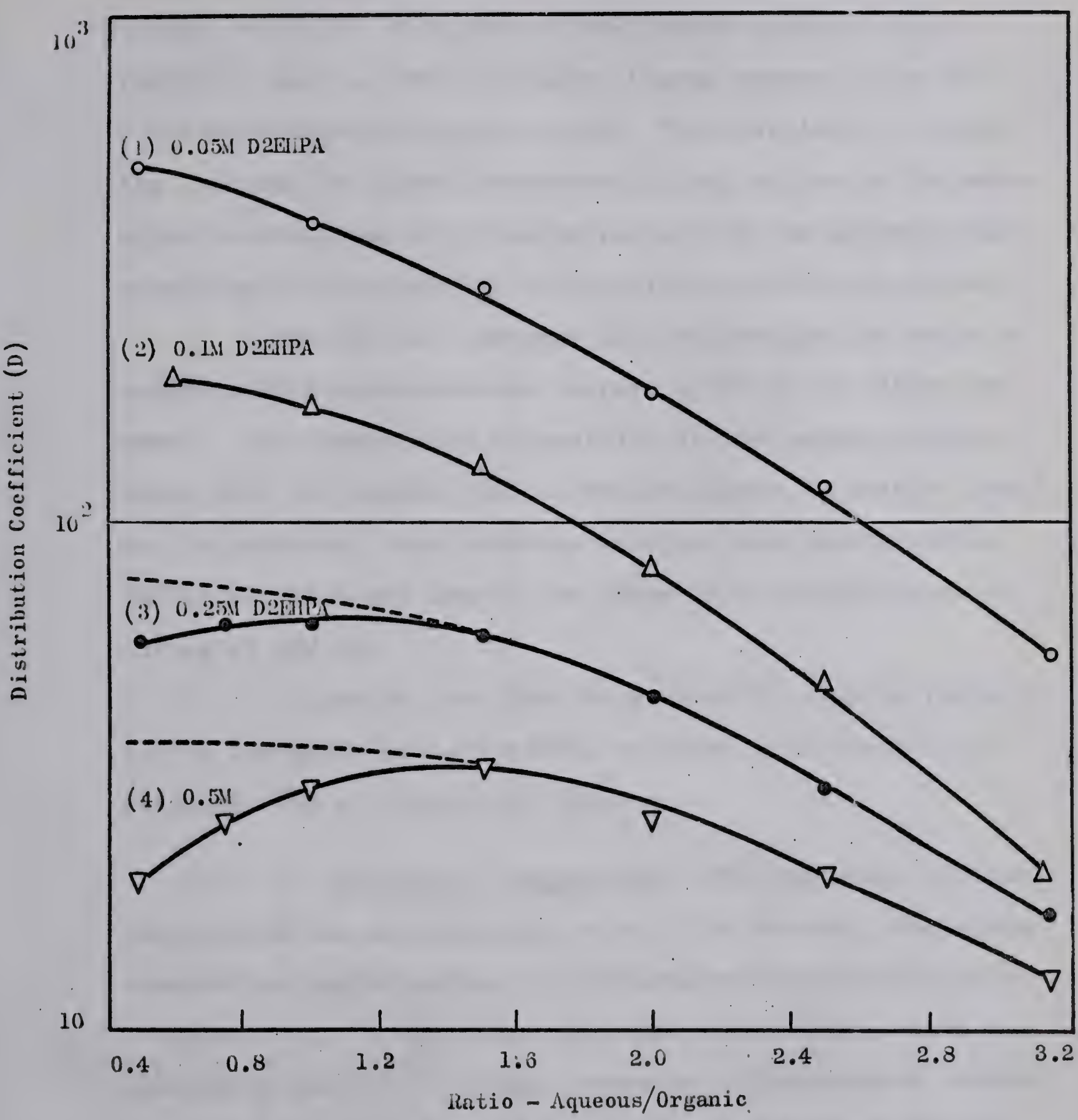

Fig. 19 Effect of aq/org ratio on the distribution coefficient of Mn at Mn/C_{D2EHPA} mole ratio of 0.48

aqueous/organic ratio consequently decreasing the distribution coefficient.

The comparison of curves reveals that the distribution ratio (D) is higher at low ligand concentration (curve 1) and is lower at higher ligand concentration for a constant aqueous/organic ratio. The lowering of D with the increase in D2EHPA concentration may be due to the molecular associations with the extractant in the aqueous phase, according to equation (63), to the effect of diluent or both.

The initial increase in the distribution ratio at higher D2EHPA concentration (curves 3 and 4) is rather unusual. The phases tend to emulsify at low aqueous/organic ratio with the result that a complete phase separation could not be achieved, thus accurate analyses were unobtainable. The dotted line may denote the trend in distribution as in curves (1 and 2).

It can be seen that an aqueous to organic ratio of 1.2 to 1.6 gives an appreciable value of distribution coefficient for all practical purposes.

6. Effect of Temperature. The influence of temperature on the distribution ratio of Mn between phases was observed on equilibrating the aqueous and organic phases in a thermostat. It was found that the distribution ratio increases up to 40°C. Further increase in temperature lowers the coefficient of distribution. The results are plotted in Figure 20.

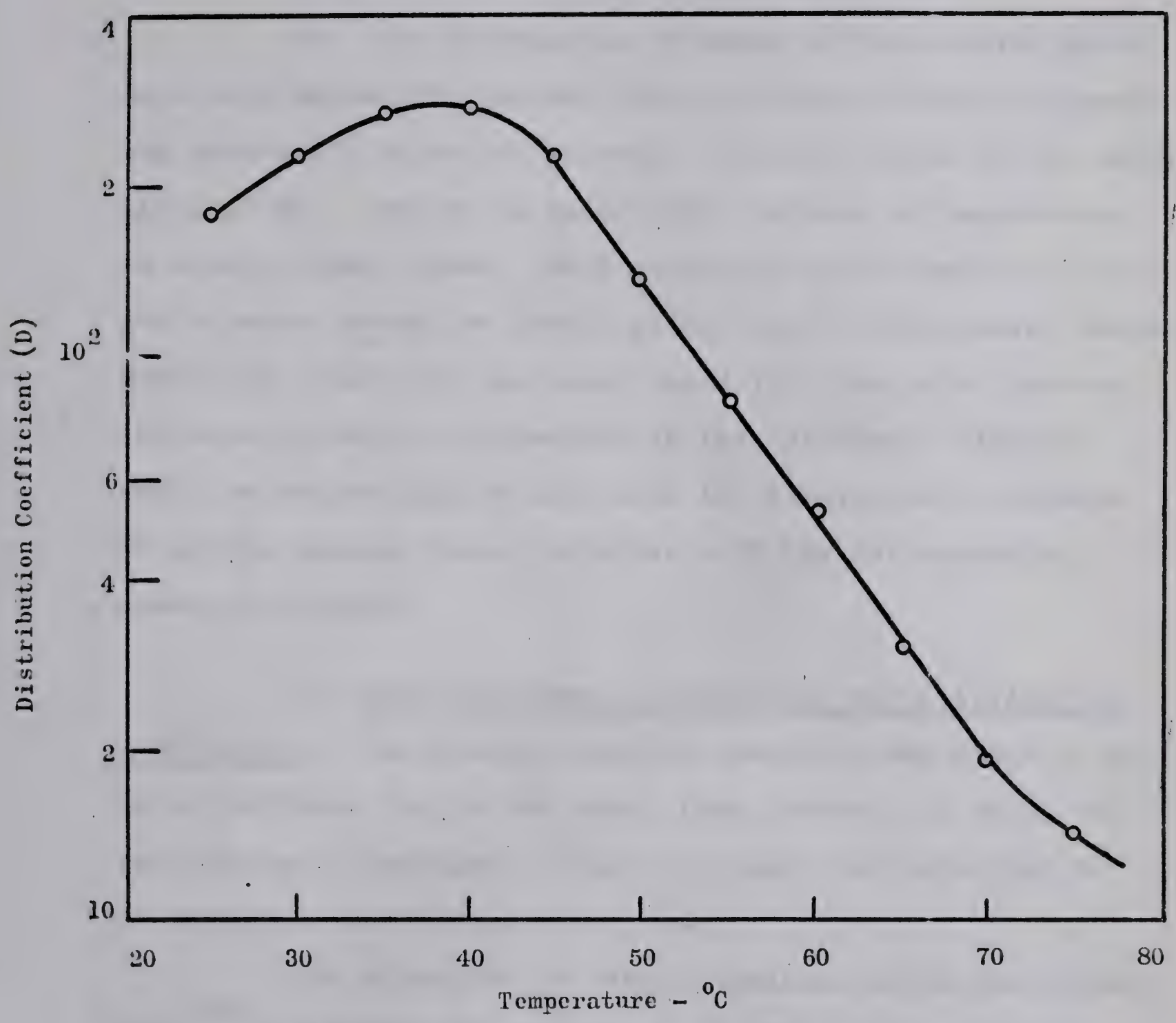

Fig.20 Effect of temperature on the distribution coefficient of Mn when 0.1M D2EHPA is contacted with 0.05M $MnSO_4$ at pH 5.4

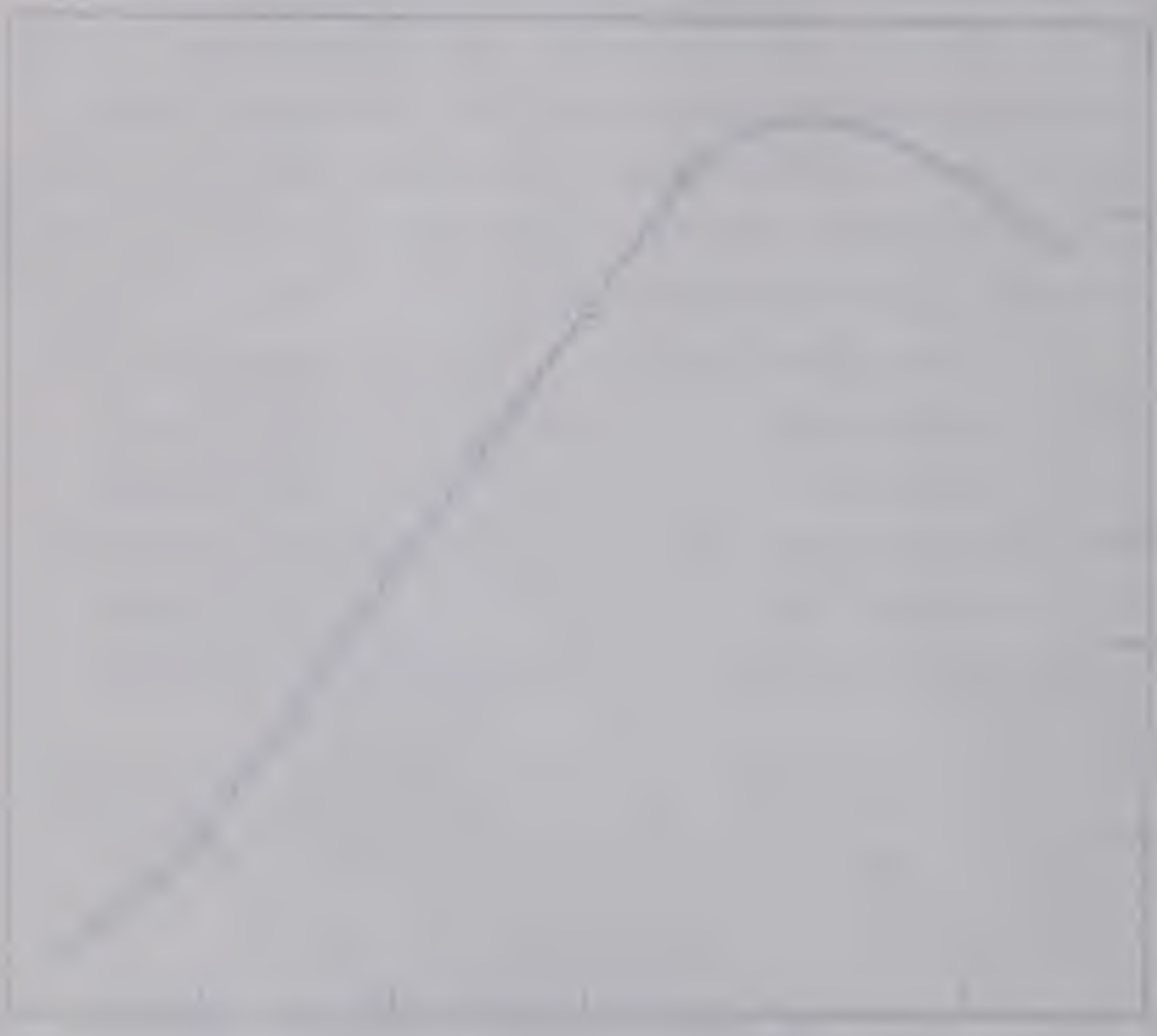

The variation in the distribution coefficient may be due to

(a) a change with temperature in the solubility of the complex in the aqueous phase, or

(b) the dissolution of water in the organic phase. Both will appreciably affect the activities of the corresponding species of solute or solvent. A drastic rise in the solubility of Mn - complex in water with increase in temperature is a very likely cause; most ionizable surfactants and their salts have a so-called Krafft point i.e., a temperature above which the solubility increases rapidly; this point denotes the onset of micelle formation in the solution; micelles would be responsible in this case for keeping more and more Mn in the aqueous phase, together with the corresponding number of ligands.

7. Effect of Time of Contact on the Distribution Coefficient. The kinetic study of reactions was found to be quite difficult due to the short time interval in which the equilibrium is attained. Figure 21 shows the variation of distribution coefficient with time.

The extraction is almost complete within one minute. Ryon[38] described the extraction of uranium by a kerosene solution of D2EHPA as a first order reaction, but, no such correlation is possible in the case of Mn extraction. Because of the high reaction speed, the reaction order is not easy to measure with ordinary analytical methods.

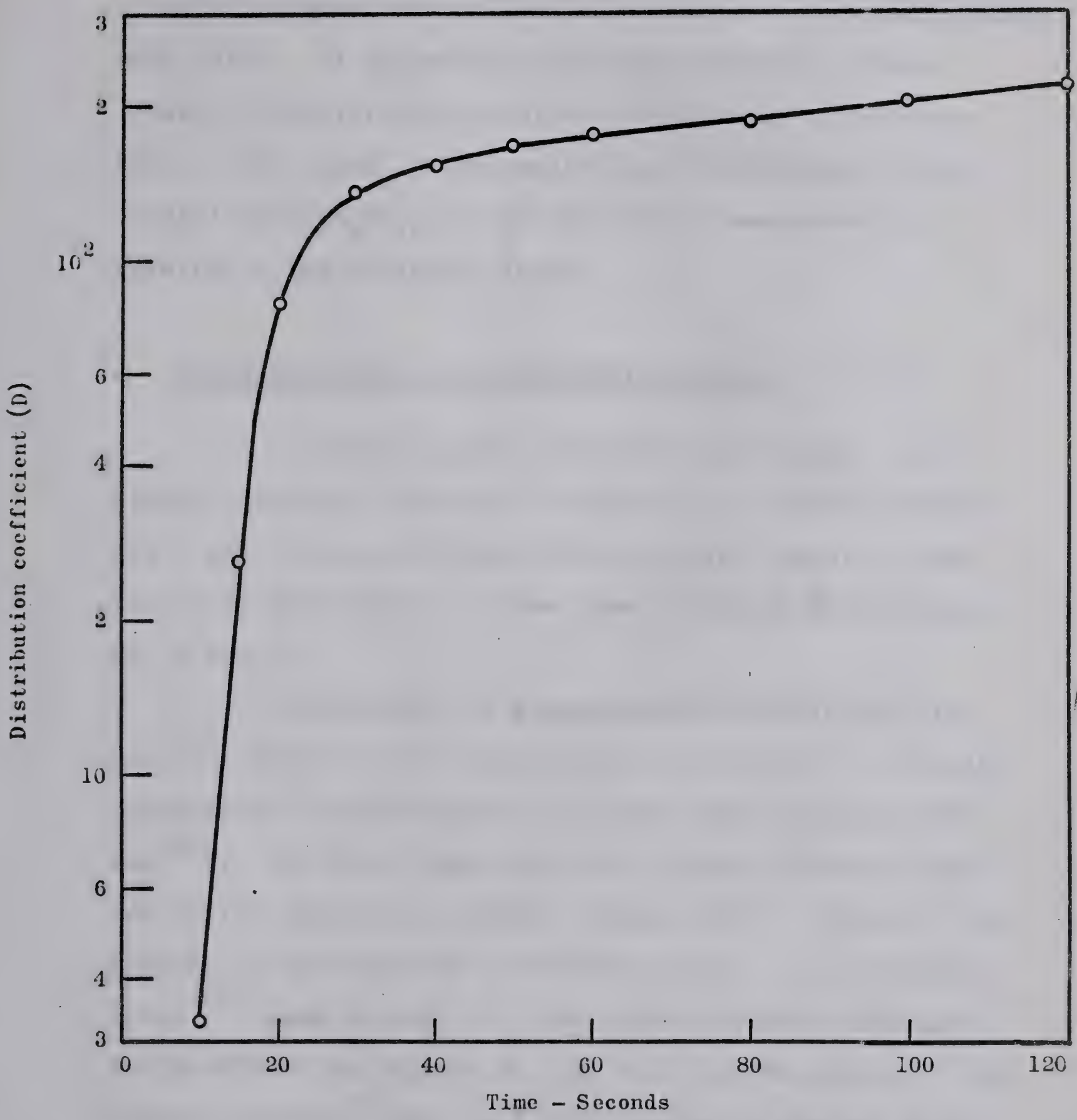

Fig. 21 Effect of time of contact of the equilibrating phase on D for 0.1M D2EHPA and 0.05M $MnSO_4$.

C. Stripping

The loaded solvent can be stripped very efficiently with 2-4 molar mineral acids, yielding corresponding manganese salts. At higher acid concentrations the solvent losses in the stripped solution are higher, in the order HNO_3 > HCl > H_2SO_4. The analysis of the stripped liquor, using 4 molar H_2SO_4, showed that 99% of manganese was recovered in the stripped liquor.

D. Infrared Study of the Mn-D2EHPA Complex

Infrared spectra of D2EHPA, Na-D2EHPA, and Mn-D2EHPA complexes are shown in Figure 22. D2EHPA spectrum No. 1 was taken as a liquid film, and as a smear of waxy solids on NaCl window, in the case of Mn and Na complexes, No. 2 and 3.

D2EHPA and its manganese salt do not show the presence of free OH in the vicinity of 3500 cm^{-1}, indicating that the ligand exists as a dimer with hydrogen bonding[39]. The broad band due to OH bending vibration present in the spectrum of D2EHPA between 1640 - 1730 cm^{-1} disappears in the spectrum of the Mn complex. The phosphoryl (P=O)[40] band at 1227 cm^{-1} for D2EHPA remains unchanged for Na-D2EHPA but shifts to 1192 cm^{-1} for Mn complex. The band at 1025 cm^{-1} (due to P-O-C) remains unchanged in all three spectra, although, it broadens in the case of Na salt of D2EHPA.

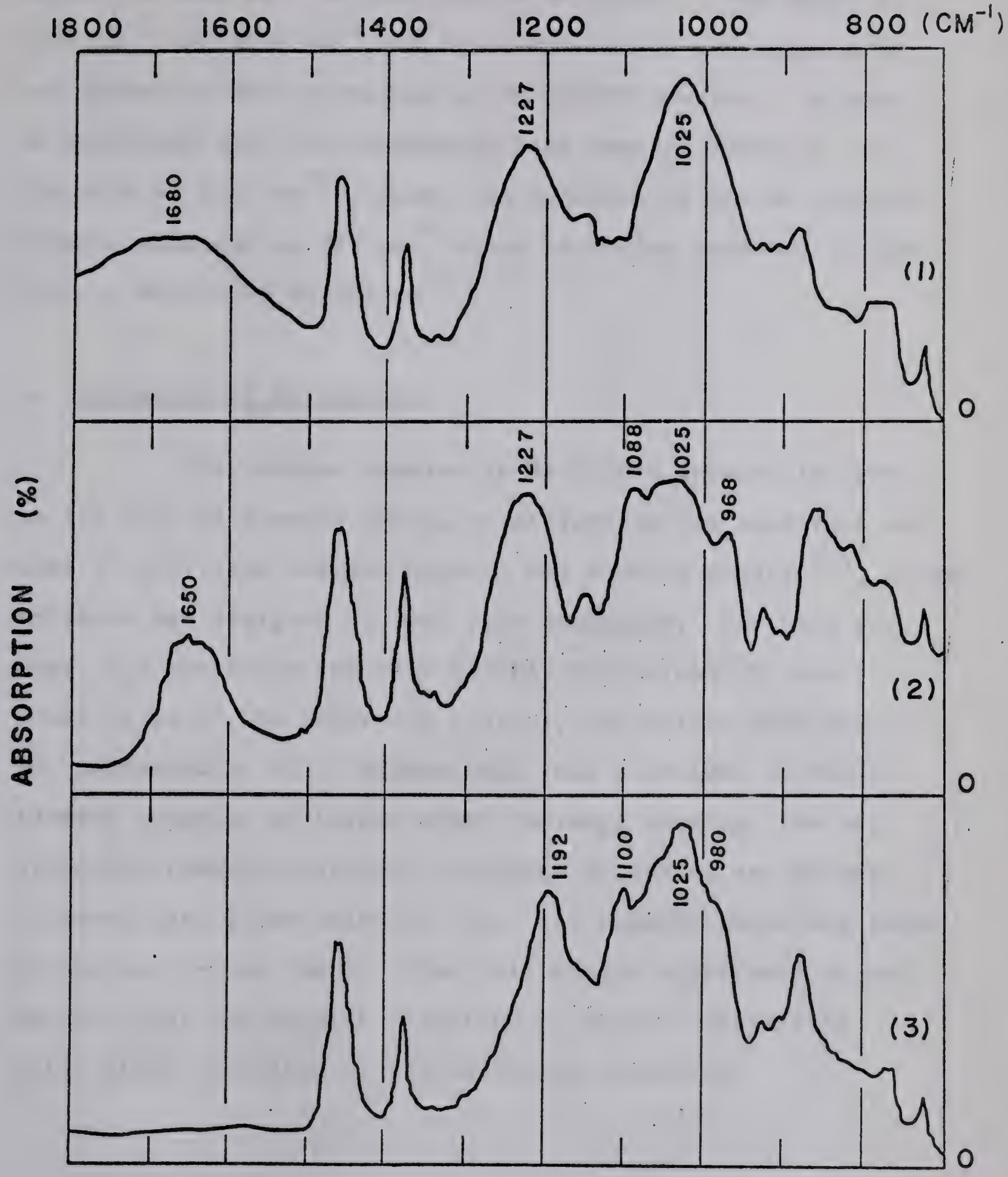

Fig.22. INFRARED SPECTRA OF D2EHPA, ITS Na AND Mn COMPLEXES

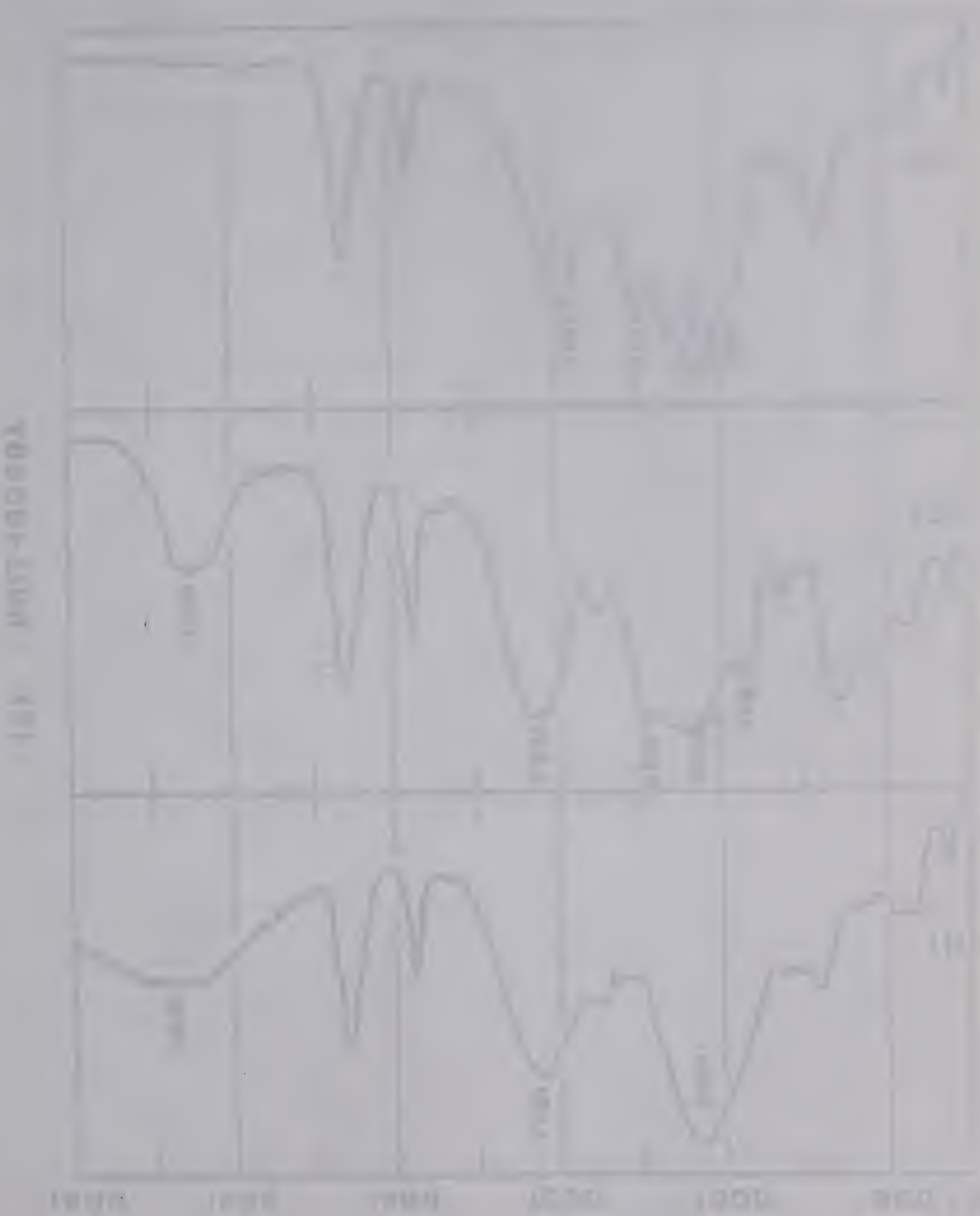

Mn complex shows a new band at 1100 cm^{-1} which shifts to 1088 cm^{-1} in the case of Na-D2EHPA. The bands at 1192 cm^{-1} and 1100 cm^{-1} may be attributed to the asymmetric and symmetric POO^- vibration of Mn-D2EHPA complex. In case of Na-D2EHPA salt the asymmetric band remains fixed as in the acid at 1227 cm^{-1}. Also, the spectrum of the Mn complex shows a shoulder at 980 cm^{-1} which is better resolved in the case of Na-D2EHPA at 968 cm^{-1}.

E. Mechanism of Extraction

The complex species of Mn-D2EHPA appears to form in the bulk of aqueous phase, to diffuse to the interface and then to partition between organic and aqueous phases[41]. An experiment was designed to test this mechanism; for this purpose, H_2O was saturated with D2EHPA (the solubility was found to be of the order 6-8 p.p.m.), and during this the pH decreased to 4.5. Excess $MnSO_4$ was dissolved in the saturated solution of ligand after thorough shaking, the solution was then equilibrated with pure kerosine, and pH was adjusted with dilute NaOH to 5.0. The organic phase was found to contain 3-4 mg. Mn/l. From this simple experiment it can be said that the complex formation in solvent extraction takes place according to the following mechanism.

1. Dissolution

$$(HL)_{2(o)} = (HL)_{2(a)} \qquad k = \frac{[HL]_{2(o)}}{[HL]_{2(a)}} \tag{86}$$

$$pk = 1.42 \pm 0.05$$

2. Dissociation

$$(HL)_{2(a)} = 2H^{+} + 2L^{-} \qquad k_1 = \frac{[H^{+}]^2[L^{-}]^2}{[HL]_{2(a)}} \tag{87}$$

$$pk_1 = 2.80 \pm 0.1$$

3. Complex formation

$$Mn^{++} + 2L^{-}_{a} = MnL_{2(a)} \qquad k_2 = \frac{[MnL_2]_a}{[Mn^{++}][L^{-}]^2_a} \tag{88}$$

4. Partition of the complex in two phases

$$MnL_{2(a)} = MnL_{2(o)} \qquad p = \frac{[MnL_2]_o}{[MnL]_a} \tag{89}$$

now

$$[MnL_2]_o = p[MnL_2]_a = k_2 p[Mn^{++}][L^{-}]^2$$

$$= k_1 k_2 p \frac{[Mn^{++}][HL]_{2(a)}}{[H^{+}]^2} \quad \frac{k_1 k_2 p}{k} \quad \frac{[Mn^{++}][HL]_{2(o)}}{[H^{+}]^2}$$

$$= \frac{K[Mn^{++}][HL]_{2(o)}}{[H^+]_2} \qquad (90)$$

where

$$K = \frac{k_1 k_2}{k} p \qquad (91)$$

F. Structure of Mn-D2EHPA Complex

The dependence of manganese extraction on D2EHPA concentration and on pH value of aqueous phase suggests that manganese extraction is directly proportional to the 2nd power of D2EHPA concentration. Equation (88) shows how the complex formation may take place between the metal cation and the ionized dimer molecule of the acid. At the C^o_{Mn}/C_{D2EHPA} ratio of 0.5 the structure of the Mn-complex could be:

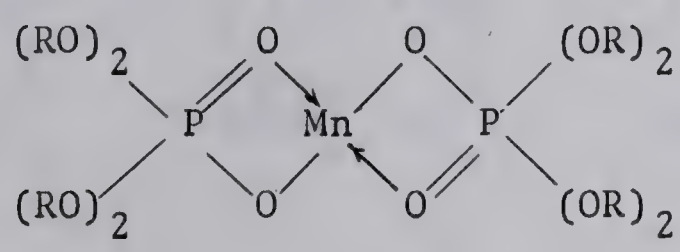

I

or

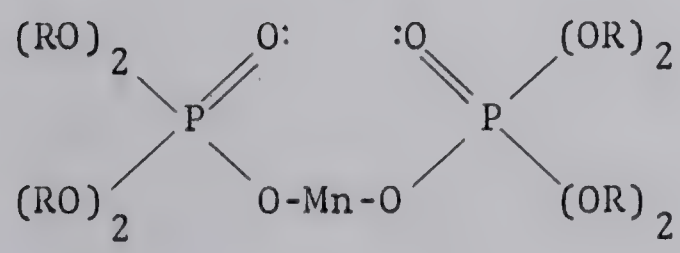

II

where R = $CH_3(CH_2)_4CH(C_2H_5($-2-ethylhexyl group.

As the saturation of ligand increases the composition of complex tends towards MnL_2. X-ray diffraction gives no clue to the structure of the complex. The material is a waxy solid of purple colour. Thus, the structure could be a chain structure, as suggested in III, or a three dimensional net work. From the analytical results of a saturated manganese complex the ratio of Mn to P is 1:2. It is likely that the three dimensional net work has an ultimate Mn to D2EHPA ratio of 1:2. Termination of the chain could occur through free P=O and P-OH groups or through the formation of a 4 membered ring with a Mn atom, e.g. $(RO)_2.P\begin{smallmatrix}O\\ \diagup\ \diagdown\\ O\end{smallmatrix}Mn$, instead of a linear structure.

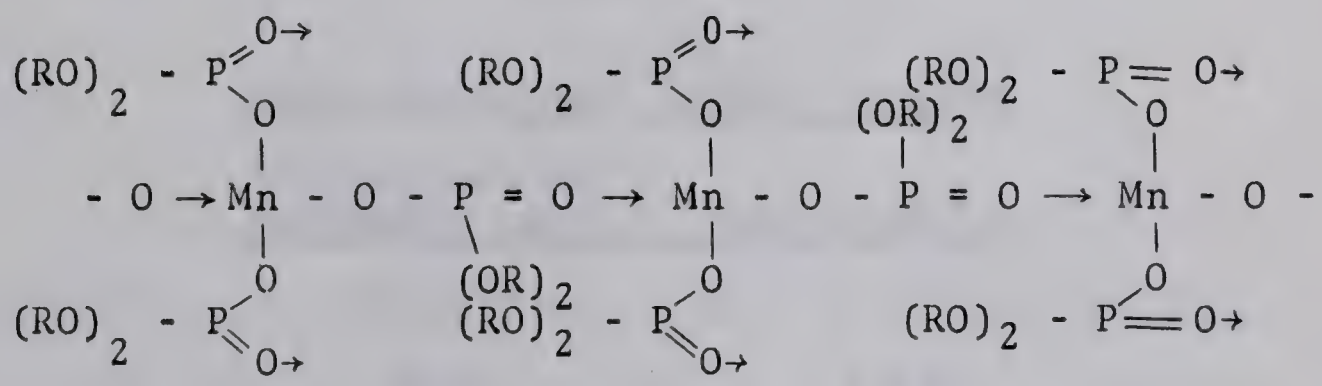

III

or

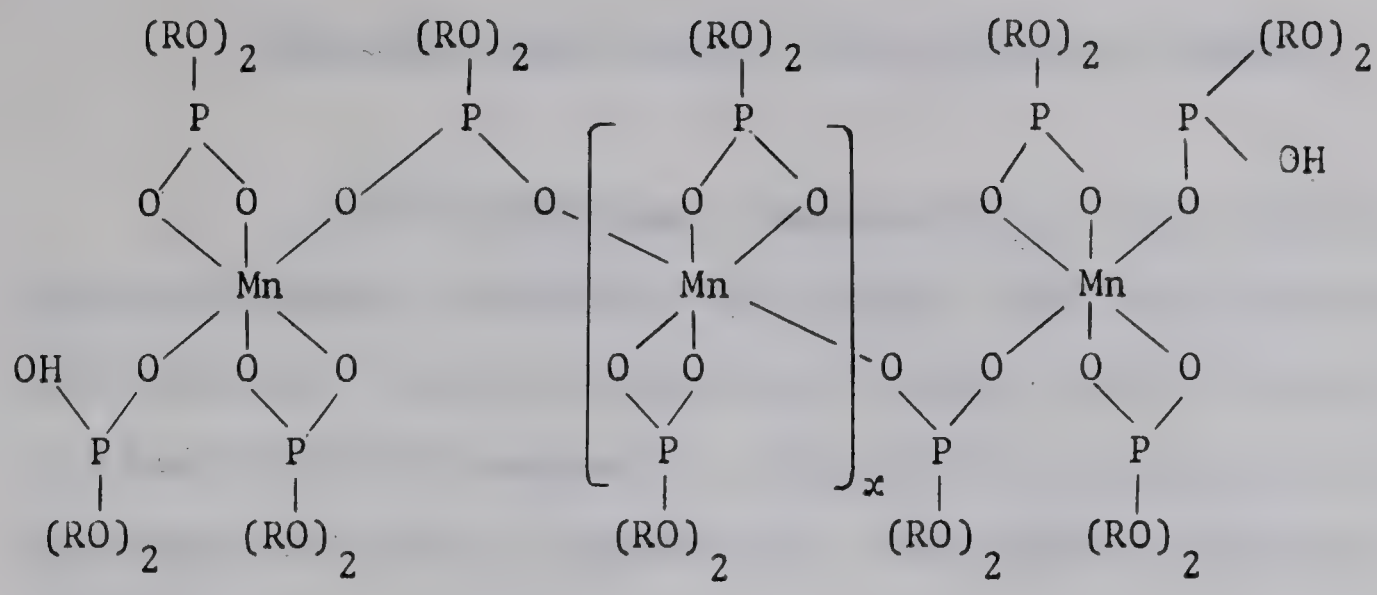

Three dimensional network

Chemical analysis of the saturated D2EHPA-Mn complex given in Table XVI shows that the ratio of ligand to Mn indeed is 1:2.

Table XVI

Analysis of Mn - D2EHPA Complex

	Theoretical at Mn-D2EHPA 1:2	Experimental
C	55.00%	55.27%
H	8.30%	8.42%
O	18.30%	--
P	9.15%	8.98%
S	nil	0.025%
Mn	7.87%	8.09%

Molar Ratio of Mn:P = 1:1.99

HYDROGEN REDUCTION OF THE Mn-D2EHPA COMPLEX

The thermodynamic evaluation of the reduction of MnO by hydrogen (reaction 45) reveals that the reduction is not favored. One may speculate, however, that the Mn-O bond in the Mn-D2EHPA complex may possibly be cleaved by the hydrogen reduction, regenerating the ligand according to the mechanism

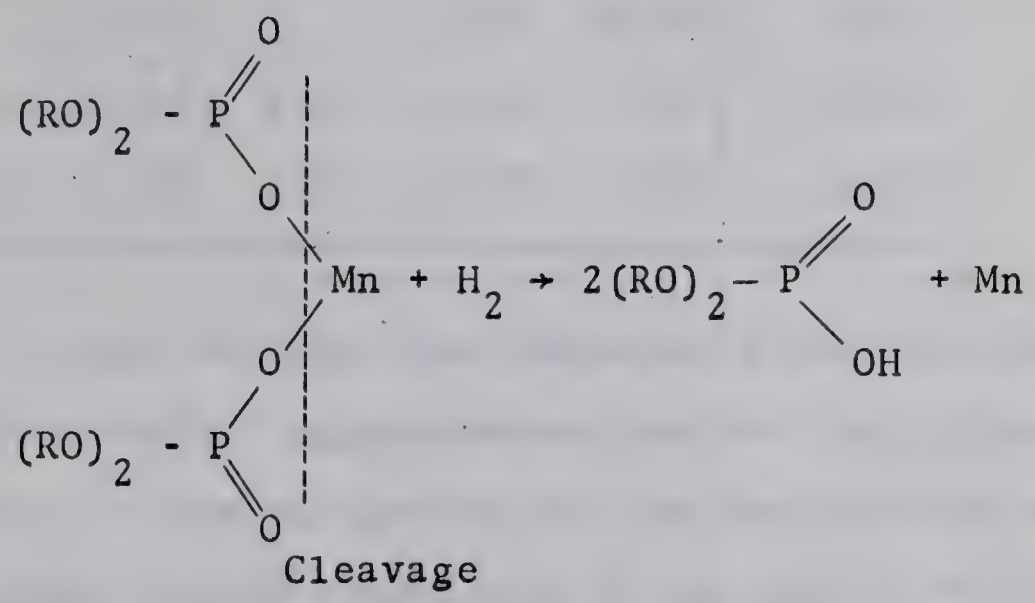

The reduction of Mn-D2EHPA solutions in benzene, and kerosene, was attempted in a rocking 1 litre autoclave, under a pressure of hydrogen ranging from 500 to 2000 Psig, and at temperatures from 50-200°C. It was observed that no noticeable change occurred below 150°C and 1000 Psig hydrogen pressure. At higher temperatures and pressures a white to grey product was obtained. The chemical analyses of the solid residues obtained from the reduction of 0.25 molar solutions of Mn-D2EHPA complex in benzene and kerosine at 200°C

and 1500 Psig are given in the Table XVII.

Table XVII

Chemical Analyses of the Reduction Product of Mn-D2EHPA

Solvent		Percent				Theoretical Mn in $Mn_2P_2O_7$	Calcd. from the Analytical Value of P.
		C	H	P	Mn		
Benzene	1	5.27	1.08	7.53	10.60	13.34	
	2	5.21	1.10	7.39	10.50	13.1	
Kerosene	1	1.13	1.70	6.10	9.87	10.8	
	2	1.70	1.67	5.79	9.36	10.25	

It can be seen from Table XVII that the composition of the product approximates that of the pyrophosphate of manganese. Infrared spectra of the precipitated solids in nujol showed strong absorption in the region 950-930 cm^{-1}. The absorption in this region is assigned to the asymmetric P-O-P absorption by Daasch and Smith[42]. Also there is a strong absorption band near 700 cm^{-1} which is assigned to P-O vibration of the pyrophosphate, by Holmstedt and Larrson[43].

The benzene phases of tests (1) and (2) were combined and subjected to fractional distillation. The fractions obtained at various temperatures were collected separately and analysed using gas chromatograph. They are given in Table XVIII.

Table XVIII

Chromatographic Analysis of Benzene Phase

Fraction		Collected at -°C
n-Hexane	$CH_3(CH_2)_4CH_3$	69
n-Heptane	$CH_3(CH_2)_5CH_3$	98.5
iSO-Octane	$(CH_3)_2CH(CH_2)_4CH_3$	116
2-ethyl hexane	$CH_3(CH_2)_3CH(C_2H_5)CH_3$	118.9

The above data indicate that reactions taking place in the autoclave are very complex. However, it would appear that the cleavage occurred at the C-O linkage rather than at the expected Mn-O, e.g.

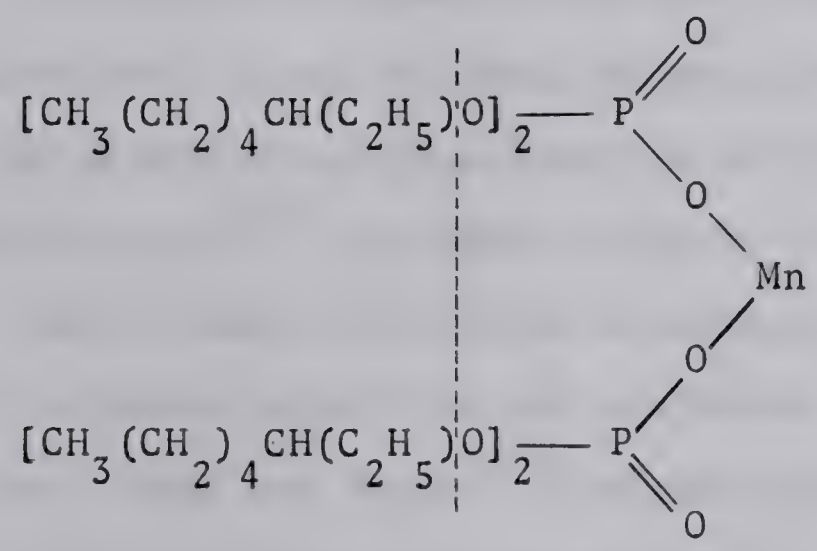

cleavage

As the metallic manganese production by hydrogen reduction of the Mn-D2EHPA complex did not succeed, the electrolytic method is investigated.

PRODUCTION OF METALLIC MANGANESE BY ELECTROLYSIS

Electrolytic production of manganese from aqueous solutions of sulphates and chlorides of manganese and of corresponding ammonium salts in a diaphragm cell has been carried out by several investigators including Allmand[44] in England, Grube[45] in Germany and Zaretskii[46] in Russia. The German work closely approximated the conditions of successful commercial production; the manganese deposited was in the ductile or gamma form.

The first work on the development of a process for the electrowinning of manganese from low grade U.S. ore was carried out by a group including Koster and Shelton[47] in the U.S. Bureau of Mines, Nevada. A process has been developed using sulphate electrolytes. The developments of the electrolytic processes up to 1945 are thoroughly covered in a review[48] in Metal Industry (London).

Until then very little attention had been directed towards cathodic deposition of manganese from chloride electrolytes. Oaks and Bradt[49] investigated extensively the use of chloride electrolytes, employing either 96 per cent Mn anodes or platinum anodes. The optimum conditions reported by them for obtaining good quality deposit are listed in the Table XIX.

Table XIX

Optimum Conditions for Electroplating Manganese
(Oaks and Bradt)

Anode	commercial 96%
Cathode	copper sheet
Cell	porous diaphragm cell
Electrolyte	300-400 g/l $MnCl_2$ + 30 g/l NH_4Cl
Current density	20 amp/cm^2
Voltage	4.5 - 5.5 volts
Temperature	26°C

Oaks and Bradt's investigations were carried out on a very small scale and in no case was the manganese obtained greater than 1 gram quantity. They concluded that the manganese chloride electrolyte was not capable of continuous use because the anode efficiency was greater than the cathode efficiency, resulting in gradual increase of manganese concentration in the solution and the subsequent formation of hydrated manganese oxide.

Thanheiser and Hubold[50] obtained good deposits at 10 amp/dm^2 current density from an electrolyte containing 47-82 g/l Mn as the chloride and 160 g/l NH_4Cl. They found that the pH of the electrolyte decreased during el-

ectrolysis and it was necessary to make continuous addition of ammonia in order to maintain the pH in the desired range. They had difficulty, however, in obtaining reproducible results because of the deterioration of the electrolyte.

Jacobs[51] has experimented extensively with deposition from chloride solutions. The conditions for the maximum current efficiency reported by him are given in Table XX.

Table XX

Conditions for Manganese Deposition from Chloride Bath

Anode	Graphite
Cathode	Stainless steel
Diaphragm	Vinyon
Mn in feed solution	54 grams per litre
NH_4Cl	110 grams per litre
Mn in catholyte	14 grams per litre
SO_2	0.05 grams per litre
Current density	45 amps per sq.ft.
Cell potential	3.4 volts
Current efficiency	70%

The chloride electrolytes are better conductors than sulphate solutions and the potential drop from

the graphite anode to the solution is less than from the oxide coated anode used in the sulphate cell. The overall result in a cell voltage of 3.57 for the chloride cell as compared with 4.83 for sulphate cell. This represents a reduction of 25% in power consumption. The pH range in which the manganese can be deposited at maximum efficiency is greater with chloride than sulphate, hence manganese recovery from the solution may be increased. The disadvantages of the chloride process are the more corrosive nature of the solution, creating equipment problems, and the loss of ammonia by decomposition at the anode. The gas evolved at the anode is approximately 99% N_2 and about 1% Cl_2.

There is no doubt that the electrolysis of aqueous solutions for the production of manganese will not loose its significance because of its unusual flexibility; it permits the use of waste products and poor ores that are unsuitable for the extraction of manganese by other means and it gives a metal requiring no further purification. However, because of high cost of electrolysis the possibility of developing a parallel cheaper process seems rather tempting.

Very little work has been done on the electrowinning of manganese from non-aqueous media. The only appropriate reference is that due to Dirkse and Brisco[52], who deposited a series of elements including manganese

from ethers, acetones and alcohols.

A. Choice of Electrolytic Media

Since manganese is on the negative or base end of the electromotive series of elements(Mn^{++}/Mn=-1.18V) it evolves hydrogen from aqueous solutions. Because of its reactivity with water metallic manganese is not plated from aqueous solutions, unless additions of 100-150 g/l of ammonium salts are made to prevent oxidation of Mn. Ammonium salts also serve as buffers for the catholyte, in addition to the increase in electrical conductivity. The disadvantages, however, are low current efficiency, low catholyte concentration, redissolution of some of the deposited Mn due to the lowering of pH as the electrolysis proceeds.

The purpose of this investigation was to develop a method of electroplating coherent and bright coating of pure manganese from organic electrolytes.

In the exploratory phase of this work chemically pure $MnSO_4$ and $MnCl_2$ were used. Detailed electrolytic studies were limited to $MnCl_2$ because of the relative insolubility of $MnSO_4$ in most of the organic solvents. The solvents in which the electrolysis of $MnCl_2$ was studied are listed in Table XXI.

Table XXI

Physical Properties of Organic Solvents

Solvent	Density g/ml	Viscosity c.p.	Sp.Conduct. mho cm^{-1}	Dielectr. const.
Formamide	1.129	0.330	1.12×10^{-5}	109.5
N-N Dimethylformamide	0.944	.0796	1.6×10^{-7}	36.71
Dimethyl sulfoxide	1.096	0.196	3×10^{-8}	46.6
N-N dimethylacetamide	0.937	.092	1.4×10^{-7}	37.8
Pyridine	0.978	.0883	1.0×10^{-9}	12.3
Nitrobenzene	1.198	0.182	1.0×10^{-10}	34.91

Electrolysis of $MnCl_2$ in dimethyl sulfoxide (DMSO), Pyridine and nitrobenzene yielded a brown to black non-metallic deposit giving qualitatively a positive test for manganese. The solutions were poorly conducting. In order to obtain a c.d. of 20-30 m amp/cm^2 the voltage had to be raised considerably with the result that the electrolyte temperature was raised to about 60°C in some cases.

Dimethyl sulfoxide also gave a black uncompacted deposit which fell off the cathode during electrolysis. The deposit contained 5-8% C and 0.5 - 1.5% S.

The electrolysis of $MnCl_2$ using amides as electrolytes gave a dark metallic deposit of manganese. In a qualitative electrolytic test when the anode and the cathode products were allowed to mix in an undivided cell a brown

coloration was produced around the anode. The cathode deposit started to redissolve as the electrolysis proceeded. In another experiment where pure amides were used as an anolyte which was separated with a fritted glass diaphragm from a $MnCl_2$ solution of amides furnishing the catholyte (using a pure graphite anode and a 18-8 stainless steel cathode), again a brown coloration appeared around the anode upon the passage of current. Infrared spectra of this brown material showed the presence C-N and C-Cl bond. This compound has been identified as cyanuric acid by Schneider[53] and later by Couch[54]. The presence of C-Cl bond indicates that the material produced may also contain cyanuric chloride. The infrared spectra of the catholyte showed the presence of secondary and tertiary amines. The catholyte however, remained clear. In order to save the electrolyte from decomposition the anolyte used in the subsequent tests was an aqueous solution of NH_4Cl. Maintaining the catholyte pH around neutral point it was observed that bright metallic microcrystalline manganese was deposited using formamide solution (Figure 23). The deposits were dull dark and contained pin holes when DMF and DMA were used (Figure 24). The chemical analyses of the deposited Mn from catholyte solutions containing 10 g/l Mn as $MnCl_2$ and anolytes containing 90 g/l NH_4Cl plus 20 g/l HCl, at a current density 40 m amp/cm^2, maintaining the catholyte pH around 7.2, are given in the

Fig. 23 Bright and smooth manganese deposited from a formamide bath.

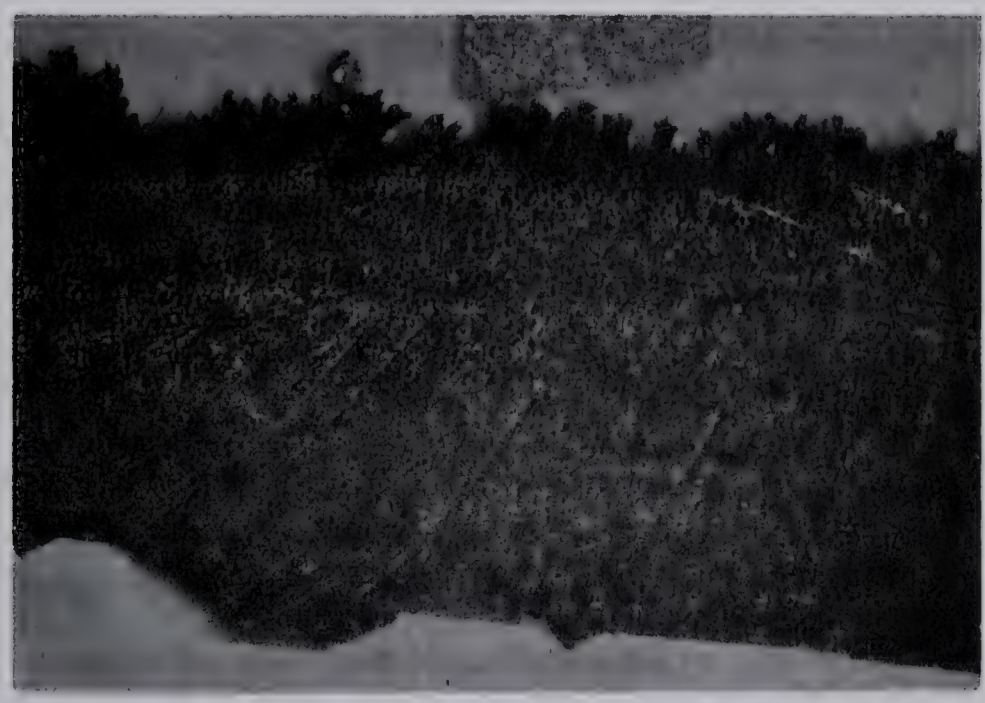

Fig. 24 Manganese deposited from Dimethyl formamide showing pin holes and "tree growth".

Table XXII.

Table XXII

Chemical Analysis of the Electrodeposited Manganese from Organic Solvents

Solvents	% Mn	% C	% O
Formamide	98.6	-	-
N-N DMF	81.4	5.7	4.4
N-N DMA	76.9	8.2	6.5

From these results it appeared that formamide was the most satisfactory electrolyte for the Mn electrolytic bath. The high dielectric constant of formamide focused our attention and decided us to undertake systematic study to investigate the influence of different variables on the current efficiency and the nature and properties of the electroplated manganese.

B. Electrolysis of Manganese from the Formamide Baths

Electrolytic studies in aqueous solutions by different workers indicate that a large number of variables have an important effect on manganese deposition. However, the most important appear to be the effect of:

1. anolyte composition and pH
2. catholyte composition and pH
3. temperature, and
4. current density.

A necessary prerequisite of a plating bath however, is that a sufficiently high concentration of the cation be maintained in solution. This made it necessary to study the solubility and conductance of $MnCl_2$ in formamide. The change in the conductivity of formamide with the increase in $MnCl_2$ concentration is plotted in Figure 25. The abrupt change in the conductivity indicates the formation of some $MnCl_2 \cdot x(HCONH_2)$ complexes. The solubility of manganous chloride in formamide at 25°C was found to be about 82.6 g/l.

1. Effect of Anolyte Composition and pH on the Current Efficiency. A series of anolyte solutions were made by dissolving 2.5 to 13 g. NH_4Cl in 100 ml of distilled water. The pH of 1-5 was adjusted with HCl. A 1% solution of Mn as $MnCl_2$ in formamide tentatively furnished the catholyte. The pH was found to be 8.6. The electrolysis was conducted in a diaphragm H-type cell using graphite anode and stainless steel cathode at a current density of 30 m amp/cm^2. The cell and the equipment used for electrodeposition of manganese is shown in Figure (26a) and (26b). The data obtained from the tests showing the effect of the variation of pH on the current efficiency at different NH_4Cl concentrations are plot-

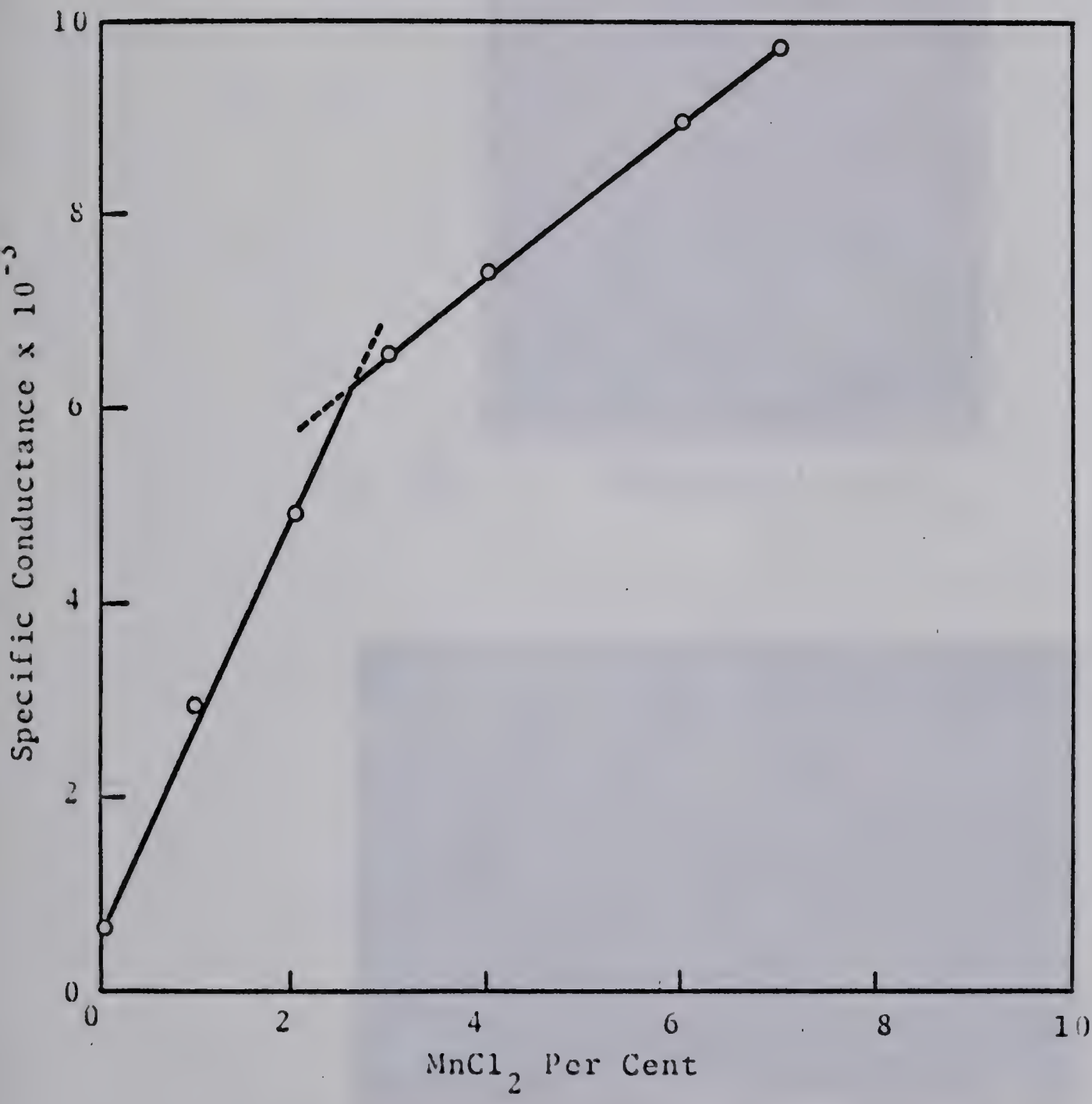

Fig. 25 Specific conductance of $MnCl_2$ - formamide solutions at 25°C.

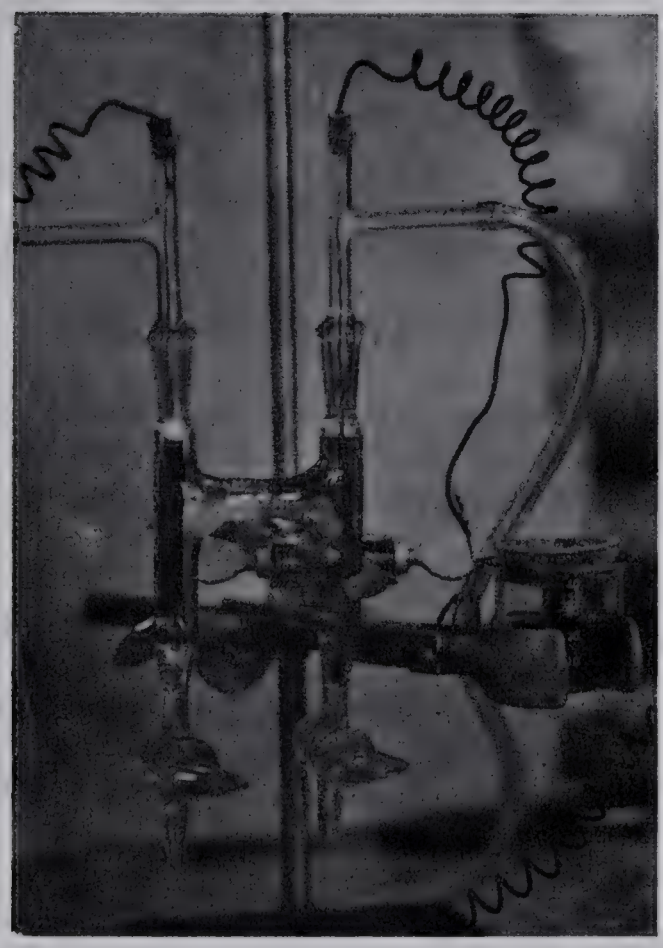

Fig. 26a. Electrolytic Cell

Fig. 26b. General View of the Set-up for the Electrodeposition of Manganese

ted in Figure 27. The current efficiency increases with the decrease in the pH; conversely, the current efficiency increases with the increase in NH_4Cl concentration up to about 90 g/l and then decreases slightly. The critical pH at low NH_4Cl concentration (10 g/l) is 1.8 which is raised to 3.0 by increasing NH_4Cl concentration to 120 g/l (c.f. curve A and D in Figure 27). The deposits at anolyte pH above 2.5 were black, flaky and tended to fall off the cathode.

2. Effect of Catholyte Composition and pH. Figure 28 shows the effect of varying pH on the current efficiency at different $MnCl_2$ concentrations. The anolyte contained 80 g/l NH_4Cl and its pH was fixed at 2.5. All other conditions were held constant. It can be observed that the critical pH, defined as the pH at which the current efficiency is maximum at a particular cationic concentration, is decreased with the increase in the manganese concentration of the catholyte. The current efficiency however, increases with the increase in the Mn concentration up to 18 g/l then it decreases. It can therefore be concluded that in order to maintain maximum current efficiency the pH of the catholyte should be decreased.

The deposits from the catholytes containing 10-20 g/l $MnCl_2$ were from bright and smooth to fine crystalline, brittle and could be readily chipped off the cathode by flexing the latter.

Figure 29 shows the smooth chipped off manganese

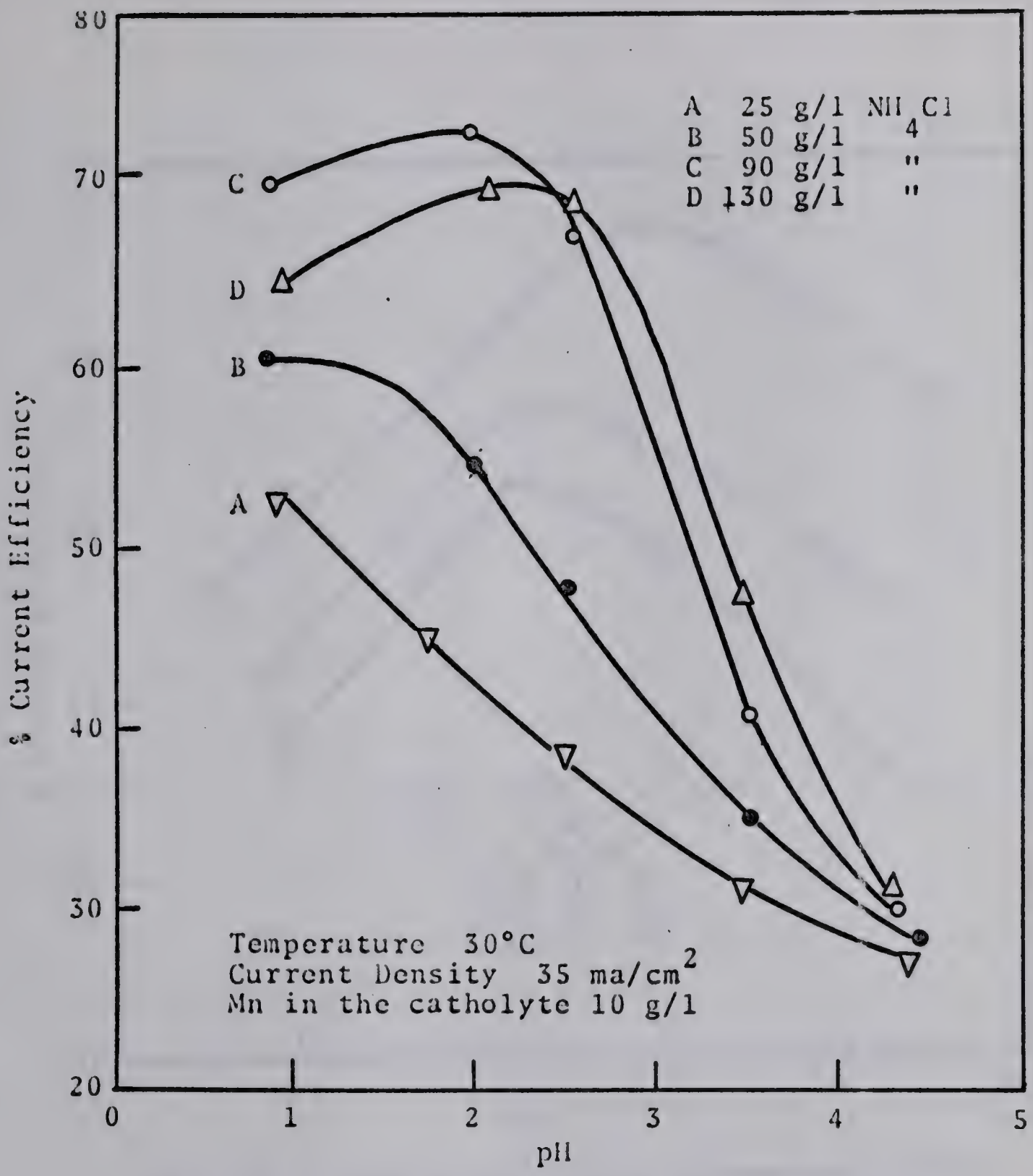

Fig. 27 Effect of anolyte pH on the current efficiency at variable NH_4Cl concentrations.

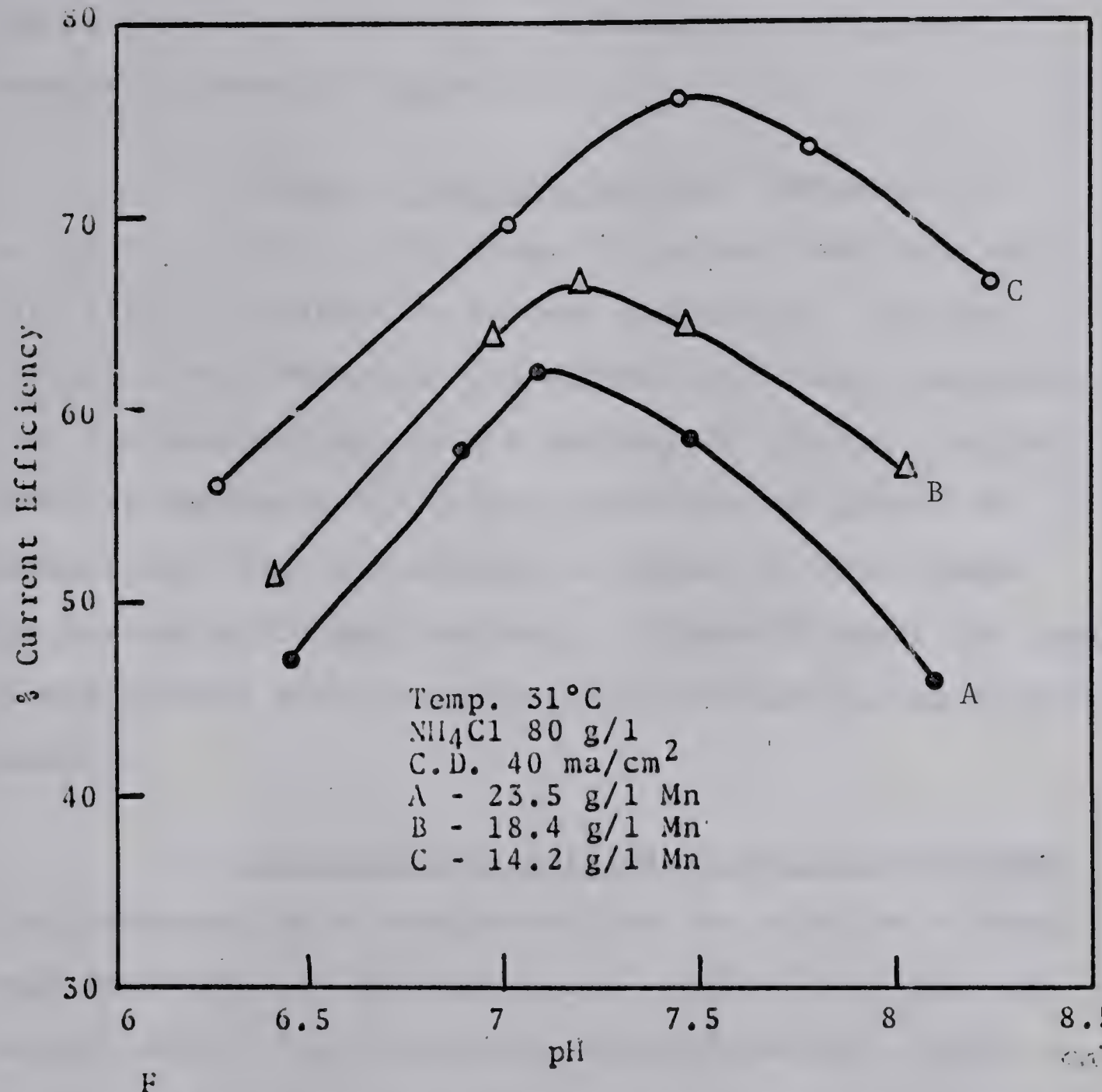

F

Fig. 28 Effect of pH on the current efficiency at variable manganese concentrations in the catholyte.

of approximately 99% purity (analysed polarographically) on the steel cathode. The overall current efficiency was 79.7%. At catholyte concentration above 20 g/l Mn the current efficiency decreases due to the nodulization of deposit particularly on the edges. A typical example is shown in Figure 30.

3. Effect of Current Density. Manganese can be deposited over a wide range of current densities with only slight variation in current efficiency. At high current density however, the current efficiency increases when the electrolysis is not prolonged. If the electrolysis is continued for longer intervals the growth of nodules and trees illustrated in Figure 31 will change the current efficiency markedly. Figure 32 shows the change in the current efficiency with the increase in the current density.

4. Effect of the Addition of Sulphur Compounds. Electrodeposition of manganese from the solution of manganese compounds and ammonium salts results in a gamma or ductile form. The commercial process however, depends on the transformation of the gamma form to the alpha form as it is deposited. This transformation is brought about by the presence of certain reducible sulphur compounds in the electrolyte. The first successful process utilized SO_2 (or sulphites).

Fig. 29 Chipped off deposit of manganese at a catholyte concentration of 14.7 g/l $MnCl_2$

Fig. 30 Nodulized manganese deposit at a catholyte concentration of 25.5 g/l $MnCl_2$

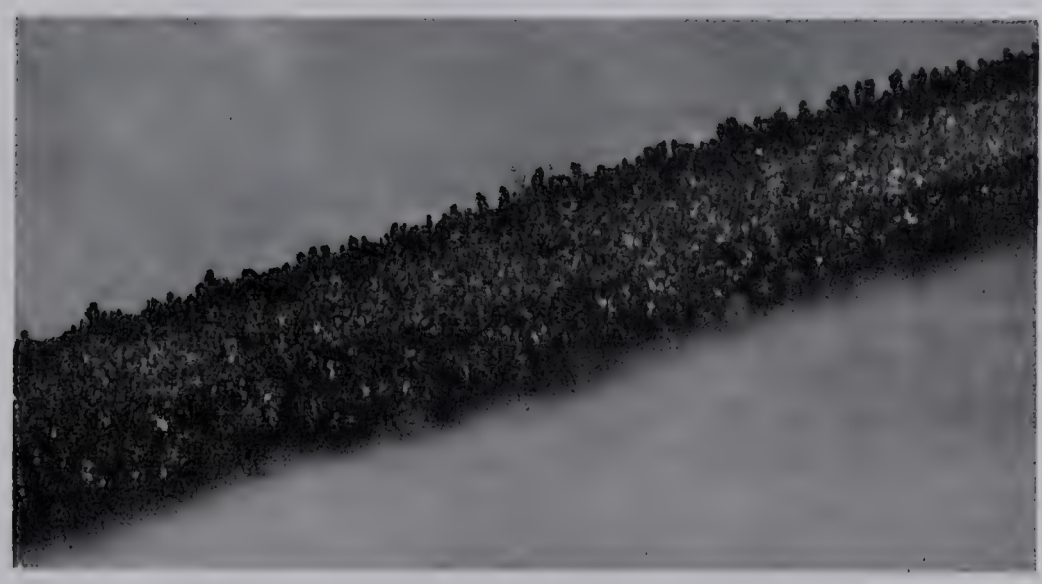

Fig. 31 "Tree growth" on prolonged electrolysis

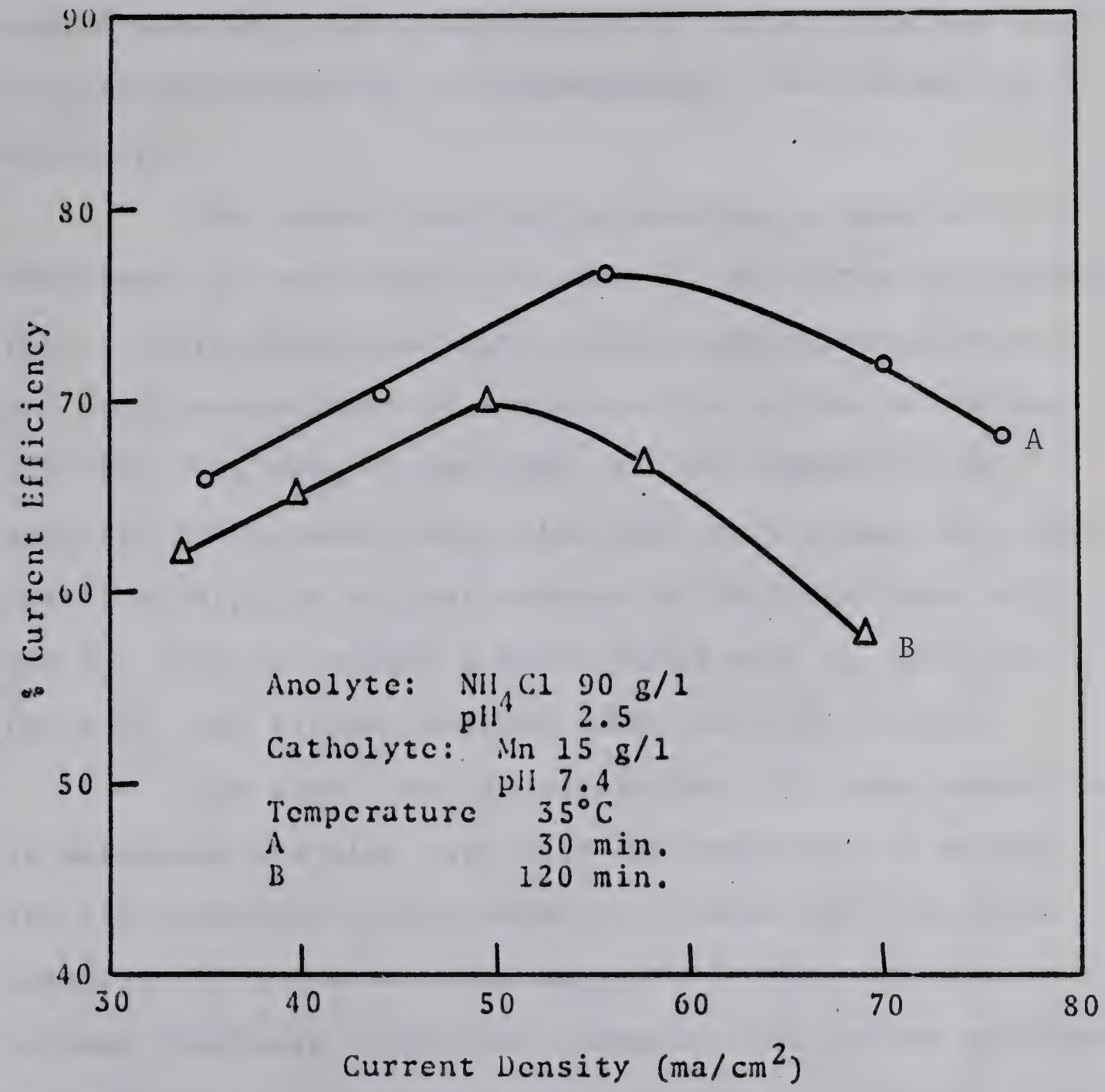

Fig. 32. Effect of current density on current efficiency.

The exact function of sulphur compounds has not been determined. Its addition in the electrolyte prevents the oxidation of the catholyte and the precipitation of manganese dioxide; the conductivity of the electrolyte is also increased and so is, consequently, the current efficiency.

The amount required to maintain a good current efficiency is only about 0.1 gram SO_2 per litre of electrolyte. It is found that with all the conditions favourable for electrodeposition of manganese the current efficiency will fall off after a few hours in the absence of SO_2. Analysis of the metal deposited with and without SO_2 shows that the sulphide sulphur content of the metal made without SO_2 does not exceed 0.0032% while with 0.1 gram per litre SO_2 the sulphur content rises to 0.02 - 0.05%.

The conditions necessary for efficient deposition of manganese are also favorable for reduction of sulphur and its inclusion in the deposit, as also for the transformation of gamma to alpha manganese. The compounds of sulphur that were tested were ammonium and sodium sulphides and sulphites, dithionates and xanthates. An amount 0.05 to 0.15 gm/l (calculated as SO_2) was found to be adequate for a good current efficiency.

5. Effect of Temperature. It is advantageous to evaluate the highest possible temperature at which Mn could be electrodeposited so that unnecessary cooling

could be prevented.

The effect of cell temperature on deposition from a catholyte containing 16 g/l Mn at pH 7.3 and anolyte containing 90 g/l NH_4Cl at pH 2.4 using a current density of 50 m amp/cm^2 is given in Table XXIII.

Table XXIII

Effect of Temperature on the Current Efficiency

Cell temp.°C	mg Mn plated	Cell pH	Cell Voltage	Current eff.
28.6	81.6	7.30	6.3	74.6
35.5	83.5	7.35	6.2	77.4
40.3	82.3	7.50	6.05	76.2
45.0	78.6	7.75	5.95	71.6
51.4	71.6	7.90	5.80	66.9

It is seen from the Table XXIII that at about 35°C maximum current efficiency is obtained. Although the cell voltage drops steadily with increasing temperature the simultaneous drop in current efficiency more than offsets this so that no overall advantage in power consumption per pound of manganese deposited is obtained.

Figure 33 shows the dependence of the cell voltage ν on the current density $\imath$ of the process of electrodeposition of manganese. We can see that with the decrease in temperature the current density decreases sharply, as re-

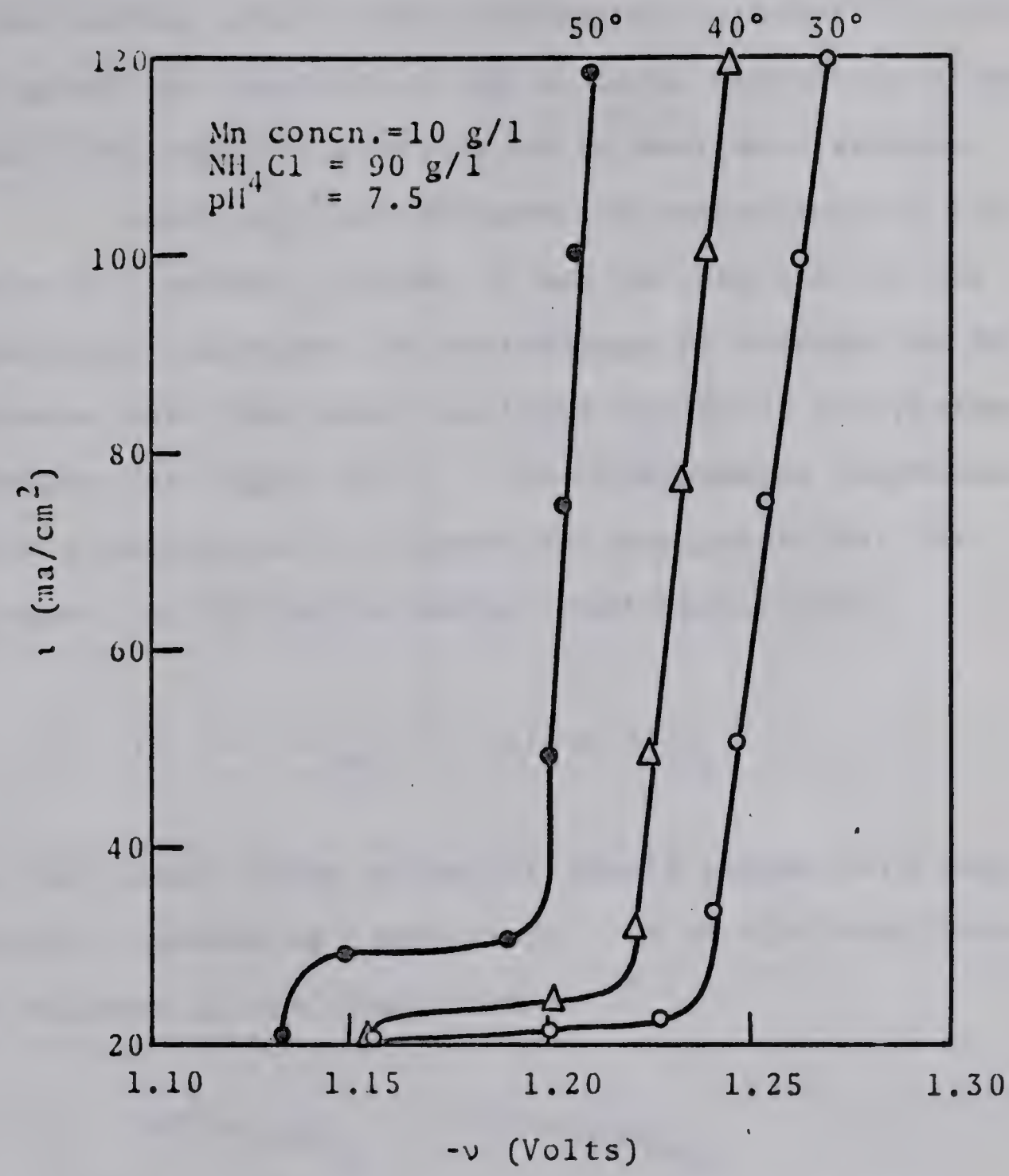

Fig. 33 Dependence of electrode potential 'v' on the current density 'i' at various temperatures.

presented by the point of inflection on the curves. After this the current density rises sharply.

A similar in character dependence of potential on the current density was obtained by Agladze[55], who investigated the kinetics of the cathodic deposition of manganese from aqueous solutions on an amalgam electrode.

Analyzing the influence of temperature on the nature of ν versus ι curve, it can be seen that as the temperature increases the overvoltage of hydrogen on Mn decreases with the result that the height of the plateau increases (in Figure 33). If the temperature dependence of the polarization is sharper for manganese than for hydrogen i.e. if the following relationship holds

$$(d\ (\Delta\nu)/dt)_{Mn} > (d(\Delta\nu)/dt)_{H_2} \qquad (93)$$

then the steady state potential should become more negative with increasing temperature. If on the other hand the contrary is the case, that is

$$(^{d(\Delta\nu)}/_{dt})_{H_2} > (^{d(\Delta\nu)}/_{dt})_{Mn} \qquad (94)$$

then a displacement of the steady-state-potential in the positive direction should be expected. In the electrodeposition of manganese this latter situation is realized; however, the change in the steady state potential is small.

Consequently $d(\Delta v)/dt$ for the Mn and H_2 differ negligibly. Thus the cathodic evolution of hydrogen in the electrodeposition of manganese takes place according to the catalytic action of the metal ion which acts as a sink for electrons and redissolves in the catholyte according to the following mechanism:

$$Mn^{2+} + 2e^{-} \rightarrow Mn \qquad (95)$$

$$Mn + 2H^{+} \rightarrow Mn^{2+} + 2H \qquad (96)$$

6. Effect of Stirring. On agitating the electrolyte the plating conditions in general are improved due to a more uniform composition of the electrolyte. Stirring proved especially beneficial for the rate of manganese deposition, although the nature of the deposit seemed to be little affected.

A statistical analysis of the influence of the parameters on the current efficiency and the nature of the deposit indicates that the most favorable bath composition would be as follows:

Table XXIV

Cell-Operation Data for Electrowinning Mn from a Formamide Bath

Catholyte	
Mn	12-16 g/l as $MnCl_2$ in formamide
pH	7.5 - 7.2
Anolyte	
NH_4Cl	80-100 g/l
pH	2.5 - 2.0
Current density	50 ma/cm^2
Temperature	35°C
Current efficiency	77%

The electrolytic conditions established for the reagent grade manganous chloride in formamide were then applied to the manganese recovered from the ore.

The loaded solvent (i.e., Mn-D2EHPA complex) was stripped with concentrated HCl or HCl gas in formamide, on the counter current principle till the formamide solution was almost neutral. The exchange reaction taking place may be as follows:

$$MnL_2 + 2HCl = MnCl_2 + 2HL \qquad (97)$$

Where L is the di(2-ethyl hexyl)-phosphate residue. The ligand is completely insoluble in formamide; the latter therefore, contains only $MnCl_2$. This solution after adjusting the pH and concentration was subjected to electrolysis in the diaphragm cell used for preliminary experiments.

The deposited manganese was analysed polarographically. X-ray diffraction pattern in Figure 34a compares with a standard alpha manganese (99.9% Mn from Electro Manganese Corporation) in Figure 34b. The three strong lines correspond to the d value of 2.09, 1.21, 1.89A°.

C. Electrode Reactions

It has been indicated [56] that formamide and other alkyl amides co-ordinate through oxygen with metal ion, as Lewis acid. This coordination through oxygen drains electron density out of the oxo bond thus lowering the bond order and decreasing the force constant. Thus the complex should be broken on electrolysis liberating the metal and regenerating the ligand. Representing formamide ($HCONH_2$) by R the equilibrium $MnCl_2$ complex with formamide may be represented as follows:

$$MnCl_2 + xR = MnCl_2.xR \qquad (98)$$

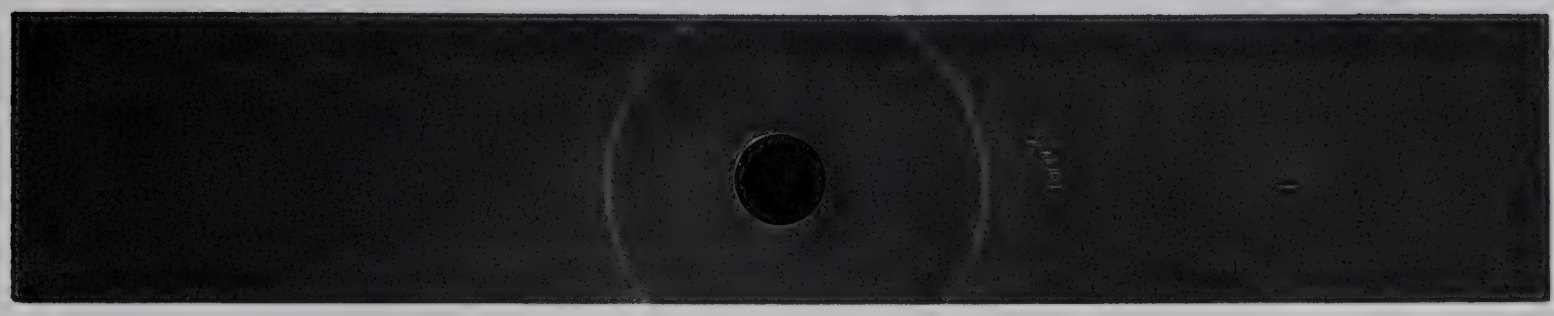

Fig. 34a X-ray diffraction pattern of the manganese deposited from the formamide bath.

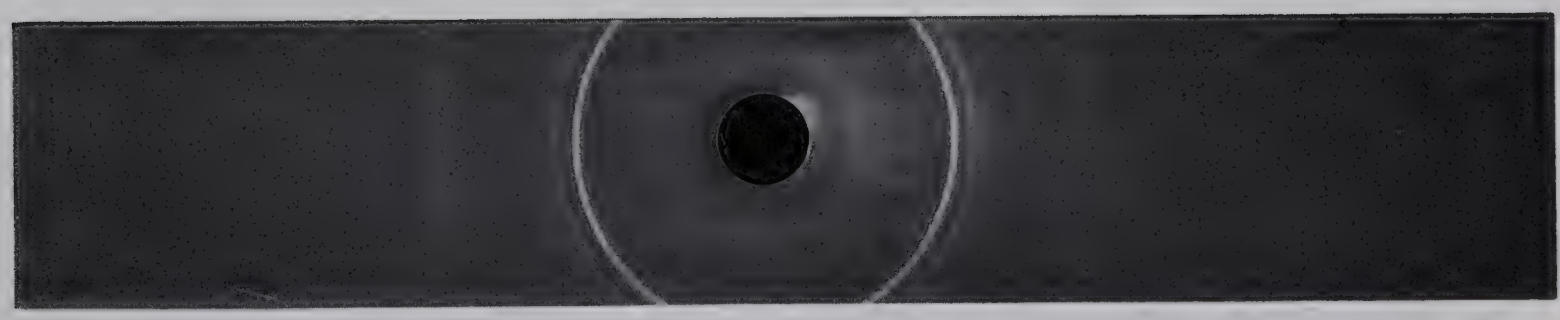

Fig. 34b X-ray diffraction pattern of the standard alpha manganese (from Electro-Manganese Corp.).

Cryoscopic determinations revealed that the $MnCl_2$ has on the average 2-4 moles of ($HCONH_2$). The solution, therefore, may contain $Mn(HCONH_2)_2Cl_2$ and $Mn(HCONH_2)_4Cl$.

The reaction at cathode may be represented as

$$[Mn(HCONH_2)_x]^{++} + 2e \rightarrow Mn + xHCONH_2 \qquad (99)$$

The anode reaction should be

$$2Cl^- \rightarrow Cl_2 + 2e \qquad (100)$$

In actual practice however, the content of chlorine in the gases produced at the anode is 1 to 2%. The titration of anolyte revealed that free acid is produced, the amount of which approximately corresponds the following reaction

$$2NH_4Cl + 3Cl_2 \rightarrow N_2 + 8HCl \qquad (101)$$

The anodic reaction therefore can be assumed to be essentially the oxidation of ammonium compounds.

The catholyte was found to be alkaline. Although theoretically it should be acidic due to the diffusion of acid from the anode compartment.

Qualitative tests and infrared spectroscopy indicated the presence of primary secondary and tertiary amines. These may have been produced by the electrolytic

reduction of amides according to the following reaction

$$HCONH_2 + 2H_2 \rightarrow CH_3NH_2 + H_2O \qquad (102)$$

Since all the byproducts formed could not be isolated and analysed a material balance for the overall cell reaction cannot be accounted for.

CONCLUSION

The laboratory scale investigation has demonstrated the feasibility of recovering manganese from a low-grade iron-manganese ore from New Brunswick. The best results were obtained when the experimental conditions were maintained as follows:

1. When a -65 mesh ore sample was leached with 16% H_2SO_4 for 30-40 minutes at 60-70°C with constant stirring, over 90% Mn was dissolved from the ore. The H_2SO_4 consumption was found to be 1.5 mole for each mole of Mn leached out.
2. Single stage batch extraction of Mn from the leach liquor into a kerosene solution containing 0.5M di(2-ethyl hexyl) - phosphoric acid (denoted D2EHPA) showed that Mn was selectively and quantitatively extracted and separated from the dissolved impurities (e.g., Fe^{++}, Ca, Mg, SiO_2, Cu, etc.) around pH 5 (as per stoichiometric equation 51). At higher ligand concentration the viscosity of the kerosene phase became too high (see Figure 18) for effective separation of aqueous and organic phases.

3. The manganese complexed by D2EHPA in kerosene was stripped with concentrated HCl into the formamide phase by counter current flow until the formamide solution becomes nearly neutralized.
4. The formamide phase containing 12-16% Mn as $MnCl_2$ was used as catholyte in the subsequent step of electroytic deposition of Mn from an organic solvent.

   The pH of the catholyte was adjusted to ~ 7.5 with NH_3.

   In order to prevent decomposition of solvent and undesirable side-reactions a diaphragm cell was used, with anolyte consisting of an aqueous solution of 90-100 g/l NH_4Cl at a pH of ~ 2.5.

   Electrolysis of $MnCl_2$-formamide at a current density of 50 ma/cm^2 and 6.5 volts in a diaphragm cell resulted in a current efficiency of about 76%.

Comparing the electrolytic processes using aqueous $MnCl_2$ with this process, using formamide solution of $MnCl_2$ it has been found that the $MnCl_2$-formamide solution has a higher conductivity. The pH of the catholyte can be raised to ~ 8.0 without precipitating $Mn(OH)_2$. The current efficiency is also higher than in the corresponding aqueous electrolytes.

The disadvantage of maintaining a higher pH was that on continued electrolysis the catholyte became turbid and the current yield was not reproducible.

The preliminary laboratory experiments point to a possibility of developing a new process for Mn reaction. The values of parameters established for the individual steps may not be the final ones for a large scale process, but nevertheless they can serve as a useful guide for the subsequent pilot-plant testing. For an evaluation of a final flowsheet it will be necessary to re-examine the effect of changes in parameters by successive approximations, to find the effects of continuous versus batch treatment, and to examine a number of new parameters like the geometry of cell and electrodes in the electrolytic step, accumulation of impurities, etc.

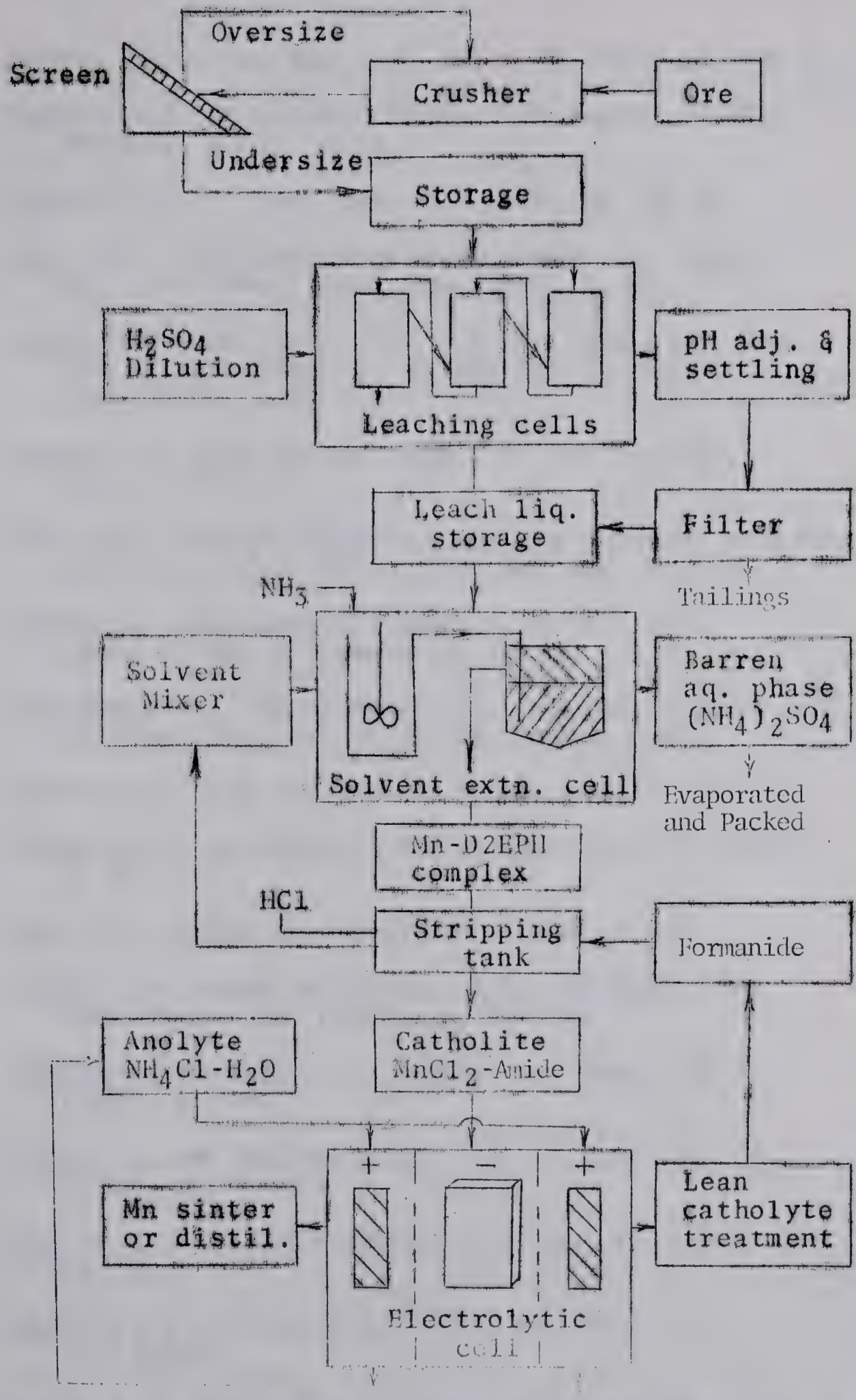

Fig. 35 A flow sheet for leaching, solvent extracting and recovering manganese by electrolysis

REFERENCES

1. Sidwell, K.O., Can. Min., Met. Bull., 50 (1957) pp. 411-16

1a. Pickett, D.E., Mine Branch Ottawa, Test Report, 894-0D, March 10, (1957), p. 12.

2. Naylor, B.F., J. Chem. Phys. 13, (1945), pp. 329-32.

3. Quazi, M.A., Hydrometallurgy of Manganese. Lit. Survey Dept. Min & Met., Univ. Alta (1965), p. 67.

4. Norman, L.D., and Kirby, R.C., U.S. Bur. Min., Inf. Circ. Part I, 8138 (1962), p. 30, and Part II, Inf. Circ. 8160 (1963), p. 35.

5. Nossen, E.S., Ind. and Eng. Chem., 43. No. 7 (1951), pp. 1695-1700.

5a. Dean, R.S., Aqueous Solutions Containing Manganese in a Complexion ..., U.S. Pat. 2, 608, 463, Aug. 26, 1952.

6. Bradley, W., (assigned to Bradley-Fitch Co.), U.S. Patent 1, 951, 341, March 20, (1934).

7. Stringham, W.S., and Summers, G.N., (assigned to Bruce Silliams), U.S. Pat. 2,724,646, Nov. 22 (1955).

8. Leaver, E.S., U.S. Pat. 243,015 (1918).

9. Blumburg, R., and Morgan, T.D., J. Appl. Chem. 3, (1953), p. 223.

10. Allen, L.N., Chem. Eng. Progr. 50, (1954), p. 9.

11. Ravitz, S.F., Wyman, W.F., Back, A.E., and Tame, K.E., AIME, Trans. 182, (1949), pp. 286-295.

12. Hoak, R.D., and Coull, J., J. Chem. Eng. Progr. 4613 (1950), p. 158.

13. Thomas, G., and Whalley, B.J.P., Can. J. Chem. Eng. 36, (1958), pp. 37-43.

14. Schrier, E., and R.W. Hoffmann, Chem. Eng. 61, (1954) pp. 152-5.

15. Engel, A.L., and Heinen, H.J., U.S. Bur. Min. R.I. 5641 (1960).

16. Jacobs, J.H., Hunter, J.W., Yarrol, W.H., and Churchward, P.E., Trans. AIME, 159 (1944), pp. 408-28.

17. Pourbaix, M., Atlas of Electrochemical Equilibrium in Aqueous Soln., Pergaman Press (1966), p.313.

18. Pourbaix, M., Atlas of Electrochemical Equilibrium in Aqueous Soln., Pergaman Press (1966), p. 290.

19. Levan, H.P., and Davis, E.G., U.S. Bur. Min. R.I. 6452 (1964).

20. Iwasaki, I., and Carlson, W.I., AIME Meeting Los Angeles, Calif., Feb. 19-23, (1967), p. 37.

21. Ambrose, P.M., Purification of Manganese Electrolyte, U.S. Pat. 2,316,750, April 20, (1943).

22. Jacobs, J.H., Hunter, J.W., Churchward, P.E., and Knickerbocker, R.G., U.S. Bur. Min. Bull. 463, (1946).

22a. Jacobs, J.H., Hunter, J.W., Yarroll, W.H., Churchward, P.E., and Knickerbocker, R.G., Trans. Am. Inst. Min & Met. Engrs., 159, (1944), pp. 408-28.

23. Charlot, G., Theorie et Methodes Nouvelles d'Analyse Qualitative, 3rd Ed., Masson, Paris (1949).

24. Jacobs, J.H., Churchward, P.E., and Knickerbocker, R.G., Trans. Elec. Chem. Soc., Preprint Oct. 16, (1944).

25. Jacobs, J.H., and Yarrol, W.H., Electrolytic Cell for Manganese Recovery, U.S. Pat. 2,456,196, Dec. 14, (1948).

26. Carosella, M.C., and Fowler, R.M., J. Elec. Chem. Soc. 104, (1957), p. 352.

27. Dyrssen, D., Acta. Chem. Scand. 11, (1957), p. 1771-

28. Richardson, F.D., and Jeffes, J.H.E., J. Iron St. Inst., Vol. 160, (1948), p. 261.

29. Mah, A.D., U.S. Bur. Min., R.I. 5600 (1960), p. 340.

30. Kimura, K., Bull. Chem. Soc. Japan, 34 (1961), pp. 63-8.

31. Peppard, D.F., Mason, G.W., Driscoll, W.J., and Sironen, R.J., J. Inorg. Nucl. Chem. 7, (1950), p. 276.

32. Brown, K.B., Coleman, C.F., Crouse, D.J., Blake, C.A., and Ryon, A.D., Proc. Second Intern. Conf. Peaceful Uses Atomic Energy, Geneva, 31 (1958), pp. 472-87.

33. Peppard, D.F., Ferraro, J.R., and Mason, G.W., J. Inorg. Nuclear Chem. 7, (1958), pp. 231-44.

34. Baes, C.F., Zingaro, R.A., and Coleman, C.F., J. Phys. Chem. 62, (1958), p. 129.

35. Szabo, E., and Szabon, J., Acta Chimica Acad. Sci. Hung. Tomus 48, (1966), pp. 299-307.

36. Healy, T.V., and Kennedy, J., J. Inorg. Nucl. Chem. 10, (1952), p. 128.

37. Gardner, A., McKay, H.A.C., and Worren, D., Trans. Farad. Soc., 48, (1952), p. 997.

38. Ryon, A.D., Daley, F.L., and Lowrie, R.S., Chem. Eng. Progr. 55, (1959), pp. 70-75.

39. Qazi, M.A., and Leja, J., Solvent Extraction Study of a Low-Grade Iron-Manganese Ore, AIME Meeting, Los Angeles, Calif., Feb. 19-23 (1967), p. 37.

40. Peppard, D.F., and Ferraro, J.R., J. Inorg. Nucl. Chem., 15 (1960), p. 365.

41. Bellamy, L.J., and Beecher, C., J. Chem. Soc. 170, (1952), p. 1701.

42. Daasch, L.W., and Smith, D.C., Analyt. Chem. 23, (1951), p. 853.

43. Holmstedt and Larsson, Acta Chem. Scand. 5, (1951), p. 1179.

44. Allmand, A.J., and Campbell, A.N., Trans. Faraday Soc. 20, (1924), p. 379.

45. Grube, G., U.S., Dept. of Commerce, B.P. 52010.

46. Zaretskii, S.A., Gosudarst Inst. Prikladnoi Khim. Sbornick Statei, (1919-39), pp. 183-91.

47. Koster, J., and Shelton, S.M., Eng. & Min. J., 137 (1936), p. 510.

48. Recorder II, Electrolytic Manganese, Production Efficiency etc., Metal Ind. (London), Feb. 16, (1945), pp. 101-102.

49. Oaks, H.H., and Bradt, W.E., Trans. Electrochem. Soc., 69 (1936), pp. 567-84.

50. Thanheiser, B., and Hubold, R., Milt. Kaiser-Wilhelm Inst. Eisenforsch, Dusseldorf, 23 (1941), pp. 1-19.

51. Jacobs, J.H., and Churchward, P.E., J. Electrochem. Soc. 94, (1948), pp. 108-21.

52. Dirkse, T.P., and Briskoe, H.T., "The Electrodeposition of Metals from non-Aqueous Solutions", Metal Ind. June (1938), pp. 284-5.

53. Schneider, V.H., Ber. Dent. Chem. Ges. 56 (1923), p. 2460.

54. Couch, D.E., Electrochimica Acta. 9, (1964), pp. 327-36.

55. Agladze, R.I., Khim. Referat Zhur, 4 (1941), p. 90.

56. Joeslen, M.D., and Drago, R.S., (in Press) (1965).